DYNAMIC RESPONSE OF PLATES ON ELASTIC FOUNDATION

Thesis for the Degree of Ph. D.

MICHIGAN STATE UNIVERSITY

Piyush C. Sharma

1964

This is to certify that the

thesis entitled

"DYNAMIC RESPONSE OF PLATES
ON ELASTIC FOUNDATION"

presented by

Piyush Chandra Sharma

has been accepted towards fulfillment
of the requirements for

Ph. D. degree in Civil Engineering

Robert K. L. Wen
Major professor

Date September 3, 1964

ROOM USE ONLY

ABSTRACT

DYNAMIC RESPONSE OF PLATES ON ELASTIC FOUNDATION

by Piyush C. Sharma

In this thesis a numerical method for the dynamic analysis of plates on elastic foundation is presented. The method is based on a discretization of the plate by use of the classical finite difference expansion of the space derivatives in the governing partial differential equation. The resulting ordinary differential equations for the discrete system (with time as the independent variable) are integrated numerically.

The purpose of this thesis is twofold: (i) To investigate the practicability of finite difference methods in solving dynamic response problems of plates, particular attention being given to the accuracy of the method and the efficient adaptation to the computer. (ii) To demonstrate the workability of this approach in handling problems whose exact solutions are not known and perhaps impossible to obtain.

For this study, computer programs have been prepared so that not only their solutions but the generations of the equations of motion (with the boundary conditions appropriately taken into account) are all done by the computer for arbitrary grid sizes.

Two methods of numerical integration are considered: (i) The Runge-Kutta method, and (ii) the Beta method. It is observed that while both methods give same order of accuracy the Beta method takes only half as much computer time as Runge-Kutta method. As regards accuracy, it is observed that for square plates a 16 x 16 grid produces reasonably accurate results (error for maximum deflection and bending moment is of the order of 0.1% and 3%, respectively).

The method is applied to study briefly several physical problems. The effect of foundation damping on the response is studied. The procedure of obtaining solutions of static problems by use of the dynamic analysis is considered. An effective method is to introduce into the system an amount of damping equal to the critical damping for the first mode and use a rectangular pulse type loading.

Some numerical results are also obtained to study the influence of boundary condition and the foundation stiffness. It is observed that stiffnesses of both have similar influence in reducing the response values.

The case of a free plate subjected to a concentrated load at the corner is studied. The distribution of principal bending moment is obtained. It is found that the maximum principal bending moment occurs in the same general area as in the case of static loading. The effect of foundation damping, and the rise rate of the loading function is also considered. It is observed that corner loading produces the most severe effects.

DYNAMIC RESPONSE OF PLATES ON ELASTIC FOUNDATION

By

Piyush C. Sharma

A THESIS

Submitted to
Michigan State University
in partial fulfillment of the requirements
for the degree of

DOCTOR OF PHILOSOPHY

Department of Civil Engineering

1964

ACKNOWLEDGEMENTS

The author wishes to express his gratitude to his major professor, Dr. Robert K. Wen for his valuable guidance during all phases of this study. The author also wishes to thank Dr. Charles E. Cutts for his continued encouragement throughout the author's graduate studies. Thanks are due to Dr. George E. Mase and Dr. J. S. Frame for their guidance and Dr. Norman L. Hills for his accepting to be on the final examination committee in place of Dr. Frame.

Acknowledgement is made to the Agency for International Development of the United States of America for their support which made this work possible. Thanks are also due to the staff of the Computer Laboratory of Michigan State University for their help and cooperation.

TABLE OF CONTENTS

Chapter			Page
ACKNOWLEDGEMENTS			ii
LIST OF TABLES			v
LIST OF FIGURES			vi
I.	INTRODUCTION		1
	1.1	Object and Scope	1
	1.2	Review of Literature	5
	1.3	Notations	12
II.	METHOD OF ANALYSIS		16
	2.1	General	16
	2.2	Non-dimensional Form	18
	2.3	Discretization of Space Domain	18
	2.4	Numerical Integration of the Set of Differential Equations of the System	20
	2.5	Evaluation of Bending Moments	23
	2.6	Use of Computer	25
III.	RESULTS AND DISCUSSION		26
	3.1	Comparison of Runge-Kutta and Beta Methods	26
	3.2	Comparison of Numerical and Exact Solutions	29
	3.3	Treatment of Concentrated Load	32
	3.4	Consideration of Foundation Damping	35
	3.5	Effects of Boundary Conditions and Foundation Stiffness	37
	3.6	Study of Free Plates	39
IV.	SUMMARY AND CONCLUSIONS		43
V.	BIBLIOGRAPHY		47

		Page
APPENDIX A	USE OF COMPUTER AND PROGRAMMING	52
A.1	Generation of Equations of Motion	52
A.2	Numerical Integration of Equations	55
A.3	Time Requirements of Computer	55
A.4	List of Fortran Variables	56
A.5	Fortran Computer Programs	60
APPENDIX B	EXACT SOLUTIONS	74

LIST OF TABLES

Table		Page
1.	Comparison of Results Obtained by Runge-Kutta and Beta Methods (τ = .0625 and τ = .025)	79
2.	Comparison of Results Obtained by Runge-Kutta and Beta Methods (for Maximum Values of Responses)	80
3.	Comparison of Numerical and Exact Values of Maximum Responses for Center Point	81
4.	Comparison of Numerical and Exact Values of Maximum Responses for Quarter Point	82
5.	Comparison of Numerical and Exact Values of Maximum Responses for Center Point for Shrinking Area Loading	83
6.	Comparison of Numerical and Exact Values of Maximum Responses for Quarter Point for Shrinking Area Loading	83
7.	Comparison of Numerical and Exact Values of Maximum Response for Center Point for Partial Loading	84
8.	Comparison of Numerical and Exact Values of Maximum Responses for Quarter Point for Partial Loading	84
9.	Maximum Deflection, Moment and Their Locations of Occurrence for a Free Plate Due to Impulse Applied at Corner	85
10.	Comparison of Maximum Values of Responses with Damping and Without Damping	86
11.	Maximum Response Values for Different Pulse Shapes Applied at Corner Point of Free Plate	87
12	Maximum Response Values for Loading Applied at Different Points Along Edge of Free Plate	88

LIST OF FIGURES

Figure		Page
1.	Plate Notation	89
2.	Pictorial Representation of the Propagation Problem	89
3.	Physical Model of Discrete System	90
4.	Biharmonic Operator	90
5.	Response Histories for Center Point Deflection for Various Grid Sizes	91
6.	Response Histories for Center Point Moment for Various Grid Sizes	92
7.	Comparison of Numerical and Exact Solutions for Center Point Moment	93
8.	Comparison of Numerical and Exact Solutions for Quarter Point Moment	94
9.	Comparison of Numerical and Exact Solutions for Center Point Deflection for Shrinking Area Loading	95
10.	Response Histories for Quarter Point Moment for Various Grid Sizes for Shrinking Area Loading	96
11.	Comparison of Numerical and Exact Solutions for Quarter Point Moment for Shrinking Area Loading	97
12.	Comparison of Numerical and Exact Solutions for Quarter Point Deflection for Shrinking Area Loading	98
13.	Comparison of Numerical and Exact Solutions for Center Point Deflection for Partial Loading	99
14.	Comparison of Numerical and Exact Solutions for Center Point Moment for Partial Loading	100

Figure		Page

15. Comparison of Numerical and Exact Solutions for Quarter Point Deflection for Partial Loading 101

16. Comparison of Numerical and Exact Solutions for Quarter Point Moment for Partial Loading 102

17. Deflection Response Histories for Various Foundation Damping Values 103

18. Moment Response Histories for Various Foundation Damping Values 104

19. Deflection Response Histories for Various Types of Boundary Conditions and Foundation Stiffness Values 105

20. Moment Response Histories for Various Types of Boundary Conditions and Foundation Stiffness Values 106

21. Deflection Response Histories for Various Types of Boundary Conditions 107

22. Center Point Deflection Response Histories for Various Grid Sizes for Free Plate 108

23. Coordinate System for Points on Free Plate for 16 x 16 Grid 109

24. Loading Pulse with Varying Rise Rate (by Varying t_o) 109

25. Response History for Deflection at Point (1, 1) Due to Load Applied at Point (1, 1) 110

26. Response History for Principal Moment M'_1 at Point (2, 2) Due to Load Applied at Point (1, 1)..... 111

27. Response History for Principal Moment M'_2 at Point (3, 3) Due to Load Applied at Point (1, 1) 112

28. Contour of Deflection 113

Figure		Page
29.	Contour of Principal Bending Moment M'_2	114
A1.	Grid Lines for Simply Supported Plate	115
A2.	Location of Points on Free Plate as Used in Programming	115
A3.	Six Different Types of "BHO" Patterns	116

CHAPTER I

INTRODUCTION

1.1 Object and Scope

The dynamic theory of plates finds many applications in modern technology such as the analysis and design of buildings, aircrafts, ship hulls, and pavements. Except for a few exceedingly simple cases (e.g., rectangular plates with opposite edges simply supported) an exact mathematical analysis of such problems is practically impossible. This is even more so for the case of plates on elastic foundation, which is important, for example, in rigid pavement design.

Many investigations have been made in the past to calculate the normal modes and natural frequencies of plates using the finite difference approach or the Raleigh-Ritz method. Presumably, one could then use these modes and frequencies to calculate the dynamic response to external loads by the method of modal analysis, although seemingly few applications of this type have been recorded in the literature.

To obtain an approximate solution for the dynamic response of structures, it is not necessary to follow the normal modes approach. By first reducing the continuous structure to a discrete system, one can directly integrate the equations of motion governing the displacements of the discrete points of the structure. This method has been applied extensively in one-dimensional structures such as beams and plane frames. A similar approach is used here for the treatment of plates.

In this thesis for the dynamic analysis of plates a method is presented that by-passes the use of normal modes concept. It is based on: (a) first replacing the continuous plate by a discrete set of lumped masses and (b) integrating the equation of motion of each mass. The replacement in (a) is effected by the usual finite difference expansion of the derivatives in the space domain. Although the integration in (b) is carried out numerically, from the theoretical viewpoint at least, the application of numerical procedure is not essential, as it is in the case (a).

With regard to the relative merits of the approximate methods of calculating normal modes using the Rayleigh-Ritz type and the finite difference methods, it may be pointed out that the former requires the use of certain sets of approximating functions which may be difficult to obtain because of boundary conditions. The use of the method is usually limited to a few degrees of freedom. Furthermore, it requires the evaluation of a number of definite integrals which could not be efficiently carried out by the computer, and have to be done by the analyst himself.

In the case of the finite difference solution, the procedure is straight forward in concept. There is also the advantage of the ease in handling the discontinuities in the structure-load system and the boundary conditions. A major disadvantage of this approach is that it requires a large amount of numerical work. This, however, has been overcome to a large extent by modern computer technology. The accuracy of finite difference method depends upon the size of the finite difference grid. By making use of the digital computer effectively, not only the solution of the equations are obtained by the computer, all the equations can be generated inside the computer also. Hence, increasing the grid divisions does not increase the work of the engineer.

Finite difference methods have been used for a variety of problems and satisfactory solutions have been obtained, particularly for the case of the static analysis of plates. However, very little work has been reported in relation to the forced vibrations of plates (see the next article on "Review of Literature"). Thus it would seem worthwhile to investigate the practicability of such an application.

The purpose of this thesis is twofold:

(1) To investigate the practicability of finite difference methods in solving dynamic response problems of plates, particular attention being given to the accuracy of the method and the efficient adaptation to the computer.

(2) To demonstrate the workability of this approach in handling problems whose exact solutions are not known, and perhaps impossible to obtain.

The method of analysis is developed in detail in Chapter II. As noted before, the continuous displacement function of the plate is represented by the displacements of a discrete set of points. The resulting equations of motion are integrated numerically. Two methods of numerical integration are considered: (a) the Runge-Kutta method (30), and (b) the Newmark Beta method (42). A comparison of the accuracy and efficiency of these methods is given in Chapter III.

In the same chapter the question of the accuracy of the finite difference method is studied by comparing numerical solutions with the mathematically exact solutions. The comparisons are made on the basis of bending moments as well as displacements. The handling of concentrated load is discussed. The effect of such parameters as foundation damping, foundation stiffness and the boundary conditions are briefly considered. It is shown also that the method can be applied efficiently to obtain the static response of plates, thus avoiding the re-formulation of the problem for a static analysis, if such is desired.

Most of the preceding solutions relate to problems for which exact solutions are not difficult to obtain. For the same reason the accuracy of the numerical methods may be discussed.

To demonstrate the applicability of the method to problems for which exact solutions seem impossible to obtain, the problem of a plate free on all edges resting on an elastic foundation is treated. It may be pointed out that this problem has important applications in the analysis and design of highway and airport pavements.

The final chapter summarizes the findings of the study and points to a few possible fruitful directions for the extension of the present work. Certain pertinent details regarding computer usage in this thesis are given in Appendix A. The mathematically exact solutions used for purposes of estimating the accuracy of the results obtained by the numerical method are presented in Appendix B.

1.2 Review of Literature

The general subject dealt with in this thesis is related to several areas. For convenience, the review of past work has been given in three groups: (a) free vibrations, natural frequencies and mode shapes, (b) forced vibrations of plates, and (c) plates on elastic foundation connected with pavement design.

1.2.1 Free Vibrations: Investigations primarily concerned with the calculation of natural frequency and normal modes for the plate are too numerous to be covered here. Therefore, only those deemed most important have been listed in the bibliography.

Sezewa (34)[1], (1931)[2] solved the problem of vibration of rectangular plates with all 4 edges clamped by making the solution

---

[1]Numbers in the first parentheses refer to reference listed in the Bibliography.

[2]Numbers in the second parentheses refer to the year of publication of the work.

satisfy the governing differential equation allowing small residual slope at some portion of the boundary. Young (46), (1950) used the Ritz method to compute the characteristic values and shapes of vibrating plates with different boundary conditions. He made use of functions which define the normal modes of vibration of uniform beams. Mindlin (23, 24), (1950, 1956) studied the effect of rotary inertia and shear in plate vibrations in a manner similar to that used by Timoshenko for the one dimensional theory of beams. Also the coupling of modes was studied for the case of one pair of parallel edges free and other pair simply supported.

Stanisic (36), (1955) considered the case of damping in the plate material and calculated the natural frequencies of plate fixed along each edge with arbitrary aspect ratio. Similarly Raskovic (31), (1959) dealt with the problem of free vibrations of elastic homogeneous plates considering the influence of internal viscous damping. He also used functions defining normal vibration mode of uniform beams and obtained the solution for a square plate with all the four edges clamped.

Feldman (4), (1959) and Bradley (1), (1961) used the finite difference method to solve the eigenvalue problem of plate vibrations. Leissa (19), (1962) used the method of point-matching to obtain the eigenvalues and eigenfunctions of vibrating plates. By setting up a digital computer program, frequencies and mode shapes were obtained for a clamped square plate. Leckie (18), (1963) applied the method of transfer matrices to plate vibrations, to obtain the natural frequencies and normal modes.

Kennedy (16), (1964) obtained the linear and non-linear vibration characteristics of rectangular plates utilizing finite difference technique on an operational analog computer. The effects of aspect ratio, large amplitudes of vibration, and grid sizes on the accuracy of natural frequency of vibration were studied.

1.2.2 Forced Vibrations: For the forced vibrations of plates, only solutions to very special cases have been obtained because of the difficulties involved in finding a general solution to such problems.

Takabayasi (37), (1936) used the method of integration in plane of complex variable to solve the problem of elastic vibration of circular clamped plate acted on at its clamped edge by an external periodic force. Yeh et.al. (44) (1955) studied the forced vibration of a clamped rectangular plate in fluid media. They used the characteristic shape functions and Lagrange equations of motion of plate to set up the equation of motion in generalized coordinates, and obtained some numerical results. Forsyth et.al. (5), (1960) studied theoretically and experimentally the transient vibration of rectangular plates. They showed that for the case of a cantilever plate subjected to an impulse load, reasonable agreement was obtained between the theoretical and experimental results.

Mase (22), (1960) solved the problem of the bending of viscous elastic plates of Maxwell and Kelvin types. He used Laplace transform to obtain the quasi-static deflection of laterally loaded plates and the dynamic response of simply supported plate under no load. The solutions for the free vibrations of Maxwell and Kelvin type plates are also obtained. Solecki (35), (1960) studied the free and forced oscillations of a triangular lamina in the form of an equilateral triangular. The bending function is expressed in the form of an infinite Fourier's series.

Kalman (15), (1962) investigated the problem of transverse vibrations of a stiffened rectangular elasto-plastic plate. The finite difference approach used in this thesis is similar to the one used by him for the dynamic response of elasto-plastic plates. He assumed that the plastic flow is proportional to the maximum moment only, and there is no interaction of moments. The report is very brief and the question of accuracy has not been considered.

Sandi (33), (1962) studied the case of dynamically loaded plates composed of hard elastic material, the rheological behavior of which is linear, resting on a half space composed of the same material. The author gives a mathematical description of the phenomenon based on the general method of expressing the dynamical displacements of bodies by means of a multiple integral equation of Volterra type with regard to time, and of Fredholm type with regard to the coordinates of the contact surface which is supposed to be prescribed. The author further discusses the phenomenon of dynamic contact.

Kurlandzki (17), (1962) considered the reduction of initial boundary value problems of elasticity to Fredholm integral equations of second kind. He reduced the dynamic problem of an elastic plate to Fredholm's integral equations of the second kind by a finite sine and cosine transformation in relation to the time variable. These equations in which integrals with respect to two variables and a relatively complicated structure appear may be solved by successive iterations. No example of application is given.

Reismann (32), (1963) studied the dynamic response of elastic plate strip to moving line load by formulating it as a boundary value problem within the framework of classical small deflection theory of thin plates and obtained solutions in terms of trigonometric series. It is shown that the shape of resulting deflection profile of plate is strongly dependent upon speed propagation of the load and magnitude of damping coefficient. In the absence of damping, denumerable infinity of critical speeds exist at which deflections become unbounded. However, with damping, deflections remain bounded.

1.2.3 Plate on Elastic Foundation: Most of the work in the area of pavements has been limited to static analysis except a few recent works like those of Holl (11), (1950), Livesley (21), (1953) and Sandi (33), (1963) which have dealt with certain highly idealized cases such as infinitely long plate or simply supported plates.

There is a great deal of literature available on the bending of plates over elastic foundation. Westergaard (43), (1925) analyzed theoretically a rigid pavement, and presented some semi-empirical formulae for evaluating the maximum bending moments. He showed that the maximum moment occurs when the load is applied at a corner. Murphy (25), (1937) calculated the stresses and deflections in loaded rectangular plates on elastic foundation by solving the classical plate equation. Similar results were presented by Holl (11), (1938).

Holl (12), (1950) studied the case of simply supported plate under dynamic loading on elastic foundation. He considered various kinds of subgrade reactions, using influence functions and transform solutions. The solutions are limited to simply supported plate or circular plates with symmetry. Similarly Livesley (21), (1953) commented on the mathematical theory of loaded elastic plates resting on elastic foundations. He studied the problem of a uniformly travelling load on an infinite plate and showed that there exists a certain critical velocity beyond which stresses and deflections become infinite.

Pickett (28, 29), (1951) studied the stresses in the corner region of concrete pavement slabs under large corner loads and calculated the influence charts for bending moment in rigid pavements under such loading.

Nagdhi (26), (1953) solved the problem of axially symmetric plates on elastic foundation taking into account the effect of transverse normal stress and shear deformation. Schleicher's functions were used to obtain the solution. Frederic (6), (1957) solved the same problem for the case of rectangular plates considering various types of fixity of edges involving 3 boundary conditions. He obtained the solution in both Levy and Navier forms. Chen (2), (1960) used both Ritz and Galerkin methods of variation to solve the problem of isotropic as well as orthotropic plates with free edges on elastic foundation.

Leonards et al. (20), (1961) dealt with the analysis of concrete slab on ground. In this paper a number of practical points such as the effect of subbase on stresses, often neglected in theoretical studies, have been considered. Harr (9), (1962) studied the effect of vehicle speed on pavement deflections. Here he considered the pavement slab as a single degree of freedom system. Jones (14), (1962) carried out detailed theoretical investigation using a digital computer to study the static effect of concentrated loads on pavement deflections.

Since this thesis is concerned with establishing the suitability of a numerical method for the dynamic response problem and its use to solve the pavement problem, no attempt has been made in this brief review to give a comprehensive survey of the published literature. The few references mentioned here are intended only to provide background information on available solutions for the dynamic response of plates on elastic foundation and problems associated closely with it.

1.3 Notations

The notation listed in the following has been adopted in this thesis. Each symbol is defined when first introduced and is collected here in alphabetical order for convenience of reference. "Fortran" notation is listed separately in Appendix A.

a	=	length of the longer side of the plate;
b	=	length of the shorter side of the plate;
BHO	=	∇^4, the biharmonic operator in finite differences form;
c	=	foundation viscous damping constant;
$c_{cr}(ij)$	=	critical damping for the mode (i,j), used in Appendix B;
D	=	$Eh^3/12(1-\nu^2)$, flexural rigidity of the plate;
e_i	=	error in deflections at point (i);
E	=	modulus of elasticity of plate material;
F_{ij}	=	$\theta \cdot P_{ij}$, non-dimensional forcing function at point (i,j);
F	=	magnitude of concentrated force used in Appendix B;
$F(t)$	=	time dependent part of the forcing function $P(x, y, t)$ used in Appendix B;
$G(x, y)$	=	space function part of the forcing function $P(x, y, t)$ used in Appendix B;
g_{ij}	=	Fourier coefficient for $G(x, y)$ used in Appendix B;

h	=	plate thickness;
i, j	=	variable subscripts to denote points in space;
k	=	foundation stiffness constant;
m	=	mass per unit area of plate;
M_x, M_y, M_{xy}	=	bending moments as used in Appendix B;
M	=	$M_x = M_y$, bending moment used in generic sense;
M_1	=	algebraically larger principal bending moment;
M_2	=	algebraically smaller principal bending moment;
M'_1	=	$M_1\, a/D$, dimensionless M_1;
M'_2	=	$M_2\, a/D$, dimensionless M_2;
M_i	=	moment at a point (i) derived from derived deflections w_i;
$\bar{M}_i$	=	moment at a point (i) derived from the deflections $\bar{w}_i$;
$\bar{\bar{M}}_i$	=	true moment at a point (i);
n	=	a/λ, number of grid divisions;
P	=	magnitude of forcing function used in Appendix B;
P_{ij}	=	forcing function at point (i, j);
$P(x, y, t)$	=	forcing function;
P_{ij}	=	natural circular frequency of the (i, j)th mode of the plate used in Appendix B;
q_{ij}	=	$\sqrt{p_{ij}^2 - r^2}$, damped natural circular frequency used in Appendix B;

$q(x, y)$ = static loading function acting over the plate;

r = $\frac{c}{2m}$, a viscous damping parameter;

$r_{cr}(ij)$ = r, corresponding to the critical damping of the (i, j)th mode;

S_{ij} = $\sin \frac{i\pi x}{a} \sin \frac{j\pi y}{b}$, used in Appendix B;

T_1 = $\frac{1}{\pi} \left(\frac{ma^4}{D}\right)^{1/2} / [1 + ka^4/4D\pi^4]^{1/2}$

first fundamental period of simply supported plate on elastic foundation;

T_o = $\left(\frac{ma^4}{D}\right)^{1/2}$; factor to divide t, to make it dimensionless;

T_s = shortest period of the plate system;

t = time;

t_o = time parameter used in Fig. 24,

t_1 = time parameter used in Fig. 24;

t_1 = duration of loading pulse used in Appendix B;

u = $\frac{w}{h}$, dimensionless deflection;

u = width along x-coordinate direction of the partially loaded area used in Appendix B;

u_{ij} = dimensionless deflection at the point (i, j);

v = width along the y-coordinate direction of the partially loaded area used in Appendix B;

v_{ij}	=	$\dot{u}_{ij}$, dimensionless velocity at the point (i, j);
w	=	deflection;
$\bar{w}_i$	=	true deflection at point (i);
w_i	=	derived deflection at point (i);
x	=	space coordinate;
y	=	space coordinate;
α	=	$\frac{ka^4}{D}$, dimensionless foundation stiffness constant;
β	=	$\frac{ca^4}{DT_o}$, dimensionless foundation damping constant;
Δ	=	prefix denoting "increment";
∇^4	=	biharmonic operator;
λ	=	grid size
τ	=	t/T_o, dimensionless time;
θ	=	a^4/Dh; factor to be multiplied to P_{ij} to make it dimensionless.

CHAPTER II

METHOD OF ANALYSIS

2.1 General

The governing differential equation for the small deflections of an elastic thin plate subjected to a lateral loading $q(x,y)$ is given[1] by:

$$\nabla^4 w = \frac{\partial^4 w}{\partial x^4} + 2\frac{\partial^4 w}{\partial x^2 \partial y^2} + \frac{\partial^4 w}{\partial y^4} = \frac{q(x,y)}{D} \tag{1}$$

in which w is the deflection, x and y are space coordinates and D is the flexural rigidity of the plate.

For the case of dynamic loading and Winkler type elastic foundation with viscous damping, the equation of motion is obtained by replacing $q(x,y)$ by $-(\frac{m\partial^2 w}{\partial t^2} + c\frac{\partial w}{\partial t} + kw) + P(x,y,t)$ where $\frac{m\partial^2 w}{\partial t^2}$ is the inertia force, and $c\frac{\partial w}{\partial t} + kw$ is the reaction of the foundation including the effect of viscous damping, and $P(x,y,t)$ is the forcing function. Thus, Eq. 1 becomes:

$$\nabla^4 w + \frac{k}{D}w + \frac{c}{D}\frac{\partial w}{\partial t} + \frac{m\partial^2 w}{D\partial t^2} = \frac{P(x,y,t)}{D} \tag{2}$$

This equation together with the appropriate boundary and initial conditions governs the dynamic response of the plate system to the dynamic loading $P(x,y,t)$.

---

[1] Timoshenko (39), pp. 79-82.

Mathematically speaking, this partial differential equation is of the parabolic type, and is referred to as a propagation problem in two space dimensions. The solution "marches" in the time domain starting with the initial conditions, and confined in space by the boundary conditions. In other words, for the case of rectangular plates, considered in this thesis, the solution has to march inside a box (as depicted in Fig. 2), whose base is made up of the initial conditions, and all the four sides are made up of the boundary conditions, the top being open.

It is difficult to find exact closed form solutions to the partial differential equation, Equation 2, except for a few simple cases where the two opposite edges of the plate are simply supported. Therefore, one has to resort to some kind of approximate or numerical procedure. The procedure used here is based on the well known finite difference method. There are two distinct steps in the numerical solution of the problem:

(1) finite difference is applied to the space domain, replacing the continuous plate by a set of discrete points; and the partial differential equation by a set of simultaneous ordinary second order linear differential equations;

(2) the set of ordinary differential equations is solved by numerical integration.

2.2 Non-dimensional Form

Since it is convenient to work with non-dimensional quantities, Equation 2 is transformed into non-dimensional form by dividing it throughout by the quantity $\frac{a^4}{Dh}$, where a is the length of the longer side of the rectangular plate and h is the thickness of the plate. Then Equation 2 may be written in the following form:

$$a^4 \nabla^4 u + \alpha u + \beta \frac{\partial u}{\partial \tau} + \frac{\partial^2 u}{\partial \tau^2} = F(x, y, \tau) \tag{3}$$

in which

u	=	w/h, dimensionless deflection	(3a)
τ	=	t/T_o, dimensionless time	(3b)
T_o	=	$(ma^4/D)^{1/2}$, a parameter	(3c)
α	=	ka^4/D, dimensionless foundation stiffness constant	(3d)
β	=	ca^4/DT_o, dimensionless foundation damping constant	(3e)
$F(x, y\tau)$	=	$\theta \cdot P(x, y, \tau)$, dimensionless forcing function	(3f)
θ	=	a^4/Dh; a parameter	(3g)

2.3 Discretization of Space Domain

The reduction of the partial differential equation (together with the boundary conditions) for the continuous system to the set of ordinary differential equations for the discrete replacement system may be accomplished "physically" or "mathematically." In the "physical" approach, a discrete model is invested with lumped physical characteristics of the continuous system. The governing equations are then obtained from the physical laws applied directly to the lumped parameter model.

In the "mathematical" approach, the continuous formulation is reduced to a discrete formulation by simply replacing the derivatives in the differential equation with finite difference expressions. The use of the "physical" approach has the advantage that the model provides something which is easily visualized, and facilitates the treatment of difficult boundary conditions. The "mathematical" approach has the advantage that it is straight-forward and does not require the judgment needed in devising an appropriate physical model.

In this thesis essentially the second approach is used. The space derivatives in Equation 3 are replaced by the second order finite difference patterns as shown in Fig. 4. Thus, for a given point (i, j) Equation 3 takes the following form:

$$n^4 \, \mathrm{BHO}\,(u_{ij}) + \alpha\, u_{ij} + \beta\, \dot{u}_{ij} + \ddot{u}_{ij} = F_{ij} \qquad (4)$$

where "BHO" denotes the biharmonic operator in finite difference form, F_{ij} denotes the value of F evaluated at point (i, j), and each dot superscript represents a differentiation with respect to τ.

Applying Equation 4 to every point in the domain and with the boundary conditions properly taken into account, one obtains a set of ordinary differential equations. Of course, the forms of "BHO" are different from Fig. 3 for points on and adjacent to the boundary in the manner similar to the case of the use of finite difference in the static analysis of plates.

In passing it might be mentioned that there is a physical model which would lead to the same equations as those given by the finite difference formulation of the static plate problem as given in (8).

2.4 Numerical Integration of the Set of Differential Equations of the System

The set of differential equations of the type of Equation 4 may be considered as representing a continuous propagation problem involving a set of mass points. However, if the time domain is also discretized simultaneously with space domain, then one obtains, for each time instant, a set of simultaneous algebraic equations. Detailed discussions of these approaches have been given by Crandall (3).

The set of differential equations can also be conveniently solved by numerical integration using a computer. There are a large number of numerical integration procedures available in the literature [for example Crandall (3), Ralston and Wilf (30)]. Among the most well known and widely used is the Runge-Kutta method. This method is generally applicable to differential equations of any order. On the other hand, there is a class of procedures developed primarily for problems of structural dynamics. In this group the "Beta Method" is representative. In the following two sub-sections these two methods are briefly commented upon. In Chapter III, a comparison of these two methods will be made from the standpoint of their applications to the method of analysis used in this thesis.

2.4.1 Runge-Kutta-Gill Method: This method comes under the general category of Runge-Kutta methods, and is a modified version of Runge-Kutta fourth order method. The derivation will not be given here, as it can be found in many textbooks on numerical analysis, e.g., (30) and (7).

The Runge-Kutta numerical integration method is a non-iterative, step by step, and self starting procedure. Accuracy is derived by using several estimates of the dependent variable for each increment of the independent variable. Usually the method is set up for first order equations. However, it can be easily adapted to higher order equations. Second order differential equations are handled by first transforming them into a set of first order differential equations. For example each of the equations (4) is transformed into two first order differential equations. Thus,

$$\dot{u}_{ij} = v_{ij} \tag{5a}$$

$$\dot{v}_{ij} = F_{ij} - n^4 \, BHO \, u_{ij} - \alpha \, u_{ij} - \beta \, v_{ij} \tag{5b}$$

The truncation error for one integration step is of order $(\Delta\tau)^5$ for this fourth order method, where $(\Delta\tau)$ is the increment of the independent variable. Theoretically, there are no limits on the increment size in regard to convergence and stability. The size of the time increment of integration is decided so that it is not too small as to require excessive computation labor or result in large round off errors; neither it should be so large as to give rise to large truncation errors.

2.4.2 Newmark Beta Method: This method of integration is a step by step, self starting and generally iterative method. It handles a set of second order differential equations. A rather comprehensive study has been made on this method and has been reported in (27, 42).

The scheme for one step of integration is as follows:

(1) Calculate the initial acceleration from the governing differential equation. For example, using the given initial conditions,

$$(\ddot{u}_{ij})_{\tau=\tau_o} = [F_{ij} - n^4 \, BHO \, u_{ij} - \alpha \, u_{ij} - \beta \, u_{ij}]_{\tau=\tau_o}$$

(2) Assume an acceleration, $(\ddot{u}_{ij})_{\tau_1=\tau_o+\Delta\tau}$

(3) Using the values from (1) and (2) calculate the values $(\dot{u}_{ij})_{\tau_o+\Delta\tau}$, $(u_{ij})_{\tau_o+\Delta\tau}$ from the following formulae which essentially represent the Beta Method:

$$\dot{u}_{ij}(\tau_o+\Delta\tau) = \dot{u}(\tau_o) + \frac{\Delta\tau}{2}[\ddot{u}_{ij}(\tau_o) + \ddot{u}_{ij}(\tau_o+\Delta\tau)]$$

$$u_{ij}(\tau_o+\Delta\tau) = u_{ij}(\tau_o) + \Delta\tau \, \dot{u}_{ij}(\tau_o) + (\Delta\tau)^2 \left(\frac{1}{2} - \text{Beta}\right) \ddot{u}_{ij}(\tau_o) + (\Delta\tau)^2 (\text{Beta}) \, \ddot{u}_{ij}(\tau_o+\Delta\tau)$$

in which "Beta" represents a fraction ranging in value from zero to one-fourth.

(4) Substitute these values of $\dot{u}_{ij}(\tau_o+\Delta\tau)$ and $u_{ij}(\tau_o+\Delta\tau)$ calculated from step (3) into the differential equation given in step (1) and obtain $\ddot{u}_{ij}(\tau_o+\Delta\tau)$.

(5) Compare $\ddot{u}_{ij}(\tau_o + \Delta\tau)$ from step (4) with the assumed one, i.e., $\ddot{u}_{ij}(\tau_o + \Delta\tau)$ of step (2). If they agree within a specified tolerance for all the variables then one step of integration is complete. If for one or more variables, $\ddot{u}_{ij}(\tau_o + \Delta\tau)$ does not converge, the whole process is repeated starting from step (1) but with the new assumed acceleration equal to that found in step (4).

It may further be pointed out that the size of time increment of integration can not be chosen arbitrarily. It has to be less than about one-third of the shortest period of the system. The method may become unstable for larger time increments.

2.5 Evaluation of Bending Moments

After the deflections at the discrete points are obtained numerically, the bending moments are calculated from these deflections using the usual second order finite difference expression to represent the curvature. Although this approach has been generally used in the past, for problems of statics, it seems that the accuracy of such a procedure has not been studied. Since bending moments are significant quantities from the engineering standpoint, it seems desirable to devote some space to consider this question.

Let w_i denote the deflection at a point (i) obtained numerically and $\bar{w}_i$ be the true deflection at the same point such that $\bar{w}_i - w_i = e_i$, is the error in the deflection at the point (i). Corresponding to the finite difference pattern used herein (Fig. 3), this error is of order λ^2, thus $e_i = O(\lambda^2)$. Let M_i and $\bar{M}_i$ represent the bending moments obtained from the deflections w_i and $\bar{w}_i$, respectively, by using the second order finite difference expressions, and $\bar{\bar{M}}_i$ be the true value of the moment. For simplicity, let D = 1 and $\nu = 0$; thus,

$$M_i = \frac{w_{i=1} - 2w_i + w_{i+1}}{\lambda^2} \tag{6a}$$

$$\bar{M}_i = \frac{\bar{w}_{i-1} - 2\bar{w}_i + \bar{w}_{i+1}}{\lambda^2} \tag{6b}$$

also

$$\bar{\bar{M}}_i = \bar{M}_i + O(\lambda^2) \tag{6c}$$

Now substituting for w_i in terms of $\bar{w}_i$ in Equation 6(a) one obtains;

$$M_i = \frac{\bar{w}_{i-1} - 2\bar{w}_i + \bar{w}_{i+1}}{\lambda^2} + \frac{e_{i-1} - 2e_i + e_{i+1}}{\lambda^2}$$

$$= \bar{M}_i + \frac{O(\lambda^2)}{\lambda^2}$$

$$= \bar{M}_i + O(\lambda^0) \tag{6d}$$

The error in moment is thus,

$$\bar{\bar{M}}_i - M_i = O(\lambda^2) - O(\lambda^0) \tag{6e}$$

It is seen that the second term of error on the right hand of Equation 6(e) cannot be made smaller by using smaller grid sizes; i.e., it will stay constant regardless of how fine a grid is used. An apparent good agreement between the values of the bending moment obtained by the numerical procedure and the exact solution would indicate that this error term is probably small in magnitude. Indeed, a preliminary study for the simple case of a beam indicates that if the loading varies linearly along the span length, the corresponding constant error term would be zero, except for errors introduced by the boundary considerations.

2.6 Use of Computer

In this study several computer programs have been prepared. They were written in a general fashion in order to handle rectangular plates of different aspect ratios, different boundary conditions, and different grid sizes. Some of the relevant details related to the programming and a representative version of the program are given in Appendix A.

CHAPTER III

RESULTS AND DISCUSSION

3.1 Comparison of Runge-Kutta and Beta Methods

As mentioned in the preceding chapter, the Runge-Kutta and Beta methods of numerical integration are being considered for use in the numerical method of dynamic plate analysis being investigated herein. While the Runge-Kutta method may seem to be more accurate, the Beta methods appear to be simpler to use. Hence, it seems a matter of practical interest to compare the relative merits of these methods from the standpoint of adaptation to the method of analysis used in this thesis.

The comparison will be made based on the study of a specific problem: a simply supported square plate resting over an elastic foundation (α = 414.7, β = 0) is loaded by a triangular pulse of peak pressure F (x, y, 0) = 36.6 acting over an 1/8 x 1/8 area of the plate at the center. The duration of the pulse is equal to .675 times the first fundamental period of the plate (T_1/T_o = .222). This problem physically corresponds to a simply supported concrete slab 12' x 12' x 1' (E = 2 x 10^6 psi), resting over a firm soil (k = 614.4 lbs/in^3, c = 0) and loaded at the center by an impulsive load of 640 psi peak value.

The problem, the boundary conditions in particular, is chosen because its exact solution can be obtained for purposes of comparison with that obtained by the numerical method. The comparison will be made on the basis of: (i) accuracy of the results; (ii) stability of integration; and (iii) computer time needed.

Before proceeding further, an estimate of the time increment in integration will be made. This increment will be expressed in terms of T_s, the smallest period of vibration of the plate which is approximately equal to the fundamental period of a plate one grid square in size. Hence, from Appendix B:

$$T_s = \frac{1}{\pi}\left(\frac{m\lambda^4}{D}\right)^{1/2} \Big/ \sqrt{1 + k\lambda^4/4\pi^4 D}$$

Assuming the physical parameters of the problem are such that the denominator is approximately equal to unity, $T_s \cong \frac{1}{\pi}\frac{m\lambda^4}{D}$ and in dimensionless form $T_s/T_o = 1/(\pi n^2)$. A fraction of this quantity is used as the increment in the numerical integration.

3.1.1 Accuracy: In Table 1 are listed the values of the center point deflections and bending moments (both in dimensionless form) for two time instants. The data presented include results as obtained by different methods of integration and different time increments used in the integrations. The numerical solutions were obtained by use of a 16 x 16 grid. In Table 2 are presented the maximum response values for the same problem.

The following observations may be made from an examination of the data: (i) The deflections obtained by these methods agree very well with each other, and with the exact answer. (ii) As expected, the agreement in bending moments is not as good as that in deflections. But it is still quite satisfactory. (iii) The size of time increment of integration is not of great importance whenever the method is stable.

Graphs of the entire deflection and moment histories of the problem as computed by the use of Runge-Kutta and Beta method (Beta = 0) also indicate very good agreement. In fact, they virtually overlap each other, and hence are not presented here.

3.1.2 Stability: When the time increment of integration is increased, less computer time is needed for the solution of a given problem. But beyond a certain limit of the increment, the solution obtained would deviate more and more from the true solution, and instability in the numerical integration is said to have occurred. Hence there is a limit as to the largest time increment that can be used in the integration. It may be seen from Tables 1 and 2 that the Runge-Kutta method has a slightly larger range of stability than the Beta methods.

3.1.3 Computer Time: For a given problem, generally speaking, the Runge-Kutta method takes about twice as much computer time as either the Beta methods considered. This difference should be regarded as of practical significance because of the cost of computer time. Between Beta = 1/6 and Beta = 0, the latter takes somewhat less time.

Since all three methods considered yield results having essentially the same order of accuracy, and since the Beta method needs only half of the computer time needed for the Runge-Kutta method, on the basis of the study of this particular problem, the Beta = 0 method is used to obtain the numerical results presented in the subsequent sections.

3.2 Comparison of Numerical and Exact Solutions

It has generally been observed, in using finite difference methods for static analysis, that the finer the grid, the better are the results. However, for the dynamic problem, this is true only to a certain extent. This is because the nature of errors in the numerical solution is quite complex. They may arise from: (i) discretization in space of the continuum; and (ii) numerical integration of the differential equations.

Since the stability of the numerical integration depends upon the size of the time increment of integration ($\Delta\tau$) in relation to the shortest period of any mode present in the system [see (42)], $\Delta\tau$ has to be inversely proportional to the square of the grid division (n). The number of differential equations of the system is proportional to the square of n. Thus the total number of numerical integrations or computer time, is proportional to the fourth power of n.

It is reasonable to assume that the round-off errors in the numerical solution increase with the computation time. Therefore, although a larger number of grid divisions will better approximate the continuous plate in the space domain, as a result of the still larger amount of numerical calculations required, the numerical solutions obtained may not necessarily be more accurate than those obtained using a smaller grid division.

The question arises naturally as to the value of n at which the advantage of a more closely approximated space domain is offset by the disadvantage of the accumulation of round-off error. In order to answer this question one would need a rigorous error analysis of this problem, which would seem quite impracticable, considering the general difficulties involved in error analysis in numerical solutions and the complexities of the problem under investigation. In view of these factors, it would seem desirable to study the problem empirically by considering the effect of grid sizes on the numerical solution of a specific problem.

The specific problem selected here is the same as described in section 3.1, except that the loading is applied uniformly over the entire plate with a peak pressure of 10 psi (thus making the total load applied over the entire plate the same as in problem of section 3.1).

In Fig. 5 are presented the deflection histories of the center point for the following grids: 4 x 4, 8 x 8, 12 x 12, 16 x 16 and 20 x 20.

It may be observed that all these curves are very close to one another. Indeed, curves corresponding to 16 x 16 and 20 x 20 grids coincide with the curve obtained by the exact solution (which is not shown here).

In Fig. 6 are shown the response histories for center point bending moments for various grid sizes. It may be observed that as the number of grid division increases the results get closer to one another. The effect of higher modes cannot be seen by using lower number of grid divisions; the response history for the 4 x 4 grid hardly shows any higher modes. In Fig. 7 is shown a comparison of the moment response history for the 16 x 16 grid and that corresponding to the exact solution. It is seen that the agreement is reasonably close.

Fig. 8 shows the comparison of the history of bending moment at $x = a/4$, $y = a/2$ (hereafter referred to as the "Quarter Point") for a 20 x 20 grid and the exact solution. Agreement between the two is seen to be as good as for the case of the center point.

In Table 3 are listed the maximum values of center point deflections and bending moments, the times of occurrence of these values and the associated errors for various grid sizes. It may be observed that for the 16 x 16 grid the error for the maximum deflection is 0.1%, and in maximum bending moment is 3%. The corresponding errors in the times of occurrence of these maximums are

0.7% and 1.9%, respectively. Similarly in Table 4 are listed the deflection and moment values for the quarter point. The error for the 16 x 16 grid in maximum deflection is 0.3%, and in maximum moment is 0.8%. The error in the times of occurrence of these maximums is 1% and 7.2%, respectively, for deflection and moment.

From Tables 3 and 4, it may further be observed that for deflections the error keeps on reducing with increasing number of grid divisions, while in case of moments it does not follow any set pattern. At the same time it is to be noted that errors for grid divisions of 4, 8, and 12 seem to reduce with increasing grid divisions, while beyond 16 grid divisions the error in moments seems to increase in the opposite direction, particularly for the quarter point. However, the errors in deflections and moments both seem to be within reasonable limits for the 16 x 16 grid. This grid therefore can be thought of as a "critical grid." Almost all the subsequent results have been obtained using this 16 x 16 grid.

3.3 Treatment of "Concentrated Load"

Because of its practical importance, the case of "concentrated load" is studied in this section. Two schemes were used to represent the concentrated load in the numerical approach. In the first approach, the loading area is kept equal to one grid square unit, and the load intensity is varied to make the total load on the plate constant. This will be referred to as the "shrinking area loading." In the second scheme the load is spread over a fixed area which is independent of the grid size. This will be referred to as the "partial loading."

The specific problem considered here for this study is the same as that described in section 3.1. In both cases of loading, the total peak load applied over the entire plate is a constant (144, 000 lbs). In the case of "shrinking area loading" a peak pressure of 10 (n^2) psi is used; hence, for an 8 x 8 grid, the peak pressure will be 640 psi. In the case of the "partial loading," the load is distributed over an 1/8 x 1/8 area of the plate with a peak pressure of 640 psi.

3.3.1 Shrinking Area Loading: The histories of the center point deflection as obtained by using the 16 x 16 grid and that from exact solution are presented in Fig. 9. The values of the maximum deflections and moments for various grid divisions are listed in Table 5. It may be observed from these data that the center point deflection as obtained by use of the 16 x 16 grid is quite close to the exact solution. It may be also observed that the bending moment under the load appears to be divergent. This is, of course, not surprising since the series representation of this moment as given by the exact solution is divergent.

In Fig. 10 are presented the response histories for the bending moment at the quarter point for different grid divisions. It may be seen that the moment response histories for different grid divisions differ from each other appreciably. This may be because of the nature of the problem, as it is known that the series for the exact solution converges very slowly. In Fig. 11 are shown the response histories for the quarter point bending moment as obtained by using the 16 x 16 grid and that from the exact solution. It is seen that the numerical solution agrees reasonably well with the exact solution. Similar comparisons of deflections are given in Fig. 12. The agreement is, as expected, excellent. In fact, the two curves practically coincide. In Table 6 are listed the values of the maximum responses (deflections and moments) at the quarter point for the various grid divisions. It is of interest to note that the values of the maximum bending moments for the different grid sizes are quite close, although the history curves differ appreciably.

The error in the maximum deflection for the center point (under the load) for the 16 x 16 grid solution is 5.5% and for the quarter point is 0.6%. The numerical solution for the maximum bending moment at the quarter point has an error of only 1.5%.

3.3.2 Partial Loading: In Fig. 13 is shown the comparison of the center point deflection histories for the 16 x 16 grid and that obtained by using the exact solution for this case of partial loading. The two results are seen to be quite close to each other. Similarly in Fig. 14 is shown a comparison of the response histories for the center point bending moment for the 16 x 16 grid and that obtained by using the exact solution. It may be observed that although the agreement is satisfactory, it is not as good as in the case of deflections. The maximum values of the responses for the center point are listed in Table 7 for the various grid sizes. The errors in the maximum center point deflection and bending moment for the 16 x 16 grid are 2.5% and 6.6%, respectively.

In Figs. 15 and 16 are presented a comparison of the quarter point response histories for deflection and bending moment, respectively. For moment, the agreement between the numerical solution and the exact solution is reasonably good, while for deflection the curves practically coincide. The maximum response values for the various grid divisions are listed in Table 8. The errors in the maximum response values for the 16 x 16 grid are 0.4% and 5.1%, respectively, for the quarter point deflection and bending moment.

Inasmuch as in actual engineering applications it is practically impossible to have a case of a real concentrated or point load, from the preceding it would seem reasonable and practical to use the "partial loading" approach to deal with the case of nominal "concentrated" loading.

3.4 Consideration of Foundation Damping

In this section numerical solutions involving foundation damping will be studied. The same plate system described in section 3.1 is considered here with the following changes. Two types of uniform loading are used: (i) a constant load is applied suddenly; and (ii) the load is increased linearly from zero to a maximum value and held constant thereafter. Varying amounts of damping are introduced into the system.

The response histories for the center point deflection are plotted in Fig. 17. The numerical solutions were obtained by use of a 16 x 16 grid. For the case of the suddenly applied loading, it may be seen that for $\beta = 56.52$ (slightly less than 1st mode critical damping) the numerical solution is practically identical to the exact solution. It may be seen also that the influence of damping in reducing the magnitude of response is quite pronounced. It can be further noted that for values of $\beta = 56.52$ the dynamic response approaches the static response monotonically from below. This would point to the possibility of obtaining static solutions by use of dynamic analysis. So far as that objective is concerned, it would seem from the data presented in this figure that the use of $\beta = 56.52$ is most efficient in the sense that larger amounts of damping would take longer for the solution to approach the static value within a given percentage.

In Fig. 17 is also shown the damped response ($\beta = 56.52$) for the case of gradually applied loading. As expected the response also approaches the static value monotonically from below. However, it approaches at a slower rate than that for the case of suddenly applied load. Hence it is considered to be a less efficient type of loading so far as obtaining the static response is concerned.

It should be pointed out that, in general, if the static solution is the only objective, one would not use this approach. However, in this case the computer program for the dynamic analysis is already available, and it would be more convenient to make use of it, instead of preparing a new program for that specific purpose. It might be mentioned also that this "pseudo-dynamic" approach for static analysis may be usefully extended to inelastic problems as recently demonstrated for the case of one dimensional structures by Heidebrecht et.al. (10).

In Fig. 18 are presented data similar to those given in Fig. 17 except that the result concerns bending moment instead of deflection. It may be seen that the trends of these results are similar to those discussed in the preceding.

3.5 Effects of Boundary Conditions and Foundation Stiffness

In this section the effects of boundary conditions and foundation stiffness will be briefly considered. Except for these particular parameters, the plate system dealt with here for this study is the same as described in sub-section 3.3.2. In addition to the simply supported, plates with all edges fixed and all edges free are considered. It is reasonable to consider the "stiffness" of a free edge to be less than that of a simply supported edge, the stiffness of which in turn, to be less than that of a fixed one.

In Fig. 19 are presented deflection histories for the simply supported and fixed plates for the case of $\alpha = 0$ (no foundation stiffness) and for $\alpha = 414.7$. It may be observed that the stiffness of the boundary conditions and that of the foundation have similar effect on the response. The effect is to reduce the magnitude of the response as well as the duration of its positive phase. Also, all the history curves remain practically identical to each other up to a certain time, $\tau = .0375$ (which is .143 times the first fundamental period of the simply supported plate with $\alpha = 0$). Thus, it seems that it takes a finite length of time for the influence of the boundary or the foundation stiffness to come into play.

Similar observations can also be made from the results on bending moments presented in Fig. 20 for the same plates considered. In Fig. 21 are presented additional data on the influence of boundary conditions including the case of a free plate also. The problem considered is the same as the preceding, except that the load is applied over an 1/16 x 1/16 area. This result also corroborates the observations made in the preceding.

3.6 Study of Free Plates

In this section the dynamic response of plates with all four edges free and resting on an elastic foundation will be studied in some detail. In contract to most of the numerical results presented in the preceding, exact solutions of this type of problem are practically impossible to obtain. However, the problem is of considerable practical interest because it may be used as an analytical model for such technical applications as studies of rigid pavements of highways and airport runways.

It is not intended here to make extensive investigation of these technical problems; the purpose here is to demonstrate the feasibility of the use of the numerical method for such problems. The great majority of the numerical data presented in this section concerns the dynamic response of such plates to a load applied at one of the corners of the plate. This is because this type of loading is thought to be most critical for such plate structures as observed in the case of pavement slabs (45). From the design standpoint, the principal bending moments are the significant quantities. These moments have been considered in the following sub-sections. The numerical problem studied here, except for the boundary conditions and the loading is the same as in section 3.1.

3.6.1 Influence of Grid Size: Before discussing the case of corner loading the effects of grid size will be considered. This is done in order to reasonably ensure the accuracy of the numerical procedure for this type of problem in the absence of an exact solution.

In Fig. 22 are shown the response histories for the center point deflection for various grid sizes for a "shrinking area type" triangular loading pulse as described in section 3.3. It may be observed that the response for the 16 x 16 grid is quite close to those for 20 x 20 and 24 x 24 grids. Moments under the load diverge as expected, and therefore they are not presented here.

3.6.2 Response Histories: For data presented in this and the subsequent sub-sections unless otherwise specified the loading is as follows: A "partial type" of triangular loading as described in sub-section 3.3.2 is applied at one of the corners over an 1/16 x 1/16 area of the plate. In order to identify the location of points on the plate the coordinate system is depicted in Fig. 23.

In Table 9 are listed the maximum deflections and principal bending moments and their locations for a number of time instants. These maximums will be referred to as "space-maximum," while the term "maximum" without a prefix will be reserved for the quantity which is the maximum with respect to both time and space. Thus it is seen that for different instants the space-maximum deflections and principal moments occur at different locations. Representative response histories are presented in Figs. 25, 26 and 27, respectively, for the corner point deflection, principal bending moment M'_1 at point

(2, 2), and principal bending moment M'_2 at point (3, 3) with the load applied at the corner point (1,1). (M'_1 and M'_2 are, respectively, the algebraically larger and smaller principal moments.) It is of interest to note from the Fig. 27 that the peak value of M'_2 is attained rather early relative to the duration of loading.

3.6.3 Contours of Response: Fig. 28 shows the deflection contour at a time close to the occurrence of the maximum deflection. It is noted that the maximum (downward) deflection occurs at the corner under the load, and at the opposite corner, the plate has the maximum negative (upward) displacement. In Fig. 29 is shown the contour for M'_2 at a time close to the occurrence of the maximum M'_2. It may be observed that the space distribution of the moment is similar to that in the case of static loading. The maximum value occurs at points a short distance away from the corner along a diagonal line.

3.6.4 Effect of Foundation Damping: In Table 10 are listed the time instants, locations of occurrence, and the values of maximum deflection and principal bending moments for the cases of foundation damping corresponding to $\beta = 0$ and $\beta = 56.52$. It may be observed that, relative to the undamped case, the magnitudes of the maximum deflection and M'_1 are about 50% smaller, and M'_2 only about 20% smaller. Furthermore, the influence of damping is to hasten the time of occurrence of the maximum response. Representative history curves of deflection and M'_2 for the damped case are also shown in Figs. 25 and 26.

3.6.5 Effect of Pulse Shape: In Table 11 are listed the time instants, locations of occurrence, and the values of maximum responses for various triangular pulse shapes obtained by varying the time parameters defined in Fig. 24. It may be seen from this table that the values of the maximum responses become slightly greater with the reducing rise rate of the loading (larger value of t_o). Meanwhile, the time instants of occurrence of these maximums are delayed.

3.6.6 Effect of Load on Point Adjacent to Corner: Listed in Table 12 are the time instants, locations of occurrence and the values of the maximum responses for a triangular loading pulse applied at the corner point (1, 1) and at the point (2, 1) next to the corner. It may be seen that the values of the maximum responses for the corner loading case are somewhat larger than those due to the loading at the adjacent point. This is in agreement with the observation in the case of static loading, that corner loading is most critical for this type of plates.

CHAPTER IV

SUMMARY AND CONCLUSIONS

In this thesis a numerical method for the dynamic analysis of plates on elastic foundation has been presented. The method is based on a discretization of the plate by use of the classical finite difference expansion of the space derivatives in the governing partial differential equation. The resulting ordinary differential equations for the discrete system (with time as the independent variable) have been integrated numerically.

As expected the accuracy of the method depends on the grid size. The finer the grid, the more accurate would be the results. However, this is true only to a certain extent. As the grid size is made smaller, the amount of computation increases, and so does the round-off error. It seems that for a square plate a grid of 16 x 16 would represent a "critical" size in the sense that any finer grid may not necessarily produce more accurate results. On the other hand, a 16 x 16 grid or even coarser ones, depending upon the degree of accuracy needed for the particular problem being considered, can yield sufficiently accurate results. For example, for the test problem considered, the errors in maximum deflection and maximum bending moment for an 8 x 8 grid are less than 1% and 6%, respectively.

The relative accuracy and efficiency of the classical Runge-Kutta method and the Beta method for the numerical integration of the equations of motion of the system have been studied by considering a specific numerical problem. Based on the data obtained it seems that, although Runge-Kutta method has a somewhat larger range of stability, the results produced do not seem to be any more accurate than those given by the Beta method. On the other hand, Beta method is more efficient in regard to programming as well as computer time for the type of problems considered--problems of structural dynamics governed usually by a system of simultaneous second order differential equations.

It has been demonstrated that the tedious part of the work associated with this method--that associated with the formulation of the equations and the lengthy computations, can all be handled by the computer. In order to obtain numerical solutions of problems one needs to supply to the computer only the most basic parameters such as the size of the plate, grid size, and loading. The generation of the differential equations (with the influence of the boundary conditions appropriately taken into account) and the solutions of these equations have all been handled by the computer. It might also be mentioned that the amount of computer time needed for a solution with sufficient accuracy for most engineering purposes is not excessive. For example, in the case of a free plate with a 16 x 16 grid, a complete history curve for about one fundamental period, including the selection of maximum response values in the space as well as time domain, takes about 9 minutes of computer time for a Control Data 3600 System.

After having established the reliability of the method it is applied to study briefly several physical problems. Among these is the case of the concentrated load. The load is first assumed to act over one grid square. It was found, as the grid size decreases the bending moment under the load does not converge to a definite value. This is, of course, not surprising in view of the static theory of plates. However, if one treats the concentrated load as a distributed load over a finite area then the bending moment under the load converges as the grid size is reduced.

The case of a free plate subjected to a concentrated load at the corner was studied and the contours at the instant of occurrence of the maximum deflection and the principal bending moment, respectively, have been obtained. It was found that the maximum principal bending moment occurs in the same general area as in the case of static loading. Also the effect of foundation damping, pulse shape and the location of loading were briefly studied for the case of a free plate. It was observed that the corner loading produced the most severe effects; and the effect of foundation damping was quite pronounced in reducing the values of maximum responses.

For the case of a simply supported plate, the maximum deflection was reduced by 50%, and the maximum principal bending moment by about 20% due to a foundation damping equal to the critical damping for the first mode and using a rectangular pulse type loading function. The practicability of getting a static solution from the dynamic analysis was also studied. It was indicated that this could be most conveniently done by introducing an amount of damping equal to the critical damping for the first mode and using a rectangular pulse type loading function.

Some numerical results were also obtained to study the influences of boundary condition and the foundation stiffnesses. It was observed that as the stiffness of either the foundation or the boundary condition is increased, the value of the maximum response and the duration of the positive phase of the response are reduced.

For further work along the line of investigation described herein, it is suggested that the technical problem of dynamic stresses in airport and highway pavements be studied. Because of the flexibility of this method, it is believed that a more realistic analytical representation of the physical system could be obtained. Furthermore, it might be fruitful to try to adapt this approach for a dynamic analysis of inelastic plates. Like most numerical problems, the propagation type in pargicular, the influence of round off error can always be a serious problem. Obviously, a systematic and rational investigation of this problem is of basic importance.

V. BIBLIOGRAPHY

1. Bradley, W. A., "Loading Approximations in Finite Difference Solutions of Plate Bending and Vibration Problems," Unpublished Report, Dept. of Applied Mechanics, Michigan State University, September, 1961.

2. Chen, S. T., "Rectangular Plates with Free Edges on Elastic Foundations," Acta Mechanica Sinica, Vol. 4, No. 1, Jan. 1960, pp. 23-35.

3. Crandall, S. H., Engineering Analysis, McGraw-Hill Book Co., Inc., New York, 1956, pp. 125-194 and pp. 337-405.

4. Fel'dman, M. R., "A Difference Method of Investigating the Stability and Oscillations of Plates (in Russian), Izie. Akad. Nauk. Arm. S.S.R. Ser. F13-Mat. 12, 3, 15-27, 1959.

5. Forsyth, E. M. et.al., "Transient Vibration of Rectangular Plates," J. Mech. Eng. Sciences, Vol. 2, No. 4, Dec. 1960, pp. 325-30.

6. Frederick, D., "Thick Rectangular Plates on Elastic Foundation," Trans. ASCE, Vol. 122, 1957, pp. 1069-87.

7. Gill, S., "A Process for the Step-by-Step Integration of Differential Equations in an Automatic Digital Computing Machine," Proc. of the Cambridge Philosophical Society, Vol. 47, 1951, pp. 96-108.

8. Grinter, L. E., Numerical Methods of Analysis in Engineering, Chapter 9 (by N. M. Newmark), The Macmillan Company, New York, 1949, pp. 141-144.

9. Harr, M. E., "Influence of Vehicle Speed on Pavement Deflections," Highway Research Board, Proc. Vol. 41, 1962, pp. 77-82.

10. Heidebrecht, A. C., Lee Seng-Lip and Fleming, J. F., "Dynamic Analysis of Elastic-Plastic Frames," Journal of the Structural Division, ASCE, Vol. 90, No. ST2, Part 1, April 1964, p. 334.

11. Holl, D. L., "Thin Plates on Elastic Foundations," Proceedings Fifth International Congress of Applied Mechanics, Cambridge, Mass., 1938, pp. 71-74.

12. Holl, D. L., "Simply Supported Plates Under Dynamic Loading on Elastic Foundation," Applied Mathematics Symposium of the American Math. Society, 3 (1950), pp. 107-16.

13. Iguti, S., "Lateral Vibrations of Rectangular Plate with Pairs of Simply Supported and Perfectly Free Two Opposite Edges," Doboku-Gakkai. Si (Civ. Eng. Soc., Japan-J), Vol. 26, No. 4, April 1940, pp. 427-40.

14. Jones, R. L., "Digital Computer Solution for Pavement Deflections," Portland Cement Assn. Research and Development Lab. J., Vol. 4, No. 3, Sept. 1962, pp. 30-36.

15. Kalman, L. S. and Utku Senol, "Transverse Vibration of Elasto-plastic Plates," Symposium on the Use of Computers in Civil Engg., Lisbon, Proc., Vol. II, Paper No. 54, 1962.

16. Kennedy, Jr., J. C., "The Linear and Non-linear Vibration Characteristics of Rectangular Plates Utilizing Finite Difference Techniques on a Operational Analog Computer, read in ASCE Engineering Mechanics Div. Specialty Conference, M.I.T., Cambridge, Mass., April 3, 1964.

17. Kurlandzki, J., "Introduction of Initial Boundary Value Problems of Elasticity to Fredholm Integral Equations of Second Kind (in Eng.)," Proc. of Vib. Prob. (Polsha Akad. Nauk, Inst. Podstawowyeh Problemow Tech.), 31 (10), 41-55, 1962.

18. Leckie, F. A., "The Application of Transfer Matrices to Plate Vibrations," Ing.-Arc, Vol. 32, No. 2, pp. 100-111, Feb. 1963.

19. Leissa, A. W., "A Method for Analyzing the Vibrations of Plates," J. Aerospace Sciences, Vol. 29, No. 4, p. 475 (Readers' Forum), April 1962.

20. Leonards, G. A. et.al., "Analysis of Concrete Slabs on Ground," Trans. ASCE, Vol. 126, Part I, 1961, p. 42.

21. Livesley, R. K., "Some Notes on Math Theory of Loaded Elastic Plates Resting on Elastic Foundation," Quarterly J. Mechanics and Appl. Math., Vol. 6, Pt. 1, Mar. 1953, pp. 32-44.

22. Mase, G. E., "Behavior of Visco-elastic Plates in Bending," Proc. ASCE, Vol. 86 (Journal Engg. Mechanics Div.), No. EM3, June 1960, Paper No. 2498, pp. 25-39.

23. Mindlin, R. D., "Influence of Rotary Inertia and Shear on Flexural Motions of Isotropic Elastic Plates," Trans. ASME (J. App. Mech.), Vol. 18, No. 1, March 1951, pp. 31-38.

24. Mindlin, R. D. et.al., "Flexural Vibrations of Rectangular Plates," Trans. ASME (J. App. Mech.), Vol. 23, No. 3, Sept. 1956, pp. 430-436.

25. Murphy, G., "Stresses and Deflections in Loaded Rectangular Plates on Elastic Foundations," Iowa State College Engineering Expt. Station, Bul. No. 135, Vol. 36, No. 5, June 30, 1937, 52 p.

26. Naghdi, P. M. and Rowley, J. C., "On Bending of Axially Symmetric Plates on Elastic Foundations," Proc. First Midwestern Conference on Solid Mechanics, University of Illinois, 1953, pp. 119-123.

27. Newmark, N. M. and Chan, S. P., "A Comparison of Numerical Methods for Analyzing the Dynamic Response of Structures," Civil Engineering Studies, Structural Research Series No. 36, University of Illinois, Oct. 1952.

28. Pickett, G. and Ray, G. K., "Influence Charts for Rigid Pavements," Trans. ASCE, Vol. 116, 1951, p. 49.

29. Pickett, G., "A Study of Stresses in the Corner Region of Concrete Pavement Slabs Under Large Corner Loads," Portland Cement Association, Chicago, Ill., 1951.

30. Ralston, A., Wilf, H., Mathematical Methods for Digital Computers, John Wiley and Sons, Inc., New York, 1960, pp. 110-120.

31. Raskovic, D., "Contribution to the Problem of Vibrations of Plates with Damping Considered," Zeit Fuer Augewandte Mathematik, U. Mechanik, Vol. 39, No. 9-11, Sept.-Nov. 1959, pp. 422-424.

32. Reismann, H., "Dynamic Response of Elastic Plate Strip to Moving Live Load, AIAA Journal, Vol. 1, No. 2, Feb. 1963, pp. 354-360.

33. Sandi, Kh., "On Plates Resting on Hard Elastic Halt Space Under the Working of Dynamic Load (in Russian), Rev. mecan. Appl., Vol. 7, No. 1, pp. 137-151, 1962.

34. Sezawa, K., "On Lateral Vibrations of Rectangular Plate Clamped at 4 Edges," Tokyo Imperial University, Aeronautical Research Inst. Report, Vol. 6, No. 70, April 1931, pp. 61-70.

35. Solecki, R., "Free and Forced Oscillations of a Triangular Lamina (in Russian), Rozprawy Inzyn. Vol. 8, No. 1, pp. 65-81, 1960, Ref. h. Mekh, No. 3, 1961, Rev. 3, Vol. 102.

36. Stanisic, M. M., "Free Vibrations of Rectangular Plate with Damping Considered," Quarterly of Applied Math., Vol. 12, No. 4, Jan. 1955, pp. 361-367.

37. Takabayari, Z., "Forced Vibration of Membranes and Plates Taking Initial Motion into Account," Soc. Mech. Engrs., Japan, Trans., Vol. 2, No. 8, Aug. 1936, pp. 327-31.

38. Timoshenko, S. and Young, D. H., Vibration Problems in Engineering, Third Edition, D. Von Nostrand Company, Inc., Princeton, N.J., 1955.

39. Timoshenko, S. and Woinowsky-Krieger, S., Theory of Plates and Shells, Second Edition, McGraw-Hill Book Co., Inc., New York, 1959.

40. Tomotika, S., "Transverse Vibration of Square Plate with 4 Clamped Edges, Tokyo Imperial University, Aeronautical Research Inst. Report, Vol. 10, No. 129, Sept. 1935, pp. 299-328.

41. Tseitlin, A. I., "On the Effect of Shear Deformation and Rotary Inertia in Vibrations of Beams on Elastic Foundations," Appl. Math. Mech. (Prikl. Mat. Mekh.), Vol. 25, No. 2, pp. 531-535, 1961.

42. Tung, T. P. and Newmark, N. M., "A Review of Numerical Integration Methods for Dynamic Response of Structures," Civil Engineering Studies, Structural Research Series No. 69, University of Illinois, March 1954.

43. Westergaard, H. M., "Computation of Stresses in Concrete Roads," Proc. Highway Research Board, Vol. 5, Part 1, 1925, pp. 90-112. Also under title "Stresses in Concrete Pavements Computed by Theoretical Analysis," Public Roads, Vol. 7, No. 2, April 1925, pp. 25-35.

44. Yeh, G. C. K. and Martinek, H., "Forced Vibration of Clamped Rectangular Plate in Fluid Media," ASME, Trans. (J. App. Mech.), Vol. 22, No. 4, Dec. 1955, pp. 568-72.

45. Yodder, E. J., Principles of Pavement Design, John Wiley and Sons, Inc., New York, 1959, pp. 52-122.

46. Young, D., "Vibration of Rectangular Plate by Ritz Method," ASME-Trans. (J.A.M.), Vol. 18, No. 2, p. 229, June 1951; also Vol. 17, No. 4, Dec. 1950, pp. 448-53.

APPENDIX A

USE OF COMPUTER AND PROGRAMMING

The computer programs used in this study are written so that only the most basic parameters need to be supplied to the computer. The generation of the equations of motion for the plate system and their integrations are carried out by the computer.

A.1 Generation of Equations of Motion

The main job in the generation of the equations of motion is the evaluation of "BHO" at each point. For simply supported and fixed plates there is only one basic "BHO" pattern, whereas in the case of free plates there are six "BHO" patterns. For convenience simply supported and fixed plates are handled by one program, and a separate program is prepared for the case of free plates.

A.1.1 Simply Supported and Fixed Plates: The first step in evaluation of "BHO" for a point is to express the deflections of points outside the plate domain in terms of deflection of the points inside the plate domain.

In the program this is done by 4 "DO" loops for points adjacent to the edges. Generality is introduced in the treatment of boundary conditions by incorporating a factor denoted by "BCF" for each edge (or a portion of the edge in the case of mixed boundary conditions for that edge). For example,[1] for the upper edge (Fig. A.1), W(I, J) = BCF1 · W(3, J), for J = 3 to NC.

After the deflections of all the relevant points outside the plate are expressed in terms of deflections inside it, the "BHO" is evaluated for all the points. In order to make use of a library subroutine for integration by the Runge-Kutta method, all variables are changed to single subscripted variables; thus:

K = (I-3) · NC + J-2

W(I, J) = Y(K)

for I = 3, to MM and J = 3, NN, and then "BHO" is evaluated thus:

BHO(K) = 20 W(I, J) - 8[W(I, J-1) + W(I, J+1), +
W(I-1, J) + W(I+1, J)]
+ 2 [W(I+1, J-1) + W(I-1, J+1) + W(I+1, J-1)+W(I+1, J+1)]
+ W(I-2, J) + W(I +2, J) + W(I, J-2) + W(I, J+2).

A.1.2 Free Plate: There are 6 basic "BHO" patterns as shown in Fig. A3. They are applied to 25 different sets of points shown in Fig. A2. These patterns have been derived after taking into consideration the boundary conditions. Therefore, all these patterns are such that they do not involve any point outside the plate region. One "BHO" pattern is taken at a time. Points which are similar in location in the

---

[1]Notations are given in the section A.4.

region of the plate are handled in a sequence using one particular kind of pattern.

To take care of the orientation of "BHO" pattern two variable subscripts IS and JS are introduced. These are added to I and J subscripts. Such that by changing IS, JS from 1 to -1, the orientation of "BHO" pattern is changed. For example, to deal with all the four corner points, 1 through 4 of the plate, pattern type 1 is used thus: for the upper left corner point 1, I = 3, J = 3, IS = 1, JS = 1 and

$$\begin{aligned} BHO(K) = {} & R_3[-W(I,J) + W(I, J+JS) + W(I + IS, J)] \\ & + R_1[W(I, J + 2JS) + W(I + 2IS, J)] \\ & + R_6 W(I + IS, J + JS). \end{aligned}$$

The expression for "BHO" remains the same for the other 3 corner points for which the values of I, J, IS and JS are as follows. For the upper right corners, point 2; I = 3, J = NC + 2, IS = 1, JS = -1, for the lower right corner, point 3; I = MR + 2, J = NC + 2, IS = -1, JS = -1; and for the lower left corner point 4; I = MR + 2, J = 3, IS = -1, JS = 1. The remaining points on the edges adjacent to corners, points 5-16 are handled in a similar manner using the patterns 2 and 3 of "BHO." Points on the edges and adjacent to edges, points 17-24 are handled as above using patterns 4 and 5. "DO" loops are used for points on the same edge. The points in the interior, points type 25 are handled all at once using "BHO" pattern 6 by a "DO" loop.

A.2 Numerical Integration of Equations

After generating the equations of motion they are numerically integrated using either the Beta method or Runge-Kutta method. A program is written for the Beta method on the basis of the description given in sub-section 2.4.2. In this case the equation of motion, Equation 4, is put in the form:

$$ACD(K) = H^2[T \cdot P(K) - AA \cdot DPA(K) - BHO(K) \cdot DV^4] - H \cdot VEA(K)$$

For the case of Runge-Kutta method, Library Function Subprogram "RKLDEQ" has been used. Equation 4 is transformed into a set of first order differential equations for I = 1 to NE, thus:

$$F(I) = Y(I + NE)$$

$$F(I+NE) = T \cdot P(I) - AA \cdot Y(I) - B \cdot Y(I+NE) - BHO(I) \cdot DV^4$$

A.3 Time Requirements of the Computer*

In order to compute the deflections, bending moments and the maximum values of these in the range of integration, the Beta method takes approximately 2.2×10^{-3} seconds per degree of freedom per step of integration. The Runge-Kutta method takes about twice as much. If the maximum responses (deflections, moments and principal moments) in the space domain for each time instant are desired in addition to the maximum values in the range of integration, an additional time of approximately 1.5×10^{-3} seconds per degree of freedom per step of integration would be needed.

*Control Data 3600.

A.4 List of Fortran Variables

A list of Fortran variables used in the programs and in this appendix is given in the following:

A = constant used in Runge-Kutta-Gill function sub-program "RKLDEQ";

AA = α, dimensionless soil elastic constant;

ACA(I) = assumed acceleration of point (I);

ACD(I) = derived acceleration of point (I);

ACF(I) = final acceleration of point (I);

ANGLE = orientation of the direction of principal moment;

ANG 1* = orientation of space-maximum M'_1;

ANG1T = orientation of the maximum M'_1;

B = β, dimensionless soil damping constant;

BETA = parameter of Beta method;

BCF 1, BCF 2, BCF 3, BCF 4 = boundary condition factors (+1 or -1) for each side;

BMX = M'_x, dimensionless bending moment M_x;

BMY = M'_y, dimensionless bending moment M_y;

BMXY = M'_{xy}, dimensionless twisting moment M_{xy};

BMP1 = M'_1, dimensionless principal bending moment;

BMP1MS = space-maximum M_i;

BMP1ST = maximum M'_1;

BMMMP = maximum center point M'_x;

---

*Number 2 in the suffix similarly will correspond to M'_2.

BMMQP = maximum quarter point M'_x;

C = $\frac{n \cdot h}{\lambda}$, factor used in the evaluation of moments;

D = D, flexural rigidity of plate;

DMMP = maximum center point deflection;

DMQP = maximum quarter point deflection;

DPA(I) = assumed deflection of point (I) obtained by using Beta-formula;

DPF(I) = final deflection of point (I);

DPFMS = space maximum deflection at any instant;

DPFST = maximum deflection;

DV = n in floating point;

E = E, modulus of elasticity;

F(I) = derivative of Y(I) with respect to time;

GS = λ, grid size;

H = $\Delta\tau$, time increment in numerical integration;

I, J, K, L, M = variable subscripts;

LR = a/b, aspect ratio;

LOCDPF = location of occurrence of maximum deflection;

LOCMP1 = location of occurrence of maximum M'_1;

MDS = location of maximum deflection at any instant;

MID = subscript for the center point;

MP1S = location of occurrence of maximum M'_1 at any instant;

MR = number of rows of grid lines;

N = number of first order differential equations;

NB = number of grid divisions on smaller side;

NC = number of columns;

NE = number of second order differential equations and also the number of dependent variables;

NL = n, number of grid divisions on larger side;

NQP = subscript for the quarter point;

NT = a variable used in "RKLDEQ";

PF = peak value of the forcing function;

P(I) = forcing function at a point (I);

PR = ν, Poisson's ratio;

Q = temporary region used by "RKLDEQ";

$R_1 = (1 - \nu^2)/2$

$R_2 = -4 + 2\nu + 2\nu^2$

$R_3 = -3 + 2\nu + \nu^2$

$R_4 = 2 - \nu$

$R_5 = -6 + 2\nu$

$R_6 = 2 - 2\nu$

$R_7 = 8 - 4\nu - 3\nu^2$

$R_8 = 7.5 - 4\nu - 2.5\nu^2$

RANGE = range of integration in Beta method;

S = a variable used in "RKLDEQ";

SIZE = a, length of the longer side of the plate;

T = θ, constant to be multiplied to p(x,y,t) to make it dimensionless;

TDMMP = time of occurrence of maximum center point deflection;

TDMQP = time of occurrence of maximum quarter point deflection;

TDPST = time of occurrence of maximum deflection;

TEND = t_1, duration of action of forcing function;

THICK = h, thickness of plate;

TIME = τ, dimensionless time;

TINT = t_o, time parameter used in Fig. 24 to denote rise rate;

TMP1ST = time of occurrence of maximum M'_1;

TO = T_o, a parameter;

TOLER = tolerance for testing the convergence in Beta method;

VEA(I) = assumed velocity of point (I) obtained by using Beta-formula;

VEF(I) = final velocity of point (I);

WCI = weight per cubic inch of plate;

W(I, J) = u(i, j), dimensionless deflection of point (i, j);

WT = m, mass per unit area of plate;

X = τ, dimensionless time in Runge-Kutta method;

XEND = final value of τ, range of integration in Runge-Kutta method;

Y(I) = dimensionless deflection of point (I) in Runge-Kutta method; and

Y(NE+I) = derivatives of Y(I) with respect to τ in Runge-Kutta method.

A.5 FORTRAN COMPUTER PROGRAMS

A.5.1 RUNGE-KUTTA METHOD FOR SIMPLY SUPPORTED AND FIXED PLATES:

```
PROGRAM DYNA2
DIMENSION Y(2048),F(2048),Q(2048),P(1024),W(36,36),BHO(1024)
1 ,BMX(1024),BMY(1024),BMXY(1024)
PLATE SIZE
LR=1
SIZE=120.
THICK=12.
NL=16
DV=FLOATF(NL)
GS=SIZE/DV
C=DV*THICK/GS
PLATE MATERIAL PROPERTIES
WCI=144./1728.
E=2.*10.**6
PR=.25
FOUNDATION MATERIAL PROPERTIES
SEK=614.4
DO 7000 IJK=2,2
FIJK=FLOATF(IJK)
SDC=3.5*(FIJK-1.)
PLATE BOUNDARY CONDITIONS
BCF1=-1.
BCF2=-1.
BCF3=-1.
BCF4=-1.
FORCING FUNCTION PARAMETERS
PF=10.
TEND=0.
PRINTING COUNTER PARAMETERS
NI=NL*NL/8
INDEPENDENT VARIABLE(TIME) INCREMENT AND LIMIT
H=1./(10.*DV**2)
XEND=.20
X=0.0
****************
DMMP=0.
DMQP=0.
BMMMP=0.
BMMQP=0.
D=(E*THICK**3)/(12.*(1.-PR**2))
WT=WCI*THICK/386.4
TO=SQRTF((WT*SIZE**4)/D)
AA=(SEK*SIZE**4)/D
B=(SDC*SIZE**4)/(D*TO)
T=(SIZE**4)/(D*THICK)
NC=NL-1
NB=NL/LR
```

```
      MR=NB-1
      NE=MR*NC
      N=2*NE
      MM=MR+2
      NN=NC+2
      MID=NC*(NL/2-1)+NL/2
      MIM=MID-1
      MIP=MID+1
      NQP=NC*(NL/2-1)+NL/4
      JJ=0
      NT=0
      PRINT 112,AA,B,T,H,BCF1,BCF2,BCF3,BCF4,TEND,PF
 112  FORMAT(1H0,3HAA=,E9.4,3X,2HB=,E9.4,3X,2HT=,E9.4,3X,2HH=,F8.7,3X,
     14HBCF=,4(F4.1,2X),1X,5HTEND=,F4.3,3X,3HPF=,F6.2)
      PRINT113,TO,NI,NL
 113  FORMAT(1H0,3HTO=,F8.6,3X,3HNI=,I3,20H,  NUMBER OF GRIDS =,I2)
      DO102 I=1,N
 102  Y(I)=0.0
      PRINT 222
 222  FORMAT(1H0,8X,1HX,13X,1HY,11X,3HBMX,11X,3HBMY,10X,4HBMXY)
      PRINT 111,X,Y(MID)
 111  FORMAT(1H0,2(F9.7,5X))
 101  IF(X-TEND)501,502,502
C     *********LOADING ROUTINE *************
 501  DO 5011 I=1,NE
 5011 P(I)=PF
C     ***********END LOADING ROUTINE*************
      GOTO 105
 502  DO 106 I=1,NE
 106  P(I)=PF
C     BEGIN GENERATION OF EQUATIONS
 105  DO 10 I=3,MM
      DO 10 J=3,NN
      K=(I-3)*(NN-2)+J-2
 10   W(I,J)=Y(K)
      DO12 J=3,NN
      W(1,J)=BCF2*W(3,J)
 12   W(MM+2,J)=BCF4*W(MM,J)
      L=NN+1
      DO 13 J=2,L
      W(2,J)=0.
 13   W(MM+1,J)=0.
      DO 14 I=3,MM
      W(I,2)=0.
      W(I,NN+1)=0.
      W(I,NN+2)=BCF3*W(I,NN)
 14   W(I,1)=BCF1*W(I,3)
      DO 15 I=3,MM
      DO 15 J=3,NN
```

```
      K=(I-3)*(NN-2)+J-2
 15   BHO(K)=20.*W(I,J)-8.*(W(I,J-1)+W(I,J+1)+W(I-1,J)+W(I+1,J))
     1+2.*(W(I-1,J-1)+W(I-1,J+1)+W(I+1,J-1)+W(I+1, J+1))
     2+W(I-2.,J)+W(I+2,J)+W(I,J-2)+W(I,J+2)
      DO 103 I=1,NE .
      F(I)=Y(I+NE)
 103  F(I+NE)=T*P(I)-AA*Y(I)-B*Y(I+NE)-BHO(I)*DV**4
C     END GENERATION OF EQUATIONS
      S=RKLDEQ(N,Y,F,Q,X,H,NT)
      IF(S-1.0)200,101,300
 200  PRINT201
 201  FORMAT(11HOERROR IN S)
 300  CONTINUE
C     **************COMPUTE MOMENTS**********************************
      DO 601 I=3,MM
      DO 601 J=3,NN
      K=(I-3)*(NN-2)+J-2
 601  W(I,J)=Y(K)
      DO 602 I=3,MM
      DO 602 J=3,NN
      K=(I-3)*(NN-2)+J-2
      BMX(K)=-C*(-(2.+2.*PR)*W(I,J)+W(I,J-1)+W(I,J+1)+PR*(W(I-1,J)+W(
     1I+1,J)))
      BMY(K)=-C*(-(2.+2.*PR)*W(I,J)+W(I-1,J)+W(I+1,J)+PR*(W(I,J-1)+W(I,J+1)))
     1+1)))
 602  BMXY(K)=C*(1.-PR)*(W(I-1,J-1)+W(I+1,J+1)-W(I+1,J-1)-W(I-1,J+1))/4.
      IF(ABSF(Y(MID))-ABSF(DMMP))603,603,604
 604  DMMP=Y(MID)
      TDMMP=X
 603  IF(ABSF(Y(NQP))-ABSF(DMQP))605,605,606
 606  DMQP=Y(NQP)
      TDMQP=X
 605  IF(ABSF(BMX(MID))-ABSF(BMMMP))607,607,608
 608  BMMMP=BMX(MID)
      TBMMMP=X
 607  IF(ABSF(BMX(NQP))-ABSF(BMMQP))609,609,700
 700  BMMQP=BMX(NQP)
      TBMMQP=X
 609  CONTINUE
      JJ=JJ+1
      IF(JJ-NI)302,303,302
 303  CONTINUE
      PRINT 804,X,Y(MID),BMX(MID),BMY(MID),BMXY(MID)
 804  FORMAT(1HO,5(F9.7,5X))
      PRINT 805,Y(NQP),BMX(NQP),BMY(NQP),BMXY(NQP)
 805  FORMAT(1HO,14HQUARTER POINT  ,4(F9.7,5X))
      JJ=0
 302  CONTINUE
      IF(X-XEND)101,400,400
```

```
 400   CONTINUE
 807   FORMAT((1H0,96H          TDMMP          DMMP          TDMQP          DMQP
     1   TBMMMP         BMMMP          TBMMQP          BMMQP)
       PRINT 807
       PRINT 806,TDMMP,DMMP,TDMQP,DMQP,TBMMMP,BMMMP,TBMMQP,BMMQP
 806   FORMAT(1H0,8F12.7)
 7000  CONTINUE
 7010  CONTINUE
       END
       FUNCTION RKLDEQ(N,Y,F,Q,X,H,NT)                                    RKLDQ
C      TEST OF ALGOL ALGORITHM
       DIMENSION Y(2048),F(2048),Q(2048)
C      REAL X,H--INTEGER N,NT--COMMENT--BEGIN INTEGER I,J,L-REAL A
       NT=NT+1
       GO TO (1,2,3,4),NT
C      GO TO S(NT)
 1     DO 11 J=1,N
 11    Q(J)=0.
       A=.5
       X=X+H/2.
       GO TO 5
 2     A=.29289321881
       GO TO 5
 3     A=1.7071067812
       X=X+H/2.
       GO TO 5
 4     DO 41 I=1,N
 41    Y(I)=Y(I)+H*F(I)/6.-Q(I)/3.
       NT=0
       RKLDEQ=2.
       GO TO 6
 5     DO 51 L=1,N
       Y(L)=Y(L)+A*(H*F(L)-Q(L))
 51    Q(L)=2.*A*H*F(L)+(1.-3.*A)*Q(L)
       RKLDEQ=1.
 6     CONTINUE
       END
       END
```

A.5.2 <u>BETA METHOD FOR FREE PLATE</u>:

```
       PROGRAM BETA2
       DIMENSION ACA(625),ACD(625),ACF(625),VEA(625),VEF(625),DPA(625)
     1,DPF(625),W(29,29),BHO(625),P(625)
     1,BMX(625),BMY(625),BMXY(625),ANGLE(625),BMP1(625),BMP2(625)
       COMMON ACA,ACD,ACF,VEA,VEF, DPA,DPF,W,BHO,P,BMX,BMY,BMXY
     1,ANGLE,BMP1,BMP2
       PRINT 8888
 8888  FORMAT(1H0,11HBETA METHOD)
 9999  FORMAT(1H0,14HALL EDGES FREE
```

```
     1/25HCONC. LOAD(CONSTANT AREA))
      PRINT 9999
      PLATE SIZE**************************
      LR=1
      SIZE=120.
      THICK=12.
      *******GRID SIZE*****************
      NL=16
      NB=NL/LR
      DV=FLOATF(NL)
      GS=SIZE/DV
      C=DV*THICK/GS
:     PLATE MATERIAL PROPERTIES********************
      WCI=144./1728.
      E=2.*10.**6
      PR=.25
      R1=(1.-PR*PR)/2.
      R2=-4.+2.*PR+2.*PR*PR
      R3=-3.+2.*PR+PR*PR
      R4=2.-PR
      R5=-6.+2.*PR
      R6=2.-2.*PR
      R7=8.-4.*PR-3.*PR*PR
      R8=7.5-4.*PR-2.5*PR*PR
C     FOUNDATION MATERIAL PROPERTIES*********************
      SEK=614.4
      SDC=0.
C     PLATE BOUNDARY CONDITIONS(FACTORS) APPLICABLE ONLY TO SIMPLY SUPPORTED
C     AND FIXED PLATES **************************************************
      BCF1=-1.
      BCF2=-1.
      BCF3=-1.
      BCF4=-1.
C     FORCING FUNCTION PARAMETERS********************************
      PF=4.*10.*64.
      TEND=.15
      TINT=0.
C     INDEPENDENT VARIABLE(TIME) INCREMENT AND LIMIT*********************
      H=1./(10.*DV*DV)
      RANGE=.15
      TIME=0.
C     PRINTING COUNTER PARAMETERS **********************
      NP=NL*NL/16
      JJ=0
C     *******BETA METHOD OF INTEGRATION PARAMETERS***********
      BETA=0.
      TOLER=.00000005
C
      D=(E*THICK**3)/(12.*(1.-PR**2))
      WT=WCI*THICK/386.4
```

```
      TO=SQRTF((WT*SIZE**4)/D)
      AA=(SEK*SIZE**4)/D
      B=(SDC*SIZE**4)/(D*TO)
      T=(SIZE**4)/(D*THICK)
C     EVALUATION OF NUMBER OF ROWS AND COLUMNS,NUMBER OF EQUATIONS ETC
C     CASE OF FREE PLATE**************************************************
      NC=NL+1                                                           FREE
      MR=NB+1                                                           FREE
      NE=MR*NC
      MM=MR+2
      NN=NC+2
      MID=NC*NL/2+(NC+1)/2                                              FREE
      MIM=MID-1
      MIP=MID+1
      PRINT 112,AA,B,T,H,BCF1,BCF2,BCF3,BCF4,TEND,PF
  112 FORMAT(1H0,3HAA=,E9.4,3X,2HB=,E9.4,3X,2HT=,E9.4,3X,2HH=,F8.7,3X,
     14HBCF=,4(F4.1,2X),1X,5HTEND=,F4.3,3X,3HPF=,F9.2)
      PRINT113,TO,NP,NL
  113 FORMAT(1H0,3HTO=,F8.6,3X,3HNI=,I3,20H,  NUMBER OF GRIDS =,I2)
      TDPST=0.
      LOCDPF=0.
      DPFST=0.
      TMP1ST=0.
      LOCMP1=0.
      BMP1ST=0.
      TMP2ST=0.
      LOCMP2=0.
      BMP2ST=0.
      ANG1T=0.
      ANG2T=0.
      DO 100 I=1,NE
      ACA(I)=0.
      ACD(I)=0.
      ACF(I)=0.
      VEA(I)=0.
      VEF(I)=0.
      DPA(I)=0.
  100 DPF(I)=0.
C     *********COMPUTE INITIAL ACCELERATION***************
      PFTI=PF*TIME/TINT
      P(1)=1.*PFTI
      P(2)=.5*PFTI
      DO 101 I=3,NC
  101 P(I)=0.
      P(NC+1)=.5*PFTI
      P(NC+2)=.25*PFTI
      DO 1011 I=20,NE
 1011 P(I)=0.
C     BEGIN COMPUTATION OF INITIAL ACCELERATION**************************
C     FREE PLATE*********************************************************
```

```
      DO 102 I=1,NE
      ACF(I)=H*H*T*P(I)
 102  ACD(I)=ACF(I)
C     END COMPUTATION OF INITIAL ACCELARATION****************************
 200  TIME =TIME+H
      IF(TIME-RANGE)300,300,900
 300  DO 301 I=1,NE
      ACA(I)=ACD(I)
      DPA(I)=DPF(I)+VEF(I)+(.5-BETA)*ACF(I)+BETA*ACA(I)
 301  VEA(I)=VEF(I)+.5*(ACF(I)+ACA(I))
      IF(TIME-TINT)402,402,403
 402  CONTINUE
C     *********BEGIN LOADING ROUTINE****************
      PFTI=PF*TIME/TINT
      P(1)=1.*PFTI
      P(2)=.5*PFTI
      DO 104 I=3,NC
 104  P(I)=0.
      P(NC+1)=.5*PFTI
      P(NC+2)=.25*PFTI
      DO 1041 I=20,NE
 1041 P(I)=0.
      GOTO 405
 403  IF(TIME-TEND)4031,4031,4032
 4031 PFTI=PF*(TEND-TIME)/(TEND-TINT)
      P(1)=1.*PFTI
      P(2)=.5*PFTI
      DO 1049I=3,NC
 1049 P(I)=0.
      P(NC+1)=.5*PFTI
      P(NC+2)=.25*PFTI
      DO 1042 I=20,NE
 1042 P(I)=0.
      GOTO 405
 4032 DO 4033 I=1,NE
 4033 P(I)=0.
C     END LOADING ROUTINE****************************
 405  CONTINUE
C     BEGIN GENERATION OF DIFFERENTIAL EQUATIONS FOR FOR PLATE WITH ALL EDGES
C     FREE************************************************************
      DO 10 I=3,MM
      DO 10 J=3,NN
      K=(I-3)*NC+J-2
 10   W(I,J)=DPA(K)
C     POINTS AT CORNER ON BOUNDARY(POINTS 1 THRU 4)
      I=3
      J=3
      IS=1
      JS=1
      CF=.25
```

```
      K=(I-3)*NC+J-2
      BHO(K)=R3*(-W(I,J)+W(I,J+JS)+W(I+IS,J))+R1*(W(I,J+2*JS)+W(I+2*IS,J))
     1))+R6*W(I+IS,J+JS)
      ACD(K)=H*H*(T*P(K)-AA*DPA(K)-BHO(K)*DV*DV*DV*DV/CF)-B*H*VEA(K)
      I=3
      J=NC+2
      IS=1
      JS=-1
      K=(I-3)*NC+J-2
      BHO(K)=R3*(-W(I,J)+W(I,J+JS)+W(I+IS,J))+R1*(W(I,J+2*JS)+W(I+2*IS,J))
     1))+R6*W(I+IS,J+JS)
      ACD(K)=H*H*(T*P(K)-AA*DPA(K)-BHO(K)*DV*DV*DV*DV/CF)-B*H*VEA(K)
      I=MR+2
      J=NC+2
      IS=-1
      JS=-1
      K=(I-3)*NC+J-2
      BHO(K)=R3*(-W(I,J)+W(I,J+JS)+W(I+IS,J))+R1*(W(I,J+2*JS)+W(I+2*IS,J))
     1))+R6*W(I+IS,J+JS)
      ACD(K)=H*H*(T*P(K)-AA*DPA(K)-BHO(K)*DV*DV*DV*DV/CF)-B*H*VEA(K)
      I=MR+2
      J=3
      IS=-1
      JS=1
      K=(I-3)*NC+J-2
      BHO(K)=R3*(-W(I,J)+W(I,J+JS)+W(I+IS,J))+R1*(W(I,J+2*JS)+W(I+2*IS,J))
     1))+R6*W(I+IS,J+JS)
      ACD(K)=H*H*(T*P(K)-AA*DPA(K)-BHO(K)*DV*DV*DV*DV/CF)-B*H*VEA(K)
C     POINTS AT INTERIOR CORNER(POINTS 5 THRU 8)
      I=4
      J=4
      IS=1
      JS=1
      CF=1.
      K=(I-3)*NC+J-2
      BHO(K)=18.*W(I,J)-8.*(W(I,J+JS)+W(I+IS,J))+2.*W(I+IS,J+JS)
     1+1.*(W(I+2*IS,J)+W(I,J+2*JS))+R4*(W(I-IS,J+JS)+W(I+IS,J-JS))
     1+R5*(W(I-IS,J)+W(I,J-JS))+R6*W(I-IS,J-JS)
      ACD(K)=H*H*(T*P(K)-AA*DPA(K)-BHO(K)*DV*DV*DV*DV/CF)-B*H*VEA(K)
      I=4
      J=NC+1
      IS=1
      JS=-1
      K=(I-3)*NC+J-2
      BHO(K)=18.*W(I,J)-8.*(W(I,J+JS)+W(I+IS,J))+2.*W(I+IS,J+JS)
     1+1.*(W(I+2*IS,J)+W(I,J+2*JS))+R4*(W(I-IS,J+JS)+W(I+IS,J-JS))
     1+R5*(W(I-IS,J)+W(I,J-JS))+R6*W(I-IS,J-JS)
      ACD(K)=H*H*(T*P(K)-AA*DPA(K)-BHO(K)*DV*DV*DV*DV/CF)-B*H*VEA(K)
      I=MR+1
      J=NC+1
```

```
      IS=-1
      JS=-1
      K=(I-3)*NC+J-2
      BHO(K)=18.*W(I,J)-8.*(W(I,J+JS)+W(I+IS,J))+2.*W(I+IS,J+JS)
     1+1.*(W(I+2*IS,J)+W(I,J+2*JS))+R4*(W(I-IS,J+JS)+W(I+IS,J-JS))
     1+R5*(W(I-IS,J)+W(I,J-JS))+R6*W(I-IS,J-JS)
      ACD(K)=H*H*(T*P(K)-AA*DPA(K)-BHO(K)*DV*DV*DV*DV/CF)-B*H*VEA(K)
      I=MR+1
      J=4
      IS=-1
      JS=1
      K=(I-3)*NC+J-2
      BHO(K)=18.*W(I,J)-8.*(W(I,J+JS)+W(I+IS,J))+2.*W(I+IS,J+JS)
     1+1.*(W(I+2*IS,J)+W(I,J+2*JS))+R4*(W(I-IS,J+JS)+W(I+IS,J-JS))
     1+R5*(W(I-IS,J)+W(I,J-JS))+R6*W(I-IS,J-JS)
      ACD(K)=H*H*(T*P(K)-AA*DPA(K)-BHO(K)*DV*DV*DV*DV/CF)-B*H*VEA(K)
C     POINTS ON BOUNDARY ADJACENT TO CORNERS(POINTS9 THRU 16)
C     ROWS(POINTS 9,10,11,12)
      I=3
      J=4
      IS=1
      JS=1
      CF=.5
      K=(I-3)*NC+J-2
      BHO(K)=R8*W(I,J)+R3*W(I,J-JS)+R2*W(I,J+JS)+R1*W(I,J+2*JS)
     1+R4*(W(I+IS,J-JS)+W(I+IS,J+JS))+R5*W(I+IS,J)+W(I+2*IS,J)
      ACD(K)=H*H*(T*P(K)-AA*DPA(K)-BHO(K)*DV*DV*DV*DV/CF)-B*H*VEA(K)
      I=3
      J=NC+1
      IS=1
      JS=-1
      K=(I-3)*NC+J-2
      BHO(K)=R8*W(I,J)+R3*W(I,J-JS)+R2*W(I,J+JS)+R1*W(I,J+2*JS)
     1+R4*(W(I+IS,J-JS)+W(I+IS,J+JS))+R5*W(I+IS,J)+W(I+2*IS,J)
      ACD(K)=H*H*(T*P(K)-AA*DPA(K)-BHO(K)*DV*DV*DV*DV/CF)-B*H*VEA(K)
      I=MR+2
      J=NC+1
      IS=-1
      JS=-1
      K=(I-3)*NC+J-2
      BHO(K)=R8*W(I,J)+R3*W(I,J-JS)+R2*W(I,J+JS)+R1*W(I,J+2*JS)
     1+R4*(W(I+IS,J-JS)+W(I+IS,J+JS))+R5*W(I+IS,J)+W(I+2*IS,J)
      ACD(K)=H*H*(T*P(K)-AA*DPA(K)-BHO(K)*DV*DV*DV*DV/CF)-B*H*VEA(K)
      I=MR+2
      J=4
      IS=-1
      JS=1
      K=(I-3)*NC+J-2
      BHO(K)=R8*W(I,J)+R3*W(I,J-JS)+R2*W(I,J+JS)+R1*W(I,J+2*JS)
     1+R4*(W(I+IS,J-JS)+W(I+IS,J+JS))+R5*W(I+IS,J)+W(I+2*IS,J)
```

```
      ACD(K)=H*H*(T*P(K)-AA*DPA(K)-BHO(K)*DV*DV*DV*DV/CF)-B*H*VEA(K)
C     COLUMNS((POINTS 13,14,15,16)
      I=4
      J=3
      IS=1
      JS=1
      K=(I-3)*NC+J-2
      BHO(K)=R8*W(I,J)+R3*W(I-IS,J)+R1*W(I+2*IS,J)+R4*(W(I-IS,J+JS)
     1+W(I+IS,J+JS))+R5*W(I,J+JS)+W(I,J+2*JS)+R2*W(I+IS,J)
      ACD(K)=H*H*(T*P(K)-AA*DPA(K)-BHO(K)*DV*DV*DV*DV/CF)-B*H*VEA(K)
      I=4
      J=NC+2
      K=(I-3)*NC+J-2
      IS=1
      JS=-1
      BHO(K)=R8*W(I,J)+R3*W(I-IS,J)+R1*W(I+2*IS,J)+R4*(W(I-IS,J+JS)
     1+W(I+IS,J+JS))+R5*W(I,J+JS)+W(I,J+2*JS)+R2*W(I+IS,J)
      ACD(K)=H*H*(T*P(K)-AA*DPA(K)-BHO(K)*DV*DV*DV*DV/CF)-B*H*VEA(K)
      I=MR+1
      J=NC+2
      IS=-1
      JS=-1
      K=(I-3)*NC+J-2
      BHO(K)=R8*W(I,J)+R3*W(I-IS,J)+R1*W(I+2*IS,J)+R4*(W(I-IS,J+JS)
     1+W(I+IS,J+JS))+R5*W(I,J+JS)+W(I,J+2*JS)+R2*W(I+IS,J)
      ACD(K)=H*H*(T*P(K)-AA*DPA(K)-BHO(K)*DV*DV*DV*DV/CF)-B*H*VEA(K)
      I=MR+1
      J=3
      IS=-1
      JS=1
      K=(I-3)*NC+J-2
      BHO(K)=R8*W(I,J)+R3*W(I-IS,J)+R1*W(I+2*IS,J)+R4*(W(I-IS,J+JS)
     1+W(I+IS,J+JS))+R5*W(I,J+JS)+W(I,J+2*JS)+R2*W(I+IS,J)
      ACD(K)=H*H*(T*P(K)-AA*DPA(K)-BHO(K)*DV*DV*DV*DV/CF)-B*H*VEA(K)
C     POINTS ON THE BOUNDARY THIRD FROM CORNERS
C     TOP ROW(POINTS TYPE 17)
      I=3
      IS=1
      CF=.5
      DO 12 J=5,NC
      K=(I-3)*NC+J-2
      BHO(K)=R7*W(I,J)+R2*(W(I,J-1)+W(I,J+1))+R1*(W(I,J-2)+W(I,J+2))
     1+R4*(W(I+IS,J-1)+W(I+IS,J+1))+R5*W(I+IS,J)+W(I+2*IS,J)
   12 ACD(K)=H*H*(T*P(K)-AA*DPA(K)-BHO(K)*DV*DV*DV*DV/CF)-B*H*VEA(K)
C     BOTTOM ROW(POINTS TYPE 18)
      I=MR+2
      IS=-1
      DO 13 J=5,NC
      K=(I-3)*NC+J-2
      BHO(K)=R7*W(I,J)+R2*(W(I,J-1)+W(I,J+1))+R1*(W(I,J-2)+W(I,J+2))
```

```
     1+R4*(W(I+IS,J-1)+W(I+IS,J+1))+R5*W(I+IS,J)+W(I+2*IS,J)
 13   ACD(K)=H*H*(T*P(K)-AA*DPA(K)-BHO(K)*DV*DV*DV*DV/CF)-B*H*VEA(K)
C     LEFT COLUMN BOUNDARY(POINTS TYPE 19)
      J=3
      JS=1
      DO 14 I=5,MR
      K=(I-3)*NC+J-2
      BHO(K)=R7*W(I,J)+R2*(W(I-1,J)+W(I+1,J))+R1*(W(I-2,J)+W(I+2,J))
     1+R4*(W(I-1,J+JS)+W(I+1,J+JS))+R5*W(I,J+JS)+W(I,J+2*JS)
 14   ACD(K)=H*H*(T*P(K)-AA*DPA(K)-BHO(K)*DV*DV*DV*DV/CF)-B*H*VEA(K)
C     RIGHT COLUMN BOUNDARY(POINTS TYPE 20)
      J=NC+2
      JS=-1
      DO 15 I=5,MR
      K=(I-3)*NC+J-2
      BHO(K)=R7*W(I,J)+R2*(W(I-1,J)+W(I+1,J))+R1*(W(I-2,J)+W(I+2,J))
     1+R4*(W(I-1,J+JS)+W(I+1,J+JS))+R5*W(I,J+JS)+W(I,J+2*JS)
 15   ACD(K)=H*H*(T*P(K)-AA*DPA(K)-BHO(K)*DV*DV*DV*DV/CF)-B*H*VEA(K)
C     POINTS INTERIOR AND ADJACENT TO BOUNDARY
C     TOP ROW(POINTS TYPE 21)
      I=4
      IS=1
      CF=1.
      DO 16 J=5,NC
      K=(I-3)*NC+J-2
      BHO(K)=19.*W(I,J)-8.*(W(I,J-1)+W(I,J+1)+W(I+IS,J))+2.*(W(I+IS,J-1)
     1+W(I+IS,J+1))+W(I+2*IS,J)+R4*(W(I-IS,J-1)+W(I-IS,J+1))+R5*W(I-IS,J
     1)+W(I,J+2)+W(I,J-2)
 16   ACD(K)=H*H*(T*P(K)-AA*DPA(K)-BHO(K)*DV*DV*DV*DV/CF)-B*H*VEA(K)
C     BOTTOM ROW(POINTS TYPE 22)
      I=MR+1
      IS=-1
      DO 17 J=5,NC
      K=(I-3)*NC+J-2
      BHO(K)=19.*W(I,J)-8.*(W(I,J-1)+W(I,J+1)+W(I+IS,J))+2.*(W(I+IS,J-1)
     1+W(I+IS,J+1))+W(I+2*IS,J)+R4*(W(I-IS,J-1)+W(I-IS,J+1))+R5*W(I-IS,J
     1)+W(I,J+2)+W(I,J-2)
 17   ACD(K)=H*H*(T*P(K)-AA*DPA(K)-BHO(K)*DV*DV*DV*DV/CF)-B*H*VEA(K)
C     LEFT COLUMN(POINTS TYPE 23)
      J=4
      JS=1
      DO 18 I=5,MR
      K=(I-3)*NC+J-2
      BHO(K)=19.*W(I,J)-8.*(W(I-1,J)+W(I+1,J)+W(I,J+JS))+2.*(W(I-1,J+JS)
     1+W(I+1,J+JS))+W(I,J+2*JS)+R4*(W(I-1,J-JS)+W(I+1,J-JS))+R5*W(I,J-JS
     1)+W(I-2,J)+W(I+2,J)
 18   ACD(K)=H*H*(T*P(K)-AA*DPA(K)-BHO(K)*DV*DV*DV*DV/CF)-B*H*VEA(K)
C     RIGHT COLUMN(POINTS TYPE 24)
      J=NC+1
      JS=-1
      DO 19 I=5,NC
```

```
      K=(I-3)*NC+J-2
      BHO(K)=19.*W(I,J)-8.*(W(I-1,J)+W(I+1,J)+W(I,J+JS))+2.*(W(I-1,J+JS)
     1+W(I+1,J+JS))+W(I,J+2*JS)+R4*(W(I-1,J-JS)+W(I+1,J-JS))+R5*W(I,J-JS
     1)+W(I-2,J)+W(I+2,J)
 19   ACD(K)=H*H*(T*P(K)-AA*DPA(K)-BHO(K)*DV*DV*DV*DV/CF)-B*H*VEA(K)
C     POINTS IN THE INTERIOR(5,5),(5,N),(M,5),(M,N)
C     POINTS TYPE 25.
      CF=1.
      DO 20 I=5,MR
      DO 20 J=5,NC
      K=(I-3)*NC+J-2
      BHO(K)=20.*W(I,J)-8.*(W(I,J-1)+W(I,J+1)+W(I-1,J)+W(I+1,J))
     1+2.*(W(I-1,J-1)+W(I-1,J+1)+W(I+1,J-1)+W(I+1, J+1))
     2+W(I-2,J)+W(I+2,J)+W(I,J-2)+W(I,J+2)
20    ACD(K)=H*H*(T*P(K)-AA*DPA(K)-BHO(K)*DV*DV*DV*DV/CF)-B*H*VEA(K)
C     END GENERATION OF EQUATIONS*************************************
C     TEST CONVERGENCE*****************
      MARK=0
      DO 500 I=1,NE
      ERROR=ABSF(ACD(I)-ACA(I))
      IF(ERROR-TOLER)500,500,600
 600  MARK=1
 500  CONTINUE
      IF(MARK)800,800,300
 800  DO 801 I=1,NE
      ACF(I)=ACD(I)
      VEF(I)=VEA(I)
 801  DPF(I)=DPA(I)
C     **************COMPUTE MOMENTS**********************************
      DO 601 I=3,MM
      DO 601 J=3,NN
      K=(I-3)*(NN-2)+J-2
 601  W(I,J)=DPF(K)
      MMM=MM-1
      NNN=NN-1
      DO 602 I=4,MMM
      DO 602 J=4,NNN
      K=(I-3)*(NN-2)+J-2
      BMX(K)=-C*(-(2.+2.*PR)*W(I,J)+W(I,J-1)+W(I,J+1)+PR*(W(I-1,J)+W(
     1I+1,J)))
      BMY(K)=-C*(-(2.+2.*PR)*W(I,J)+W(I-1,J)+W(I+1,J)+PR*(W(I,J-1)+W(I,J
     1+1)))
 602  BMXY(K)=C*(1.-PR)*(W(I-1,J-1)+W(I+1,J+1)-W(I+1,J-1)-W(I-1,J+1))/4.
C     TOP ROW***************************
      I=3
      IS=1
      DO 603 J=4,NNN
      K=(I-3)*NC+J-2
      BMX(K)=-C*(W(I,J-1)-2.*W(I,J)+W(I,J+1)+PR*(2.*W(I,J)-5.*W(I+IS,J)
     1+4.*W(I+2*IS,J)-W(I+3*IS,J)))
```

```
      BMY(K)=0.
  603 BMXY(K)=0.
C     BOTTOM ROW*************************
      I=MM
      IS=-1
      DO 604 J=4,NNN
      K=(I-3)*NC+J-2
      BMX(K)=-C*(W(I,J-1)-2.*W(I,J)+W(I,J+1)+PR*(2.*W(I,J)-5.*W(I+IS,J)
     1+4.*W(I+2*IS,J)-W(I+3*IS,J)))
      BMY(K)=0.
  604 BMXY(K)=0.
C     LEFT HAND COLUMN*****************
      J=3
      JS=1
      DO 605 I=4,MMM
      K=(I-3)*NC+J-2
      BMX(K)=0.
      BMY(K)=-C*(W(I-1,J)-2.*W(I,J)+W(I+1,J)+PR*(2.*W(I,J)-5.*W(I,J+JS)
     1+4.*W(I,J+2*JS)-W(I,J+3*JS)))
  605 BMXY(K)=0.
C     RIGHT HAND COLUMN
      J=NN
      JS=-1
      DO 606 I=4,MMM
      K=(I-3)*NC+J-2
      BMX(K)=0.
      BMY(K)=-C*(W(I-1,J)-2.*W(I,J)+W(I+1,J)+PR*(2.*W(I,J)-5.*W(I,J+JS)
     1+4.*W(I,J+2*JS)-W(I,J+3*JS)))
  606 BMXY(K)=0.
      DO 607 I=1,NE
      ANGLE(I)=ATANF(2.*BMXY(I)/(BMX(I)-BMY(I)))*.5*57.2958
      BMP1(I)=(BMX(I)+BMY(I))*.5+SQRTF(((BMX(I)-BMY(I))*.5)**2+BMXY(I)**
     12)
  607 BMP2(I)=(BMX(I)+BMY(I))*.5-SQRTF(((BMX(I)-BMY(I))*.5)**2+BMXY(I)**
     12)
C     END MOMENT EVALUATION**********************
C     BEGIN MAXIMUM QUANTITIES EVALUATION IN SPACE*********************
      BMP1MS=0.
      BMP2MS=0.
      DPFMS=0.
      DO 608 I=1,NE
      IF(ABSF(BMP1(I))-ABSF(BMP1MS))608,608,609
  609 BMP1MS=BMP1(I)
      ANG1=ANGLE(I)
      MP1S=I
  608 CONTINUE
      DO 700 I=1,NE
      IF(ABSF(BMP2(I))-ABSF(BMP2MS))700,700,701
  701 BMP2MS=BMP2(I)
      ANG2=ANGLE(I)
```

```
      MP2S=I
 700  CONTINUE
      DO 702 I=1,NE
      IF(ABSF(DPF(I))-ABSF(DPFMS))702,702,703
 703  DPFMS=DPF(I)
      MDS=I
 702  CONTINUE
C     ENDIN MAXIMUM QUANTITIES EVALUATION********************************
C     BEGIN MAXIMUM QUANTITIES EVALUATION IN TIME***********************
      IF(ABSF(BMP1MS) -ABSF(BMP1ST))704,704,705
 705  BMP1ST=BMP1MS
      LOCMP1=MP1S
      ANG1T=ANG1
      TMP1ST=TIME
 704  IF(ABSF(BMP2MS) -ABSF(BMP2ST))706,706,707
 707  BMP2ST=BMP2MS
      LOCMP2=MP2S
      ANG2T=ANG2
      TMP2ST=TIME
 706  IF(ABSF(DPFMS)-ABSF(DPFST))708,708,709
 709  DPFST=DPFMS
      LOCDPF=MDS
      TDPST=TIME
 708  CONTINUE
C     END MAX EVALUATION IN TIME****************************************
      JJ=JJ+1
      IF(JJ-NP) 802,803,803
 803  CONTINUE
      PRINT 8031,TIME
 8031 FORMAT(1H0,55X,5HTIME=,F8.7)
      PRINT 804,MDS,DPFMS,MP1S,BMP1MS,MP2S,BMP2MS
 804  FORMAT(1H0,4HMDS=,I3,3X,6HDPFMS=,F9.7,3X,5HMP1S=,I3,3X,7HBMP1MS=,
     1F9.7,3X,5HMP2S=,I3,3X,7HBMP2MS=,F9.7)
      PRINT 8044,ANG1,ANG2
 8044 FORMAT(1H ,5HANG1=,F7.3,5X,5HANG2=,F7.3)
      JJ=0
 802  GOTO 200
 900  CONTINUE
      PRINT 8050,TDPST,LOCDPF,DPFST
 8050 FORMAT(1H0,6HTDPST=,F9.7,3X,7HLOCDPF=,I3,3X,6HDPFST=,F9.7)
      PRINT 8051,TMP1ST,LOCMP1,BMP1ST
 8051 FORMAT(1H ,7HTMP1ST=,F9.7,3X,7HLOCMP1=,I3,3X,7HBMP1ST=,F9.7)
      PRINT 8052,TMP2ST,LOCMP2,BMP2ST
 8052 FORMAT(1H ,7HTMP2ST=,F9.7,3X,7HLOCMP2=,I3,3X,7HBMP2ST=,F9.7)
      PRINT 8053,ANG1T,ANG2T
 8053 FORMAT(1H ,6HANG1T=,F7.3,5X,6HANG2T=,F7.3)
 1000 CONTINUE
 1001 CONTINUE
      END
      END
```

APPENDIX B
EXACT SOLUTIONS

The "exact" solution of the problem of forced vibrations of a simply supported rectangular plate resting on an elastic foundation is presented here. It has been used as a basis of comparison for the evaluation of the accuracy of method presented in the thesis.

Referring to the same plate as described in section 2.1, the exact solution of Equation 1 may be written as:

$$w = \sum_{i=1}^{\infty} \sum_{j=1}^{\infty} S_{ij} T_{ij} \tag{B1}$$

where $S_{ij} = \sin \frac{i\pi x}{a} \sin \frac{j\pi y}{b}$, and T_{ij} is a function of time only. Also assume the loading function be given as:

$$P(x, y, t) = G(x, y) F(t) \tag{B2}$$

where, G(x, y) is a function of the space coordinates, "x" and "y" only and F(t) is a function of time, t only.

Let G(x, y) be expanded in a double sine series:

$$G(x, y) = \sum_{i-1}^{\infty} \sum_{j=1}^{\infty} g_{ij} \sin \frac{i\pi x}{a} \sin \frac{j\pi y}{b} \tag{B3}$$

in which

$$g_{ij} = \frac{4}{ab} \int_{o}^{a} \int_{o}^{b} G(x, y) \sin \frac{i\pi x}{a} \sin \frac{j\pi y}{b} \, dxdy \tag{B4}$$

Substituting the preceding expressions (B1), (B2), and (B3) into the equation of motion, Equation 1 of section 2.1, the following equation is obtained:

$$\sum_{i=1}^{\infty} \sum_{j=1}^{\infty} \left(\frac{i\pi}{a}\right)^4 S_{ij} T_{ij} + \frac{2(i\pi)^2 (j\pi)^2}{ab} S_{ij} T_{ij} + \left(\frac{j\pi}{b}\right)^4 S_{ij} T_{ij}$$

$$+ \frac{k}{D} S_{ij} T_{ij} + \frac{c}{D} S_{ij} \dot{T}_{ij} + \frac{m}{D} S_{ij} \ddot{T}_{ij} - \frac{q_{ij}}{D} S_{ij} F(t) = 0 \qquad (B5)$$

Since S_{ij} is not identically zero, one obtains:

$$\ddot{T}_{ij} + 2r \dot{T}_{ij} + p_{ij}^2 T_{ij} = \frac{q_{ij}}{m} F(t) \qquad (B6)$$

where $r = \frac{c}{2m}$, and p_{ij} is the natural undamped circular frequency of the $(i, j)^{th}$ mode of the plate:

$$p_{ij} = \sqrt{\frac{D}{m} \left[\left\{ \left(\frac{i\pi}{a}\right)^2 + \left(\frac{j\pi}{b}\right)^2 \right\}^2 + \frac{k}{D} \right]} \qquad (B7)$$

For the case of zero initial displacement and velocity the solution of Equation (B6) may be written[1] as

$$T_{ij} = \frac{q_{ij}}{mq_{ij}} \int_0^t F(\tau)\, e^{-r(t-\tau)} \sin q_{ij}(t-\tau)\, d\tau \qquad (B8)$$

in which q_{ij} is the damped natural circular frequency given by

$$q_{ij} = \sqrt{p_{ij}^2 - r^2} \qquad (B9)$$

The "critical damping" c_{cr} for the system can be obtained by setting $q_{ij}^2 = 0$, thus;

$$c_{cr}(i, j) = 2\sqrt{km}\sqrt{\left[1 + \frac{D}{k} \left\{ \left(\frac{i\pi}{a}\right)^2 + \left(\frac{j\pi}{b}\right)^2 \right\}^2 \right]} \qquad (B10)$$

[1] Timoshenko (38), pp. 104-109.

It may be observed that the factor inside the bracket shows effect of the flexural rigidity of the plate and the mode shapes (value of i and j) on the value of the critical damping for the $(i, j)^{th}$ mode.

For any given loading the solution can be obtained from Equation Bl by use of Equations B4 and B8. The exact solutions of the various problems that have been used for purposes of comparison in the text of this thesis are given in the following.

1. <u>Triangular Pulse Loading</u>: In this case $P(x, y, t) = P(1 - \frac{t}{t_1})$ is constant over the entire plate and taking $r = 0$ (no damping), for a square plate, Equation B4 yields:

$$q_{ij} = \frac{16P}{\pi^2 ij}$$

Equation B8 yields:

$$T_{ij} = \frac{16P}{\pi^2 mij\, p_{ij}^2} \int_o^t (1 - \frac{\tau}{t_1}) \sin p_{ij} (t-\tau)\, d\tau$$

$$= \frac{16P}{\pi^2 mij\, p_{ij}^2} \left(1 - \frac{t}{t_1} - \cos p_{ij} t + \frac{\sin p_{ij} t}{t_1 p_{ij}}\right)$$

finally substituting into Equation Bl one has

$$w(x, y, t) = \frac{16P}{\pi^2 m} \sum_{i=1}^{\infty} \sum_{j=1}^{\infty} \frac{1}{ij\, p_{ij}^2} \left[1 - \frac{t}{t_1} + \frac{\sin p_{ij} t}{t_1\, p_{ij}} - \cos p_{ij} t\right]$$

$$\sin \frac{i\pi x}{a} \sin \frac{j\pi y}{b} \qquad \text{(B11)}$$

for $t < t_1$.

Bending moments are calculated from:

$$M_x = -D\left(\frac{\partial^2 w}{\partial x^2} + \nu \frac{\partial^2 w}{\partial y^2}\right)$$

$$M_y = -D\left(\frac{\partial^2 w}{\partial y^2} + \nu \frac{\partial^2 w}{\partial x^2}\right) \qquad \text{(B12)}$$

$$M_{xy} = D\,(1-\nu)\,\frac{\partial^2 w}{\partial x \partial y}$$

2. Partial Loading: The loading is the same as the preceding one except that it is applied over an area u x v whose center is located at (ζ, η). In this case Equation B4 yields:

$$q_{ij} = \frac{16P}{\pi^2 ij\, uv} \sin\frac{i\pi\zeta}{a} \sin\frac{j\pi\eta}{b} \sin\frac{i\pi u}{2a} \sin\frac{\partial\pi v}{2b}$$

When the load is concentrated, i.e., $u, v \rightarrow 0$ and $P \cdot u \cdot v \rightarrow F$ (a constant), the above equation yields:

$$q_{ij} = \frac{4F}{ab} \sin\frac{i\pi\zeta}{a} \sin\frac{j\pi\eta}{b}$$

The complete solution can be written as before.

3. Rectangular Pulse: The load P is applied uniformly over the plate. In this case the effect of foundation damping is also included. From Equations B4 and B8 one obtains, respectively

$$q_{ij} = \frac{16P}{\pi^2 ij}$$

$$T_{ij} = \frac{16P}{m\pi^2 ij q_{ij}} \int_o^t e^{-r(t-\tau)} \sin q_{ij}(t-\tau)\, d\tau$$

$$= \frac{16P}{\pi^2 ij\, m} \left[\frac{1}{r^2 + q_{ij}^2} \left\{ 1 - \frac{e^{-rt}}{q_{ij}} (r \sin q_{ij} t + q_{ij} \cos q_{ij} t) \right\} \right]$$

The complete solution is given by Equation B1 as:

$$w(x,y,t) = \frac{16P}{m\pi^2} \sum_{i=1}^{\infty} \sum_{j=1}^{\infty} \frac{1}{ij(r^2 + q_{ij}^2)} \left[1 - e^{-rt} \left(\frac{r}{q_{ij}} \sin q_{ij} t + \cos q_{ij} t \right) \right]$$

$$\sin \frac{i\pi x}{a} \sin \frac{j\pi y}{b}$$

for all $t > 0$ and $c_{ij} < c_{cr}(ij)$ (B13)

TABLE 1. COMPARISON OF RESULTS OBTAINED BY RUNGE-KUTTA AND BETA METHODS (τ = .0625 AND τ = .125)

Time increment $\Delta\tau$	Method of solution	τ = .0625		τ = .125	
		Deflection (u = w/h)	Moment (Ma/D)	Deflection (u = w/h)	Moment (Ma/D)
	Exact	.0027852	.0054363	.0024640	.0023591
$1/10\ n^2$	Runge-Kutta	.0027480	.0048949	.0025019	.0027559
	Beta = 0	.0027512	.0048474	.0025021	.0027973
	Beta = 1/6	.0027462	.0046217	.0025019	.0027462
$1/5\ n^2$	Runge-Kutta	.0027478	.0046850	.0025018	.0027483
	Beta = 0	.0027589	.0051735	.0024948	.0023365
	Beta = 1/6	.0027412	.0044529	.0025025	.0027645
$1/4\ n^2$	Runge-Kutta	.0027477	.0046896	.0025017	.0027365
	Beta = 0	.0027619	.0052392	.0025015	.0027001
	Beta = 1/6	.0027401	.0044650	.0025034	.0028201
$1/3\ n^2$	Runge-Kutta	.0027481	.0047205	.0025018	.0027367
	Beta = 0	unstable	unstable	unstable	unstable
	Beta = 1/6	unstable	unstable	unstable	unstable
$1/2.5\,n^2$	Runge-Kutta	unstable	unstable	unstable	unstable
	Beta = 0	unstable	unstable	unstable	unstable
	Beta = 1/6	unstable	unstable	unstable	unstable

TABLE 2. COMPARISON OF RESULTS OBTAINED BY RUNGE-KUTTA AND BETA METHODS FOR MAXIMUM VALUES OF RESPONSES

Time increment $\Delta\tau$	Method of solution	Maximum deflection ($u = w/h$)		Maximum moments (Ma/D)	
		Instant	Magnitude	Instant	Magnitude
	Exact	.0906250	.0044553	.0812500	.0114936
$1/10\ n^2$	Runge-Kutta	.0933594	.0045647	.0941406	.0120576
	Beta = 0	.0933594	.0045688	.0937500	.0122500
$1/5\ n^2$	Runge-Kutta	.0937500	.0045633	.0937500	.0119689
	Beta = 0	.0927688	.0045739	.0929688	.0123821
$1/4\ n^2$	Runge-Kutta	.0937500	.0045624	.0937500	.0119323
	Beta = 0	.0927734	.0045718	.0917969	.0123091
$1/3\ n^2$	Runge-Kutta	.0937500	.0045606	.9375000	.0118662
	Beta = 0	unstable	unstable	unstable	unstable

TABLE 3. COMPARISON OF NUMERICAL AND EXACT VALUES OF MAXIMUM RESPONSES FOR CENTERPOINT

(DEFLECTION)

Method of solution	Time ($\tau = t/T_o$)	Maximum deflection ($u = w/h$)	% error in time	% error in deflections
Exact	.0927083	.0014727		
n = 4	.0937500	.0014904	1.1	1.2
n = 8	.0890625	.0014720	-3.9	0
n = 12	.0951389	.0014700	2.6	- 0.1
n = 16	.0933594	.0014747	0.7	0.1
n = 20	.0937500	.0014738	1.1	0.1
n = 24	.0927083	.0014750	0	0.2

(MOMENT)

Method of solution	Time ($\tau = t/T_o$)	Maximum moment (Ma/D)	% error in time	% error in moment
Exact	.1135000	.0019342		
n = 4	.0937500	.0018623	-17.4	-3.7
n = 8	.0765625	.0018244	-31.6	-5.7
n = 12	.0666670	.0018835	-41.3	-2.6
n = 16	.1156250	.0019921	1.9	3.0
n = 20	.1135000	.0019908	0	2.9
n = 24	.1177083	.0019823	3.7	2.5

TABLE 4. COMPARISON OF NUMERICAL AND EXACT VALUES OF MAXIMUM RESPONSES FOR QUARTER POINT

(DEFLECTION)

Method of solution	Time ($\tau = t/T_o$)	Maximum deflection ($u = w/h$)	% error in time	% error in deflection
Exact	.0955000	.0010955		
n = 4	.0937500	.0010249	-1.8	-6.5
n = 8	.0953125	.0010781	-0.2	-1.6
n = 12	.0951389	.0010904	-0.4	-0.5
n = 16	.0945313	.0010922	-1.0	-0.3
n = 20	.0955000	.0010939	0	-0.1
n = 24	.0937500	.0010945	-1.8	-0.1

(MOMENT)

Method of solution	Time ($\tau = t/T_o$)	Maximum moment (Ma/D)	% error in time	% error in moment
Exact	.0989583	.0015198		
n = 4	.1000000	.0011621	1.1	-23.5
n = 8	.1000000	.0014512	1.1	-4.5
n = 12	.1013889	.0014479	2.4	4.7
n = 16	.1058594	.0015324	7.2	0.8
n = 20	.0970000	.0015515	2.0	2.1
n = 24	.0989583	.0015682	0	3.2

TABLE 5. COMPARISON OF NUMERICAL AND EXACT VALUES OF MAXIMUM RESPONSES FOR CENTER POINT FOR SHRINKING AREA LOADING

Method of solution	Maximum deflection (u = w/h)		Maximum moment (Ma/D)	
	Instant	Magnitude	Instant	Magnitude
Exact	.0885417	.0045861	-	-
n = 4	.1250000	.0039174	.0375000	.0094701
n = 8	.1062500	.0046439	.1078125	.0128272
n = 12	.0930556	.0048937	.0916667	.0177950
n = 16	.0937500	.0048373	.0941406	.0186278
n = 20	.0905000	.0047537	.0880000	.0190685
n = 24	.0885417	.0047438	.0881944	.0200436

TABLE 6. COMPARISON OF NUMERICAL AND EXACT VALUES OF MAXIMUM RESPONSES FOR QUARTER POINT FOR SHRINKING AREA LOADING

Method of solution	Maximum deflection (u = w/h)		Maximum moment (Ma/D)	
	Instant	Magnitude	Instant	Magnitude
Exact	.0968750	.0027068	.0750000	.0039659*
n = 4	.1062500	.0028196	.1062500	.0040440
n = 8	.0890625	.0026812	.0687500	.0037722
n = 12	.1048611	.0027166	.1055556	.0041591
n = 16	.0976563	.0027224	.0781250	.0040260
n = 20	.0980000	.0027008	.0752500	.0046592
n = 24	.0993056	.0027086	.0756944	.0048213

*Slowly convergent series (i, j = 61).

TABLE 7. COMPARISON OF NUMERICAL AND EXACT VALUES OF MAXIMUM RESPONSES FOR CENTER POINT FOR PARTIAL LOADING

Method of solution	Maximum deflection ($u = w/h$)		Maximum moment (Ma/D)	
	Instant	Magnitude	Instant	Magnitude
Exact	.0906250	.0045530	.0812500	.0114936
n = 4	.1250000	.0039174	.0375000	.0094701
n = 8	.1062500	.0046439	.1078125	.0128272
n = 16	.0933594	.0045688	.0937500	.0122500

TABLE 8. COMPARISON OF NUMERICAL AND EXACT VALUES OF MAXIMUM RESPONSES FOR QUARTER POINT FOR PARTIAL LOADING

Method of solution	Maximum deflection ($u = w/h$)		Maximum moment (Ma/D)	
	Instant	Magnitude	Instant	Magnitude
Exact	.0968750	.0026678	.0718750	.0035596
n = 4	.1062500	.0028196	.1062500	.0040440
n = 8	.0890625	.0026812	.0687500	.0037722
n = 16	.0980469	.0026583	.0789063	.0033425

TABLE 9. MAXIMUM DEFLECTION, MOMENT AND THEIR LOCATIONS OF OCCURRENCE FOR A FREE PLATE DUE TO IMPULSE APPLIED AT CORNER

Time $\tau = (t/T_o)$	Maximum deflection ($u = w/h$)		Maximum principal moment ($M'_2 = M_2 a/D$)		
	Location	Magnitude	Location	Magnitude	Angle (^{o})
.00625	(1, 1)	.0020594	(2, 3)	-.0106407	-33.99
.01250	(1, 1)	.0052294	(3, 3)	-.0155448	45
.01875	(1, 1)	.0084516	(4, 2)	-.0170862	31.11
.02500	(1, 1)	.0115648	(4, 3)	-.0173257	39.06
.03125	(1, 1)	.0144917	(2, 5)	-.0173016	-29.54
.03750	(1, 1)	.0171819	(2, 6)	-.0168504	-26.78
.04375	(1, 1)	.0195983	(2, 6)	-.0164369	-27.95
.05000	(1, 1)	.0217115	(6, 2)	-.0157487	28.90
.05625	(1, 1)	.0235093	(8, 2)	-.0152735	22.58
.06250	(1, 1)	.0249184	(7, 2)	-.0147616	26.34
.06875	(1, 1)	.0260576	(5, 5)	-.0143696	-45
.07500	(1, 1)	.0269365	(4, 3)	-.0129368	42.06
.08125	(1, 1)	.0272545	(3, 10)	-.0135985	-26.42
.08750	(1, 1)	.0267395	(11, 1)	-.0130943	0
.09375	(1, 1)	.0264301	(8, 9)	-.0118132	-41.86
.10000	(1, 1)	.0261363	(9, 8)	-.0124041	39.31
.10625	(1, 1)	.0253643	(10, 6)	-.0108537	26.76
.11250	(1, 1)	.0241840	(4, 8)	-.0075699	-36.19
.11875	(1, 1)	.0229904	(6, 6)	-.0099431	-45
.12500	(1, 1)	.0216093	(16, 10)	-.0093487	-22.02
.13125	(1, 1)	.0196472	(16, 10)	-.0081454	-31.43
.13750	(1, 1)	.0165115	(17, 7)	-.0099522	0
.14375	(1, 1)	.0131160	(17, 6)	-.0109074	0
.15000	(1, 1)	.0092761	(17, 6)	-.0102734	0
.15625	(6, 1)	.0067519	(17, 4)	-.0093470	0
.16250	(8, 1)	.0060155	(7, 17)	-.0076295	0
.16875	(8, 1)	.0054800	(17, 7)	-.0076760	0
.17500	(17, 17)	-.0052681	(3, 3)	-.0059784	-45
.18125	(17, 17)	-.0063015	(3, 3)	-.0055748	-45
.18750	(17, 17)	-.0071057	(10, 7)	-.0043090	-40.75
.19375	(17, 17)	-.0079991	(12, 12)	-.0056715	45
.20000	(17, 17)	-.0090625	(14, 14)	-.0082439	-45

TABLE 10. COMPARISON OF MAXIMUM VALUE OF RESPONSES WITH DAMPING AND WITHOUT DAMPING

MAXIMUM DEFLECTION (u)

Amount of damping	Time ($\tau = t/T_o$)	Location	Magnitude	Angle (°)
$\beta = 0$	.0796875	(1, 1)	.0272863	-
$\beta = 56.52$	.0757813	(1, 1)	.0133758	-

MAXIMUM PRINCIPAL MOMENT (M'_1)

$\beta = 0$	.1757812	(1, 8)	.0144665	0
$\beta = 56.52$	.0355469	(2, 2)	.0077713	-45

MAXIMUM PRINCIPAL MOMENT (M'_2)

$\beta = 0$	.0285156	(5, 2)	-.0174413	28.82
$\beta = 56.52$	.0222656	(3, 3)	-.0140118	-45

TABLE 11. MAXIMUM RESPONSE VALUES FOR DIFFERENT PULSE SHAPES APPLIED AT CORNER POINT OF FREE PLATE

MAXIMUM DEFLECTION ($u = w/h$)

Rise time (Fig. 24)	Time ($\tau = t/T_o$)	Location	Magnitude	Angle (°)
$t_o = 0$	.0796875	(1, 1)	.0272863	-
$t_o = .025$	.0933594	(1, 1)	.0282670	-
$t_o = .05$	.1062500	(1, 1)	.0293000	-
$t_o = .075$	.1175781	(1, 1)	.0301443	-

PRINCIPAL MOMENT ($M'_1 = M \cdot a/D$)

$t_o = 0$	.01757812	(1, 8)	.0144665	0
$t_o = .025$	.0535156	(2, 2)	.0109976	0
$t_o = .05$	.0710938	(2, 2)	.0115884	45
$t_o = .075$	.0863281	(2, 2)	.0117586	45

PRINCIPAL MOMENT ($M'_2 = M_2 a/D$)

$t_o = 0$	.0285156	(5, 2)	-.0174413	28.82
$t_o = .025$	.0441406	(2, 5)	-.0182763	-29.47
$t_o = .05$	.0644531	(2, 5)	-.0185709	-30.71
$t_o = .075$	.0843750	(2, 5)	-.0185767	40.19

TABLE 12. MAXIMUM RESPONSE VALUES FOR LOADING APPLIED AT DIFFERENT POINTS ALONG EDGE OF FREE-PLATE

MAXIMUM DEFLECTION ($u = w/h$)

Position of load	Time ($\tau = t/T_o$)	Location	Magnitude	Angle (^{o})
(1, 1)	.0796875	(1, 1)	.0272863	-
(2, 1)	.081250	(1, 1)	.0251775	-

MAXIMUM PRINCIPAL MOMENT ($M'_1 = M_1 a/D$)

(1, 1)	.1757812	(1, 8)	.0144665	0
(2, 1)	.1765625	(1, 8)	.0133560	0

MAXIMUM PRINCIPAL MOMENT ($M'_2 = M_2 a/D$)

(1, 1)	.0285156	(5, 2)	-.0174413	28.82
(2, 1)	.0289062	(2, 5)	-.0153038	-24.54

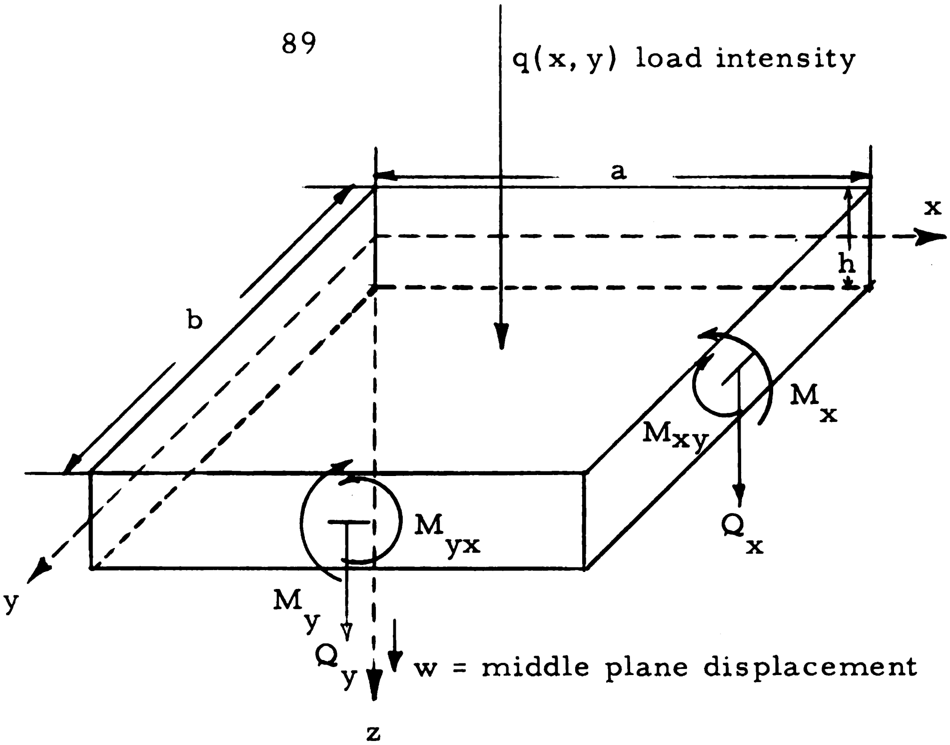

FIG. 1. PLATE NOTATION

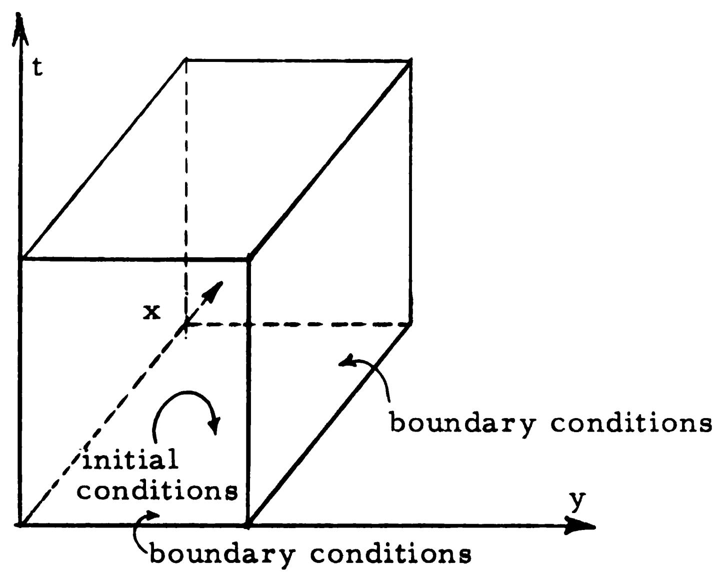

FIG. 2. PICTORIAL REPRESENTATION OF PROPAGATION PROBLEM

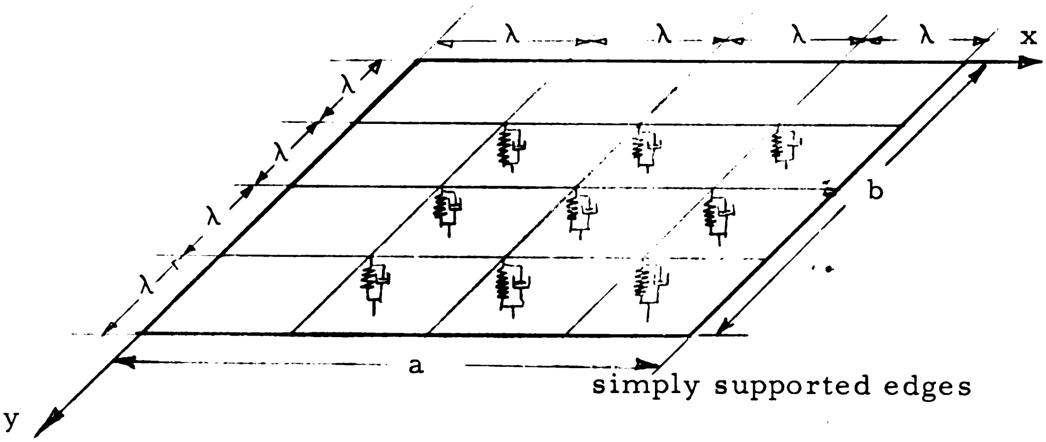

FIG. 3. PHYSICAL MODEL OF DISCRETE SYSTEM

$$\nabla^4 u = \frac{1}{\lambda^4}\begin{bmatrix} & & 1 & & \\ & 2 & -8 & 2 & \\ 1 & -8 & 20 & -8 & 1 \\ & 2 & -8 & 2 & \\ & & 1 & & \end{bmatrix} u + O(\lambda^2)$$

FIG. 4. BIHARMONIC OPERATOR

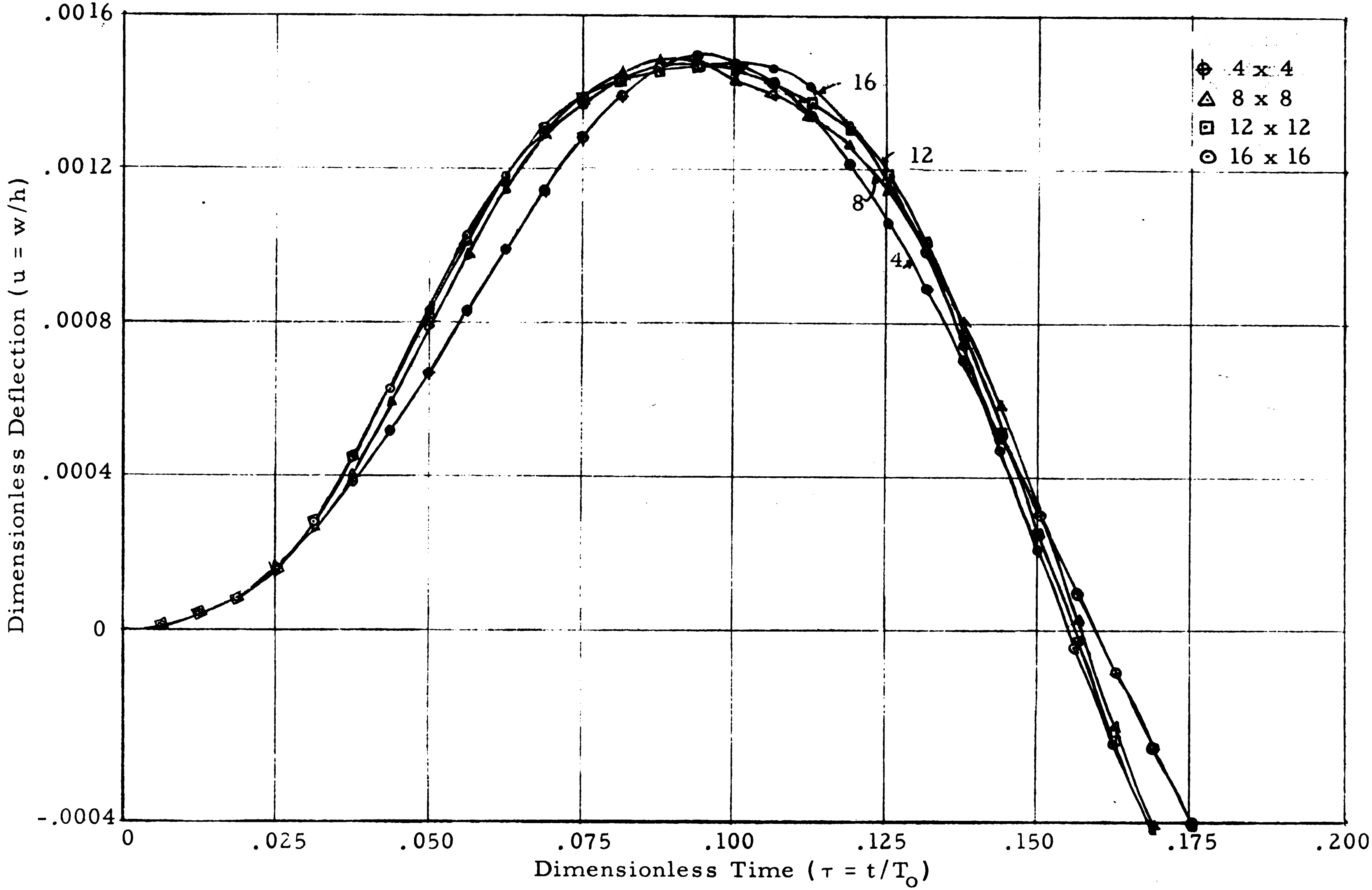

FIG. 5. RESPONSE HISTORIES FOR CENTER POINT DEFLECTION FOR VARIOUS GRID SIZES

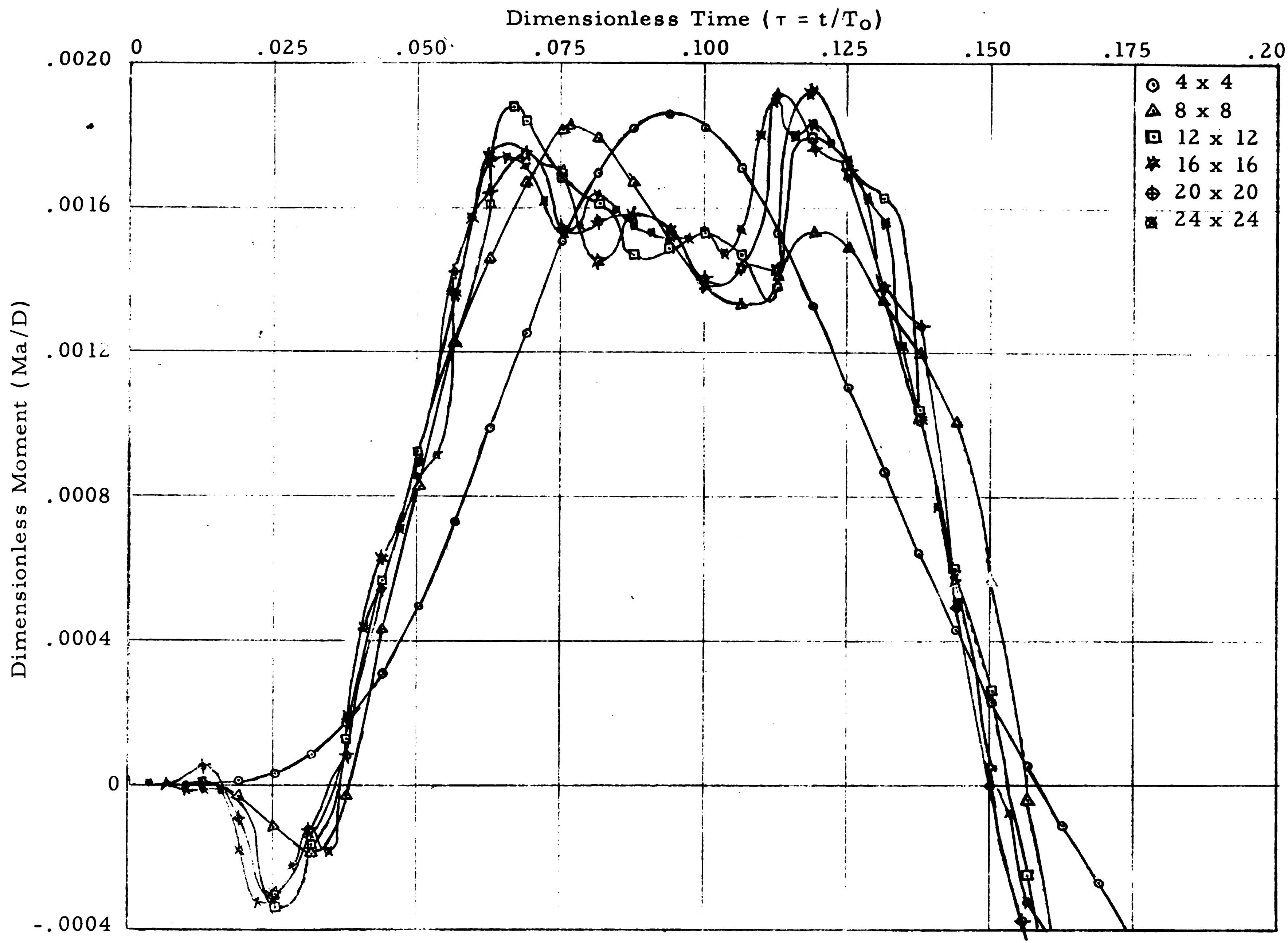

FIG. 6. RESPONSE HISTORIES FOR CENTER POINT MOMENT FOR VARIOUS GRID SIZES

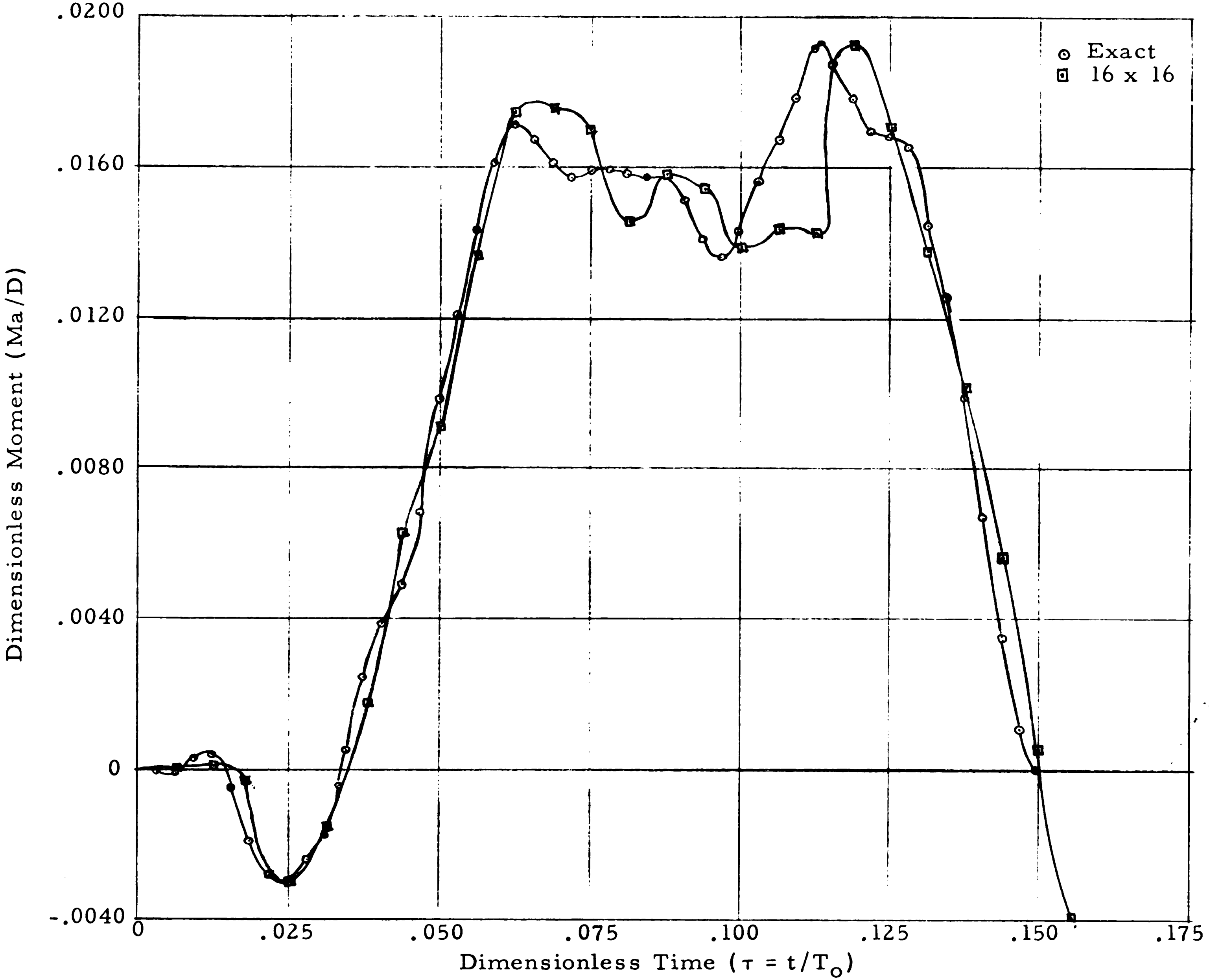

FIG. 7. COMPARISON OF NUMERICAL AND EXACT SOLUTIONS FOR CENTER POINT MOMENT

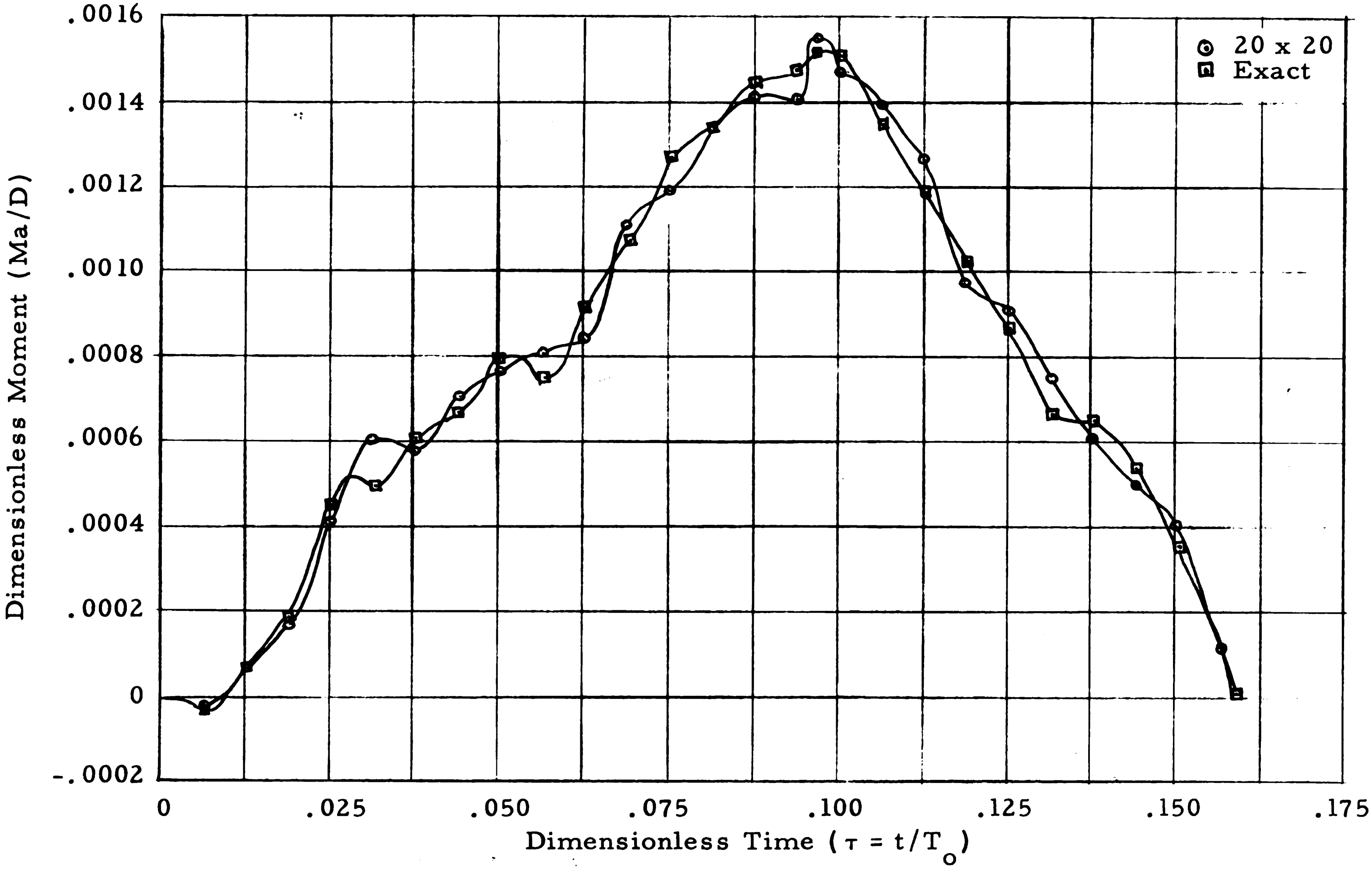

FIG. 8. COMPARISON OF NUMERICAL AND EXACT SOLUTIONS FOR QUARTER POINT MOMENT

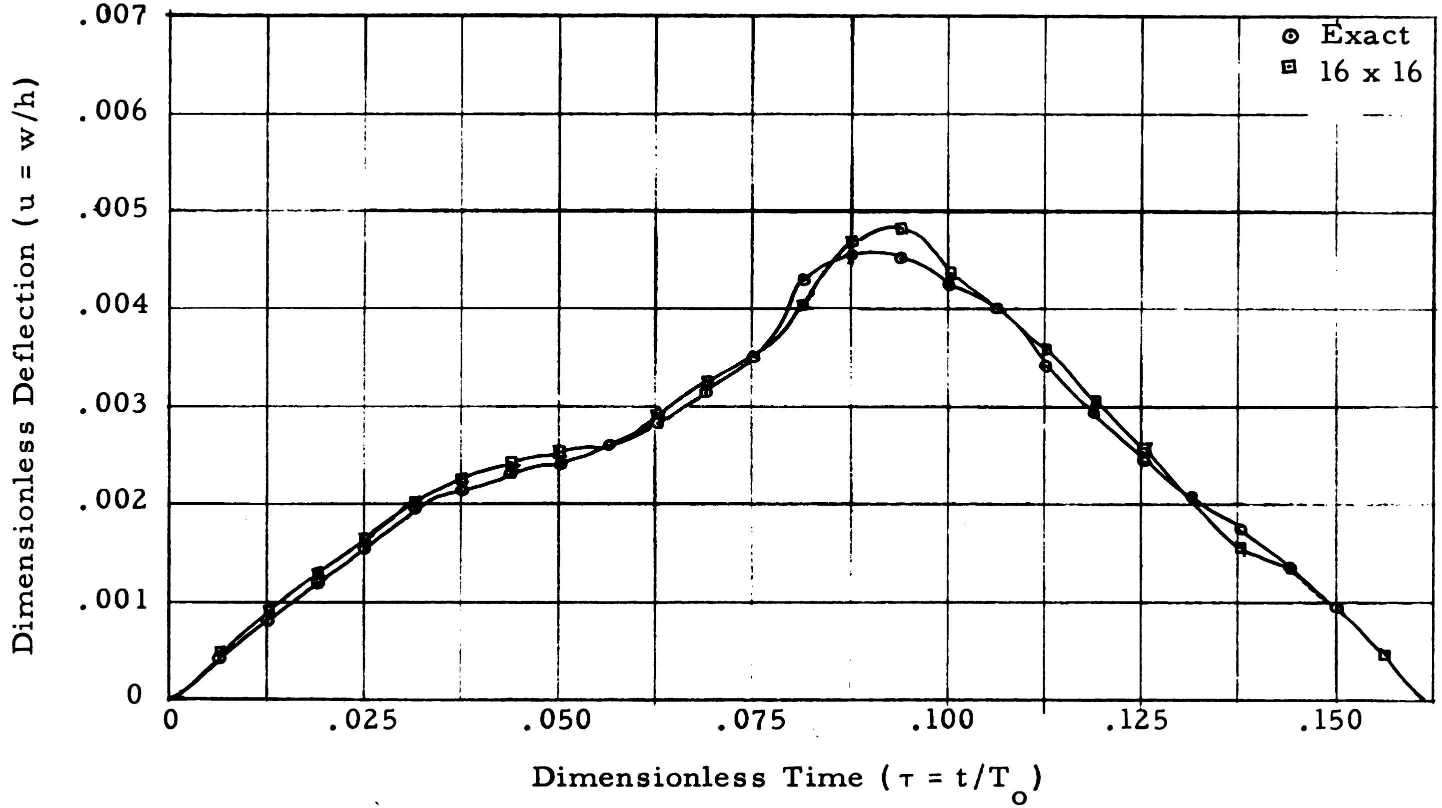

FIG. 9. COMPARISON OF NUMERICAL AND EXACT SOLUTIONS FOR CENTER POINT DEFLECTION FOR SHRINKING AREA LOADING

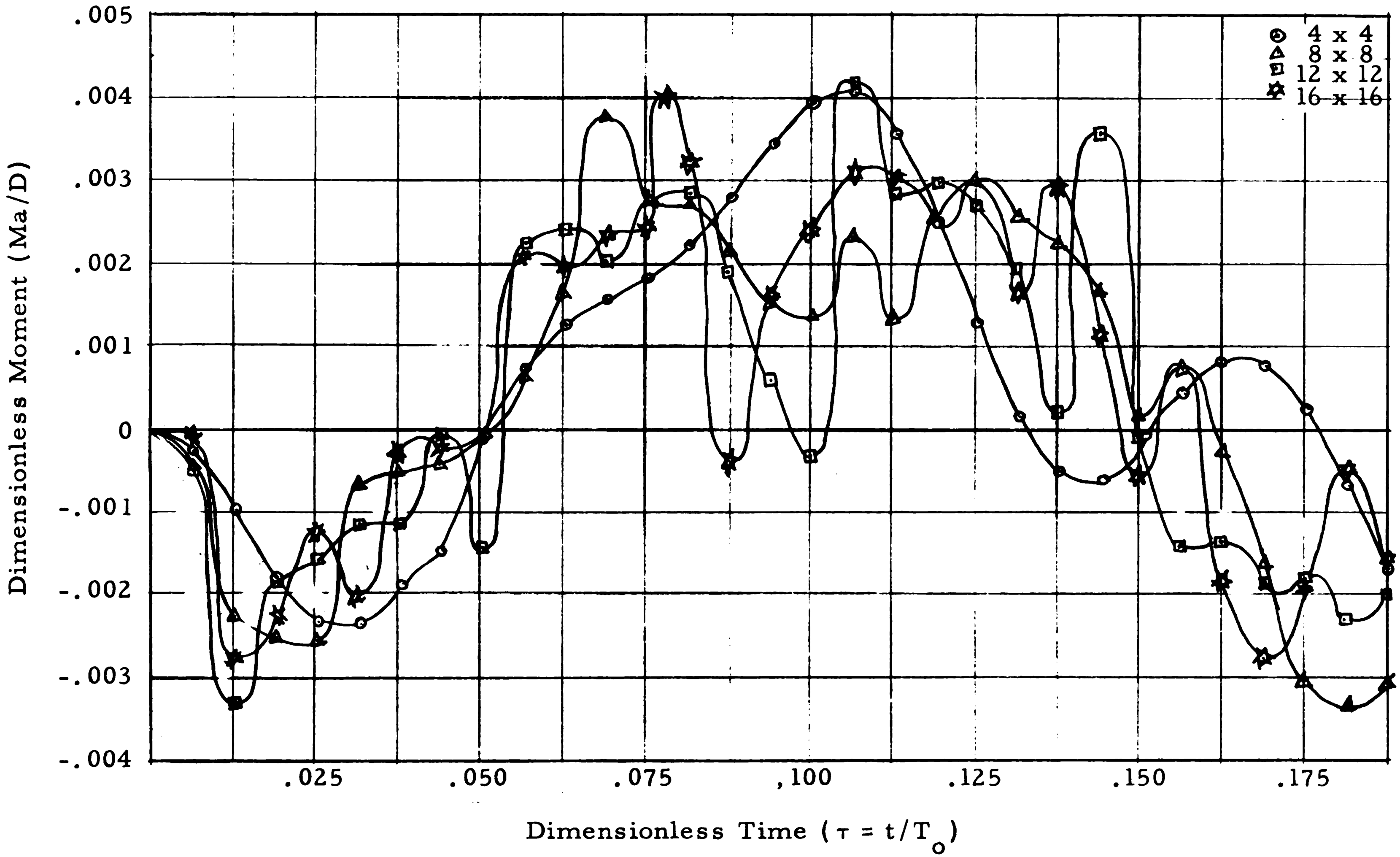

FIG. 10. RESPONSE HISTORIES FOR QUARTER POINT MOMENT FOR VARIOUS GRID SIZES FOR SHRINKING AREA LOADING

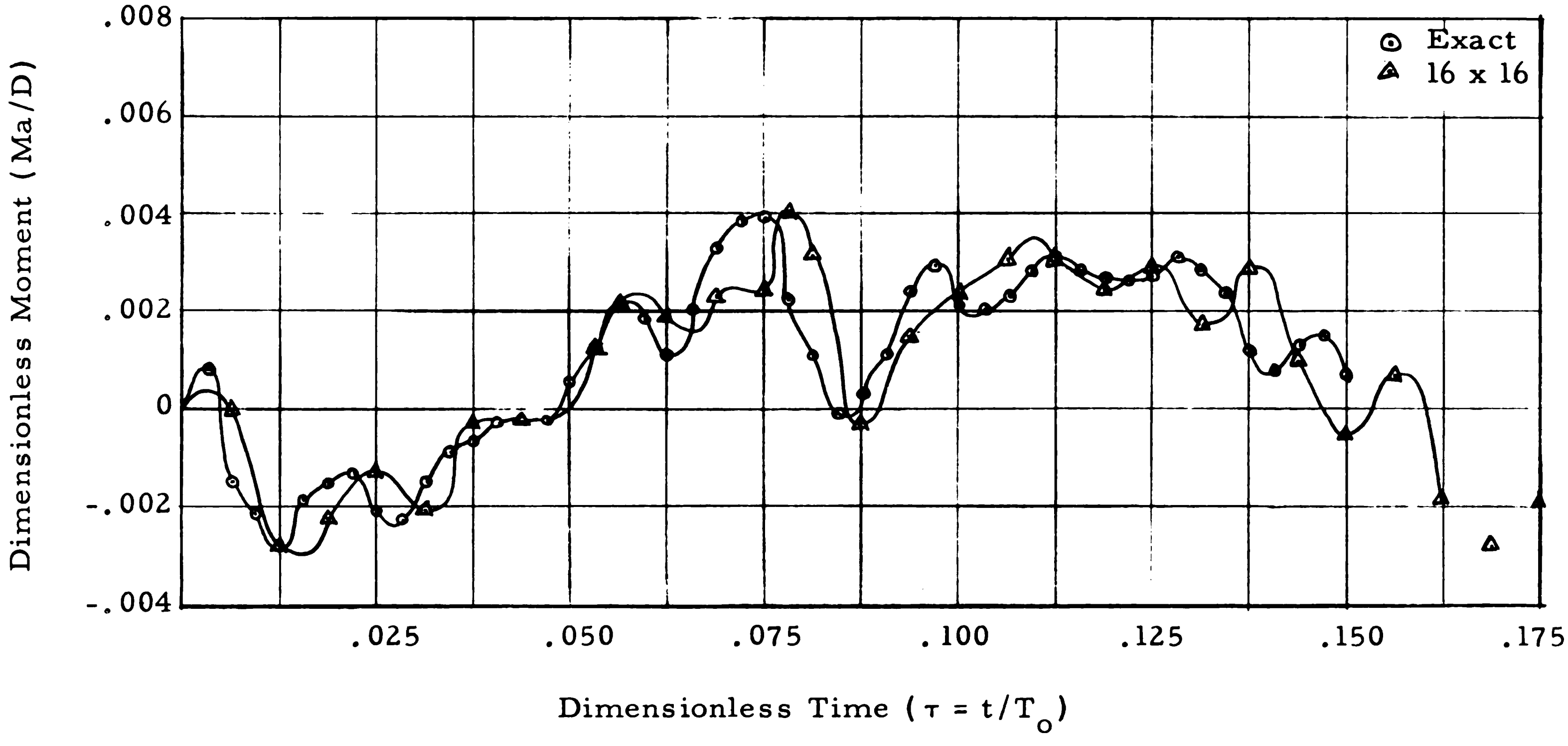

FIG. 11. COMPARISON OF NUMERICAL AND EXACT SOLUTIONS FOR QUARTER POINT MOMENT FOR SHRINKING AREA LOADING

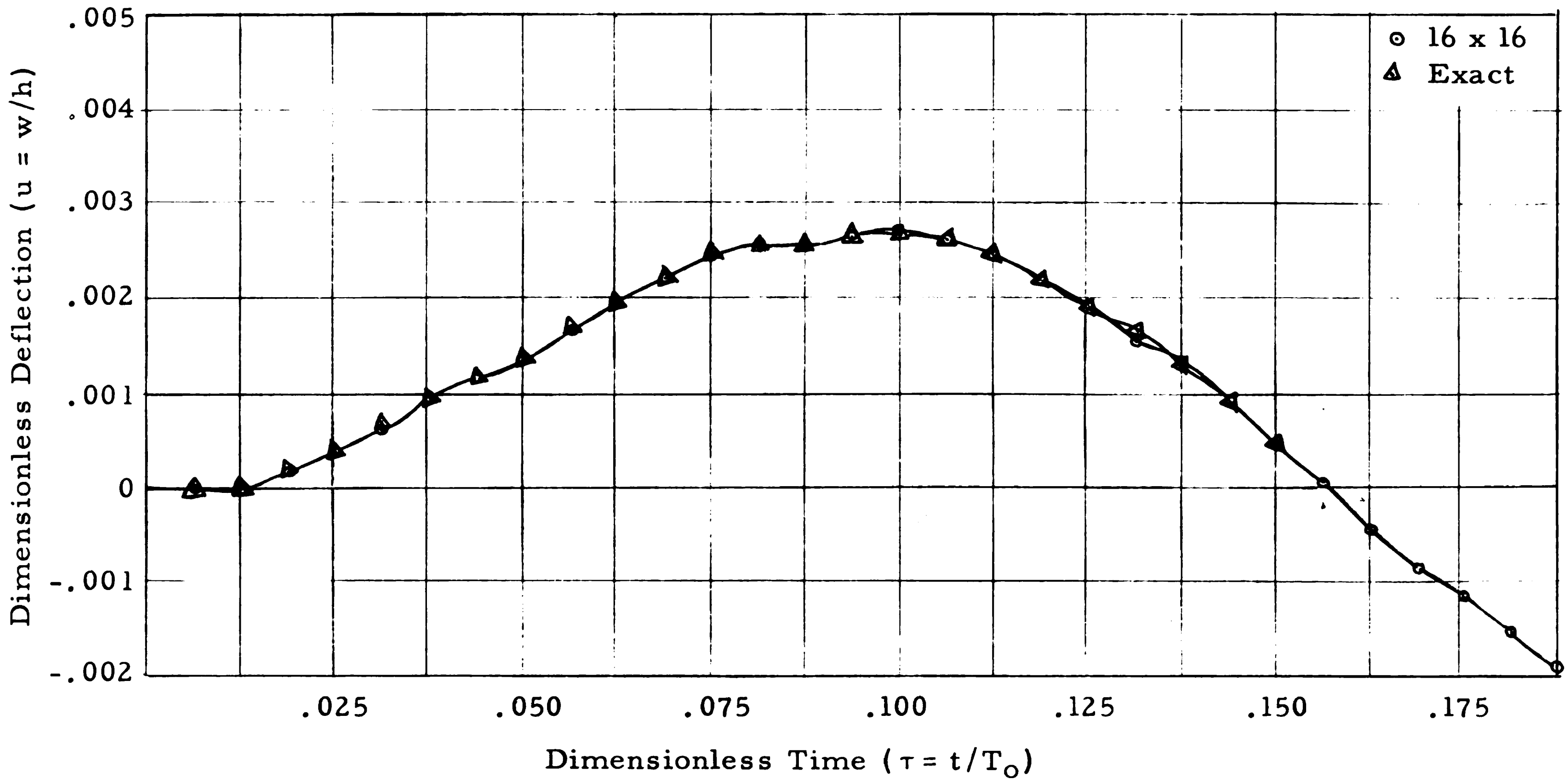

FIG. 12. COMPARISON OF NUMERICAL AND EXACT SOLUTIONS FOR QUARTER POINT DEFLECTION FOR SHRINKING AREA LOADING

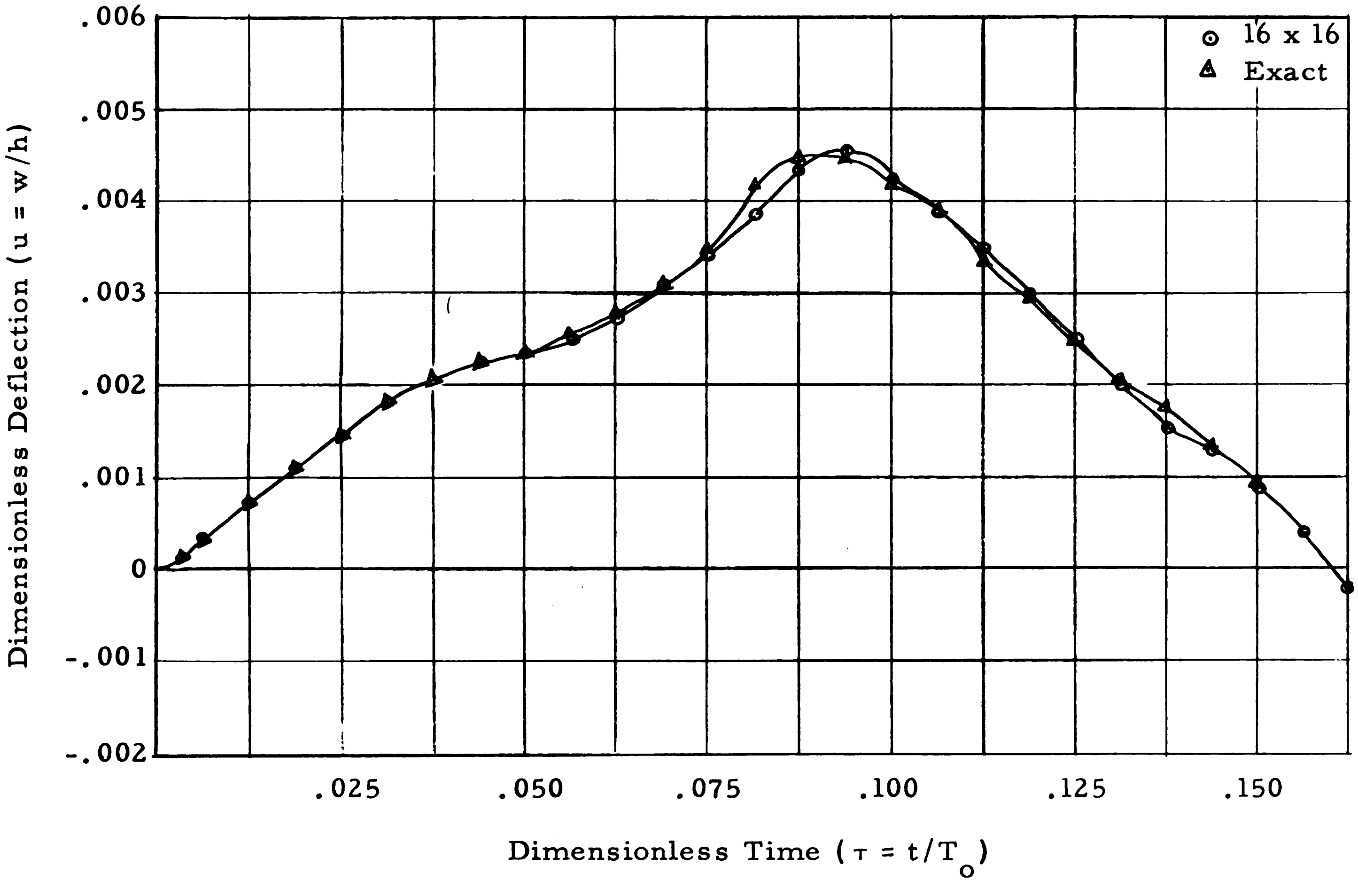

FIG. 13. COMPARISON OF NUMERICAL AND EXACT SOLUTIONS FOR CENTER POINT DEFLECTION FOR PARTIAL LOADING

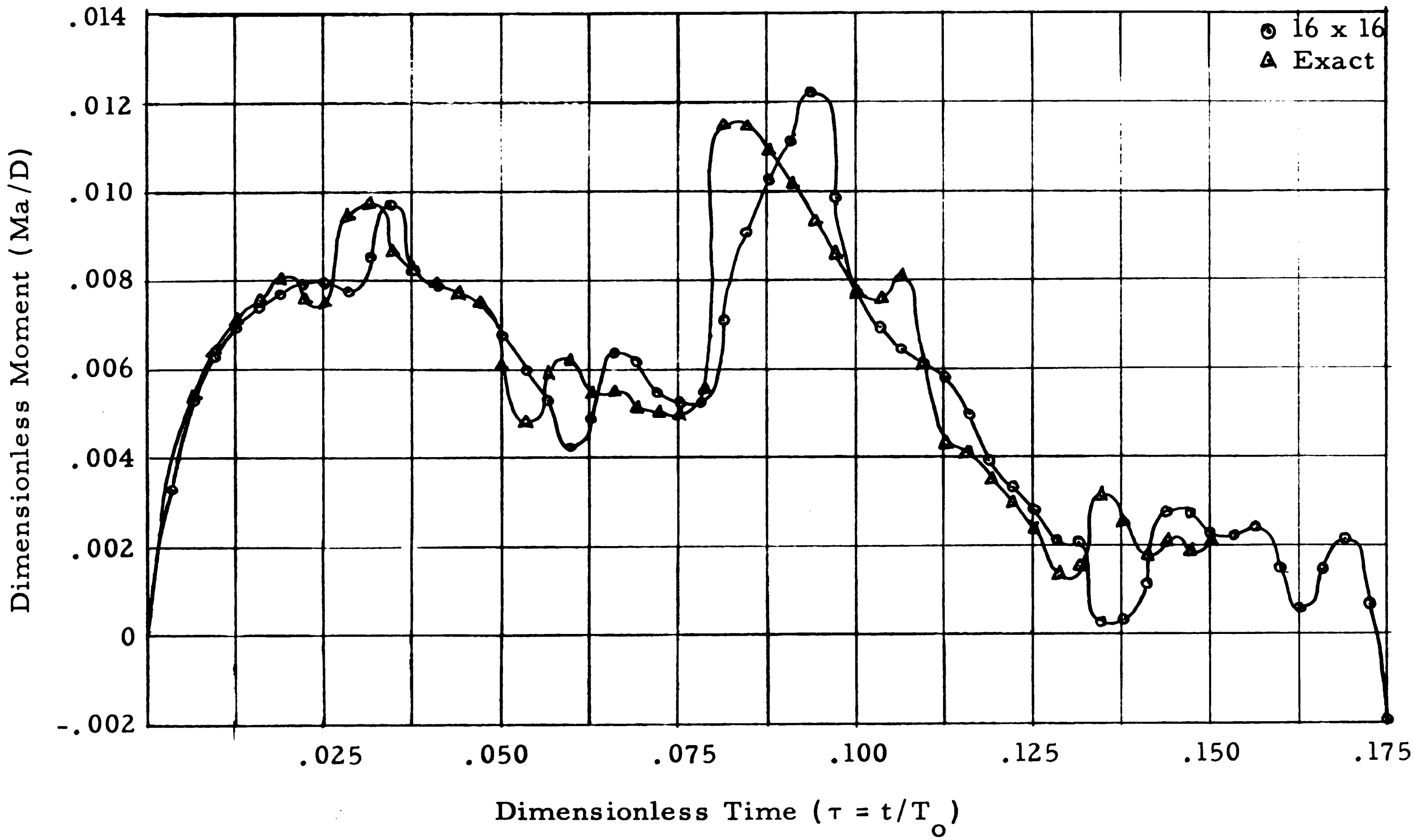

FIG. 14. COMPARISON OF NUMERICAL AND EXACT SOLUTIONS FOR CENTER POINT MOMENT FOR PARTIAL LOADING

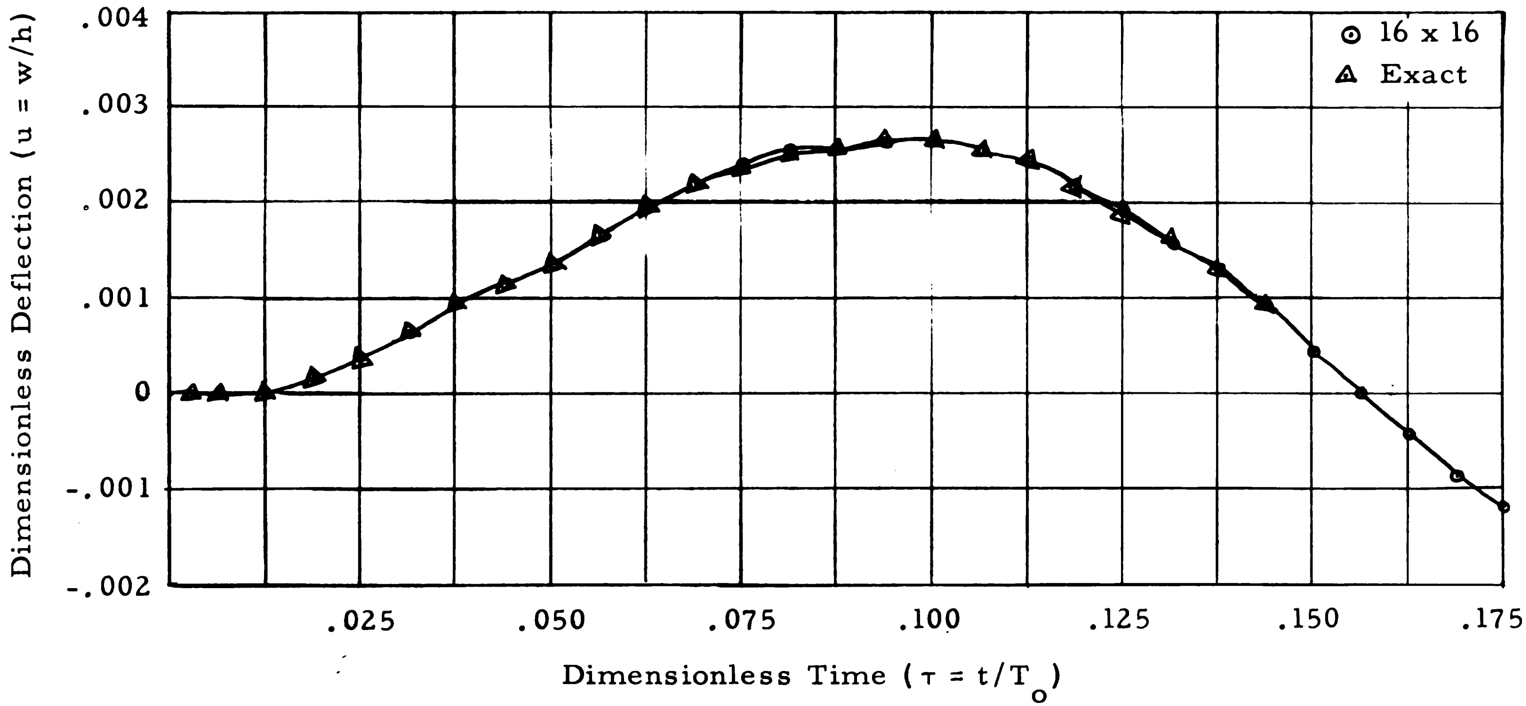

FIG. 15. COMPARISON OF NUMERICAL AND EXACT SOLUTIONS FOR QUARTER POINT DEFLECTION FOR PARTIAL LOADING

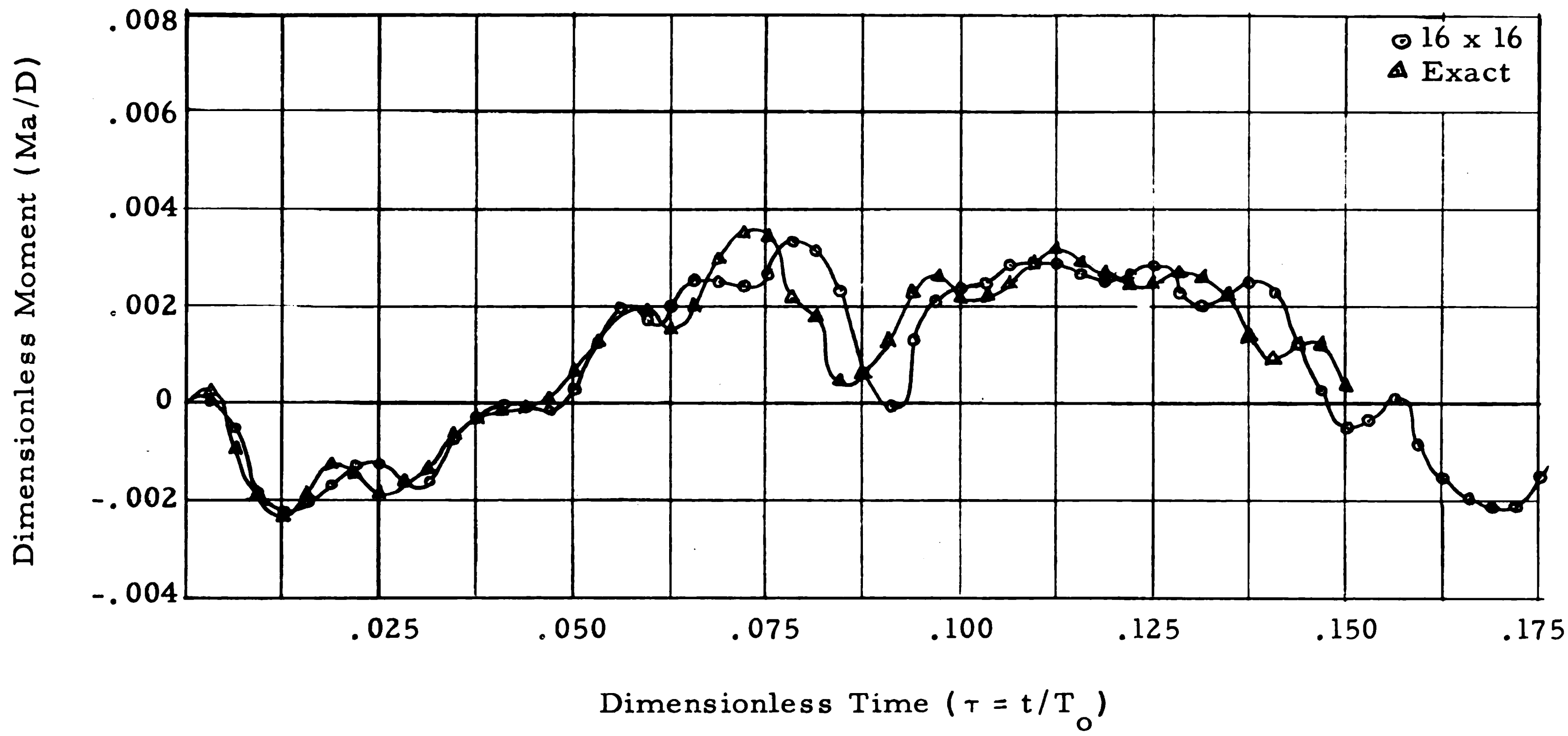

FIG. 16. COMPARISON OF NUMERICAL AND EXACT SOLUTIONS FOR QUARTER POINT MOMENT FOR PARTIAL LOADING

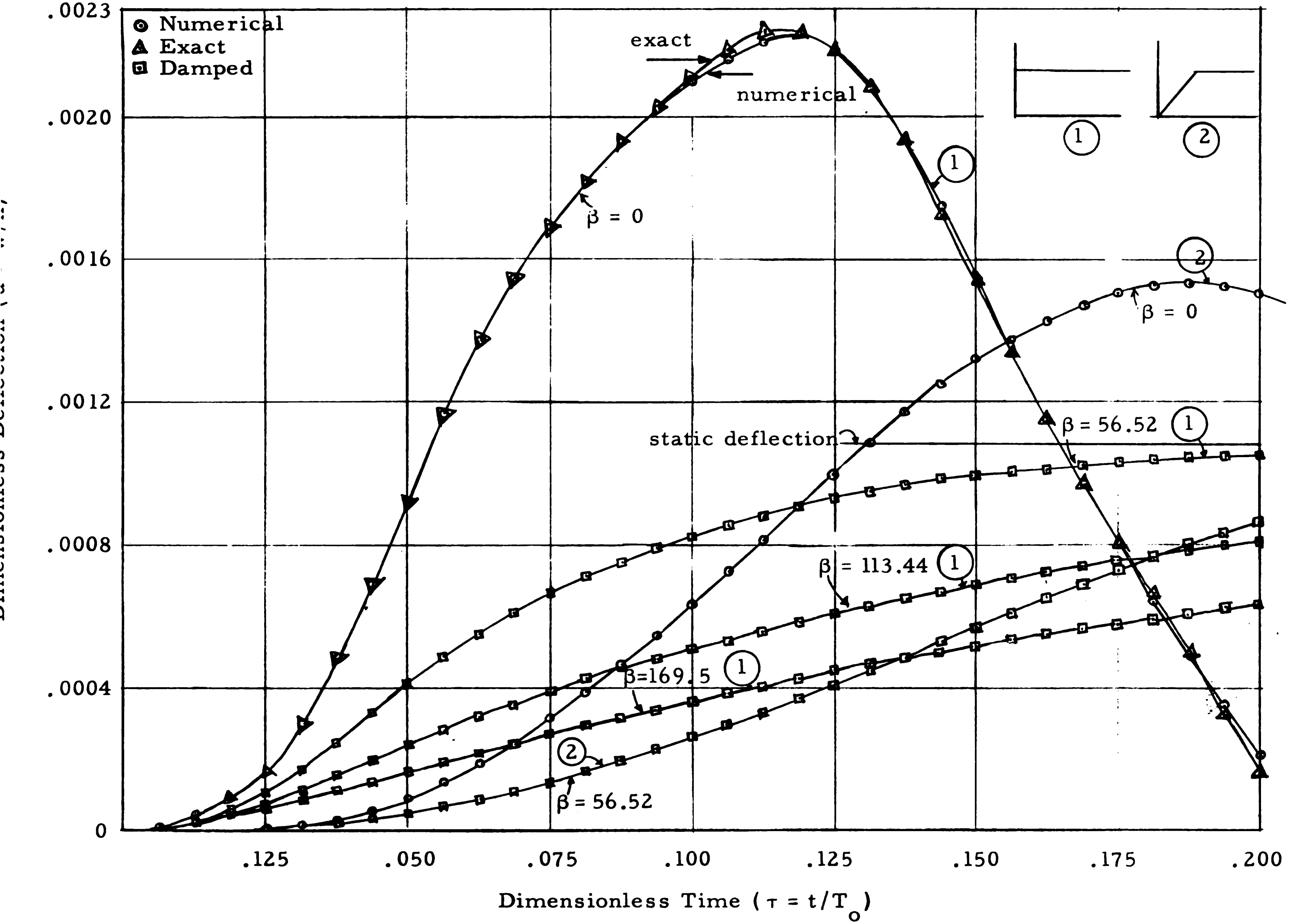

FIG. 17. DEFLECTION RESPONSE HISTORIES FOR VARIOUS FOUNDATION DAMPING VALUES

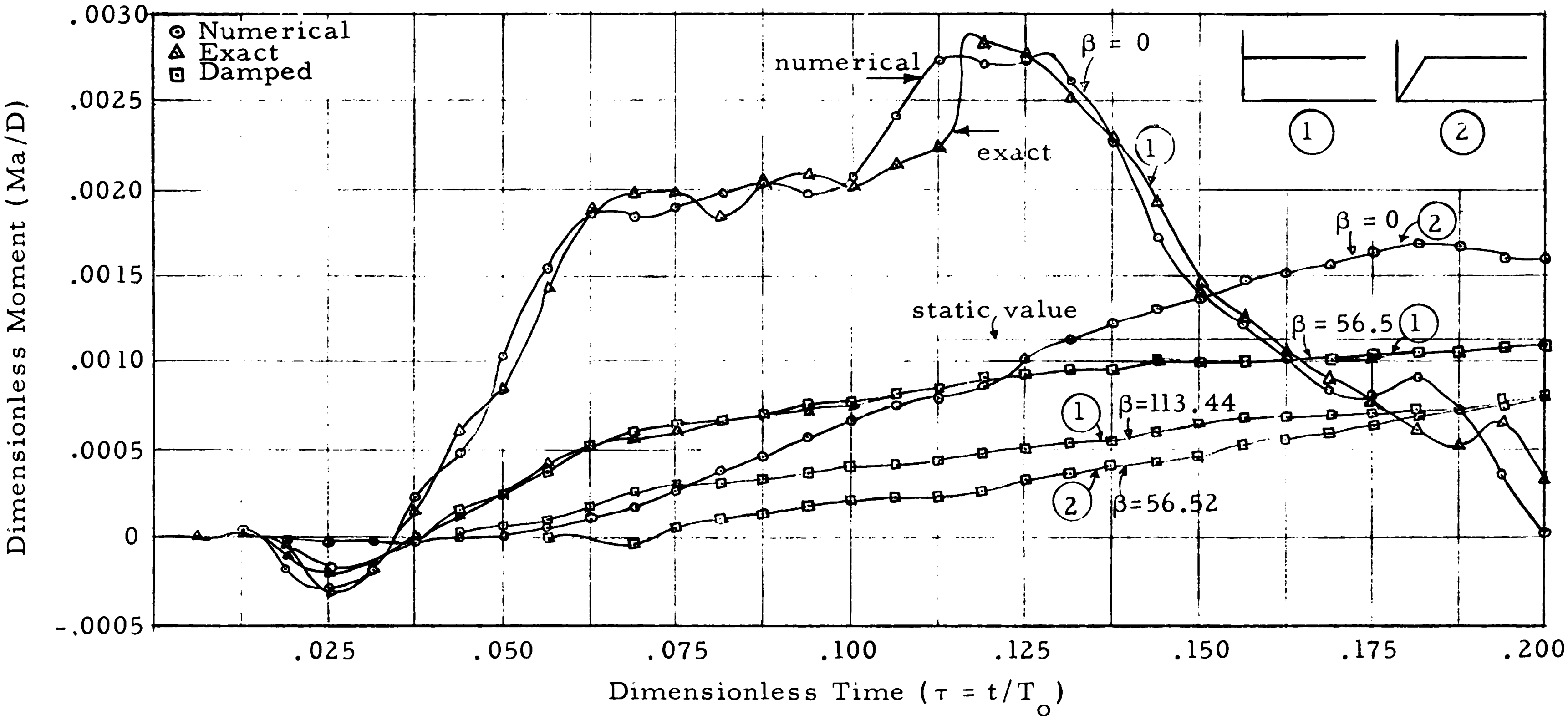

FIG. 18. MOMENT RESPONSE HISTORIES FOR VARIOUS FOUNDATION DAMPING VALUES

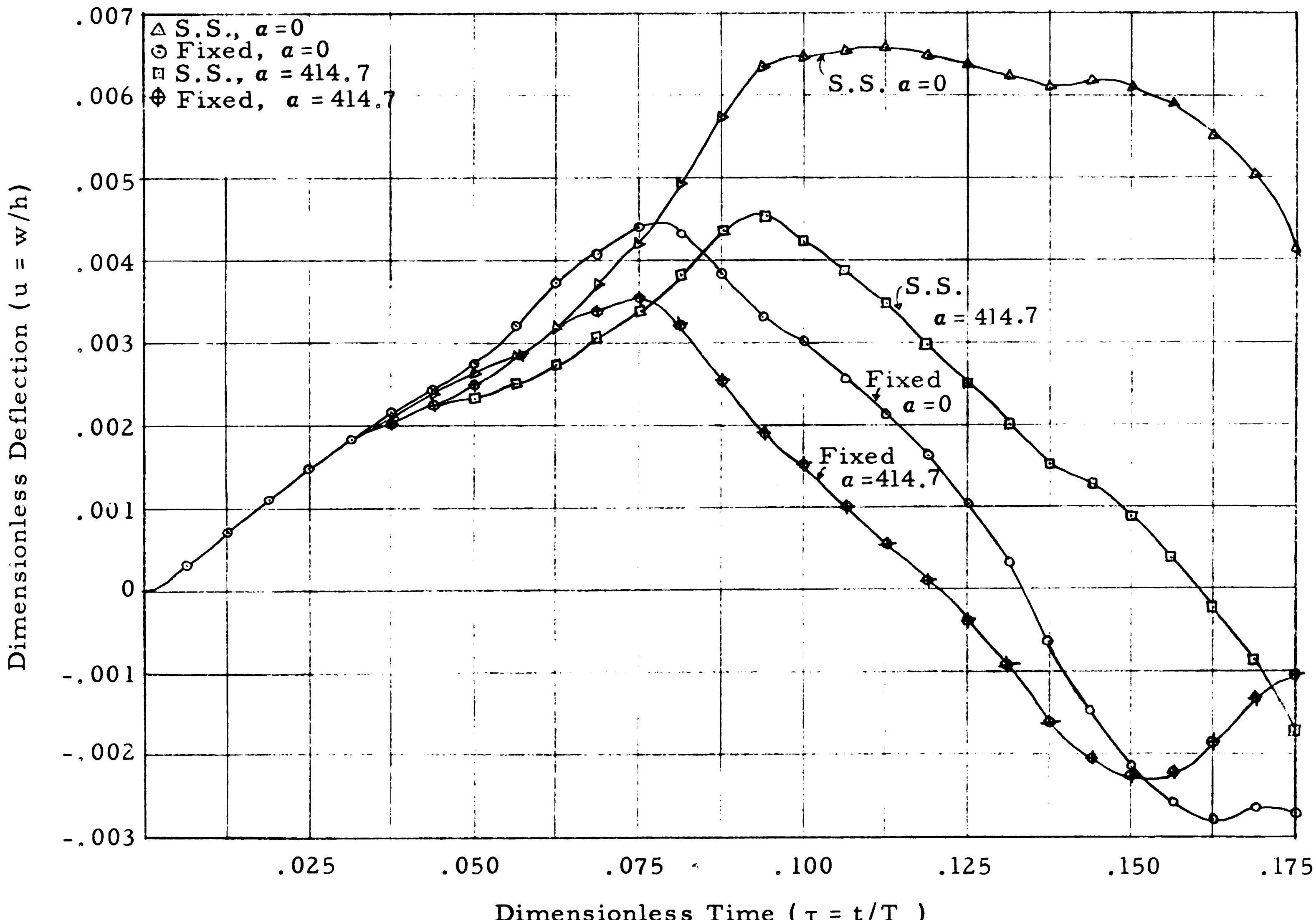

FIG. 19. DEFLECTION RESPONSE HISTORIES FOR VARIOUS TYPES OF BOUNDARY CONDITIONS AND FOUNDATION STIFFNESS VALUES

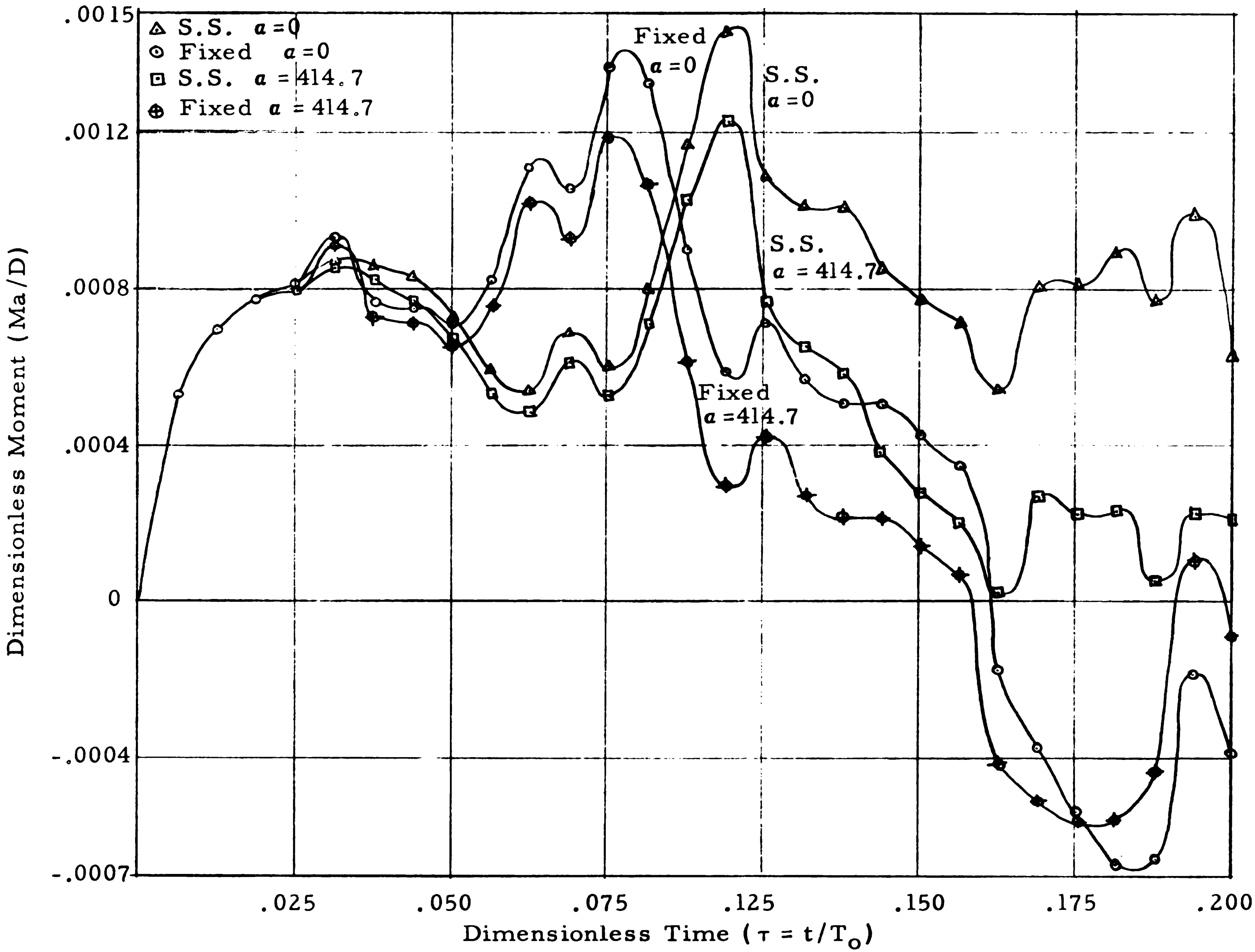

FIG. 20. MOMENT RESPONSE HISTORIES FOR VARIOUS TYPES OF BOUNDARY CONDITIONS AND FOUNDATION STIFFNESS VALUES

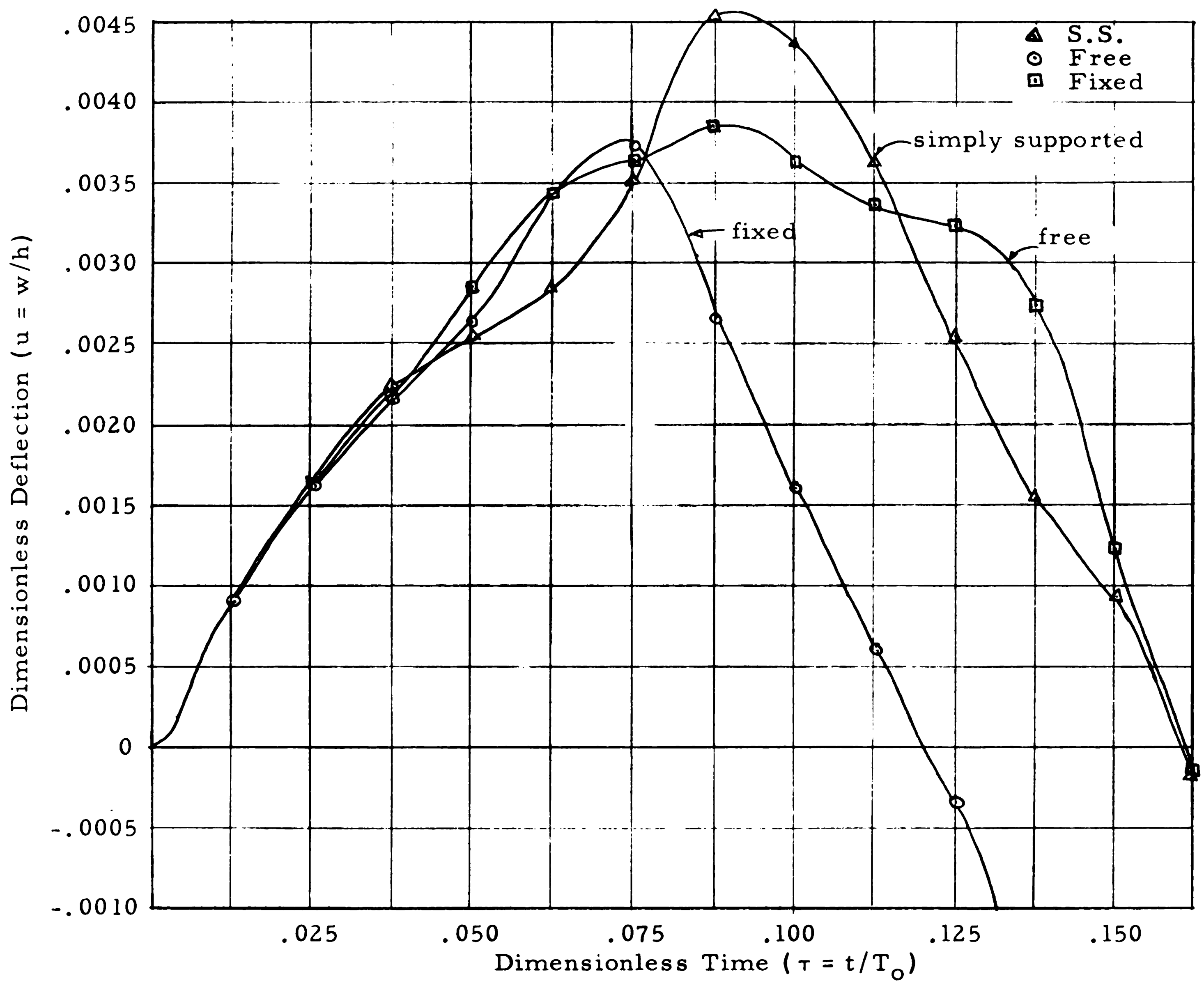

FIG. 21. DEFLECTION RESPONSE HISTORIES FOR VARIOUS TYPES OF BOUNDARY CONDITIONS

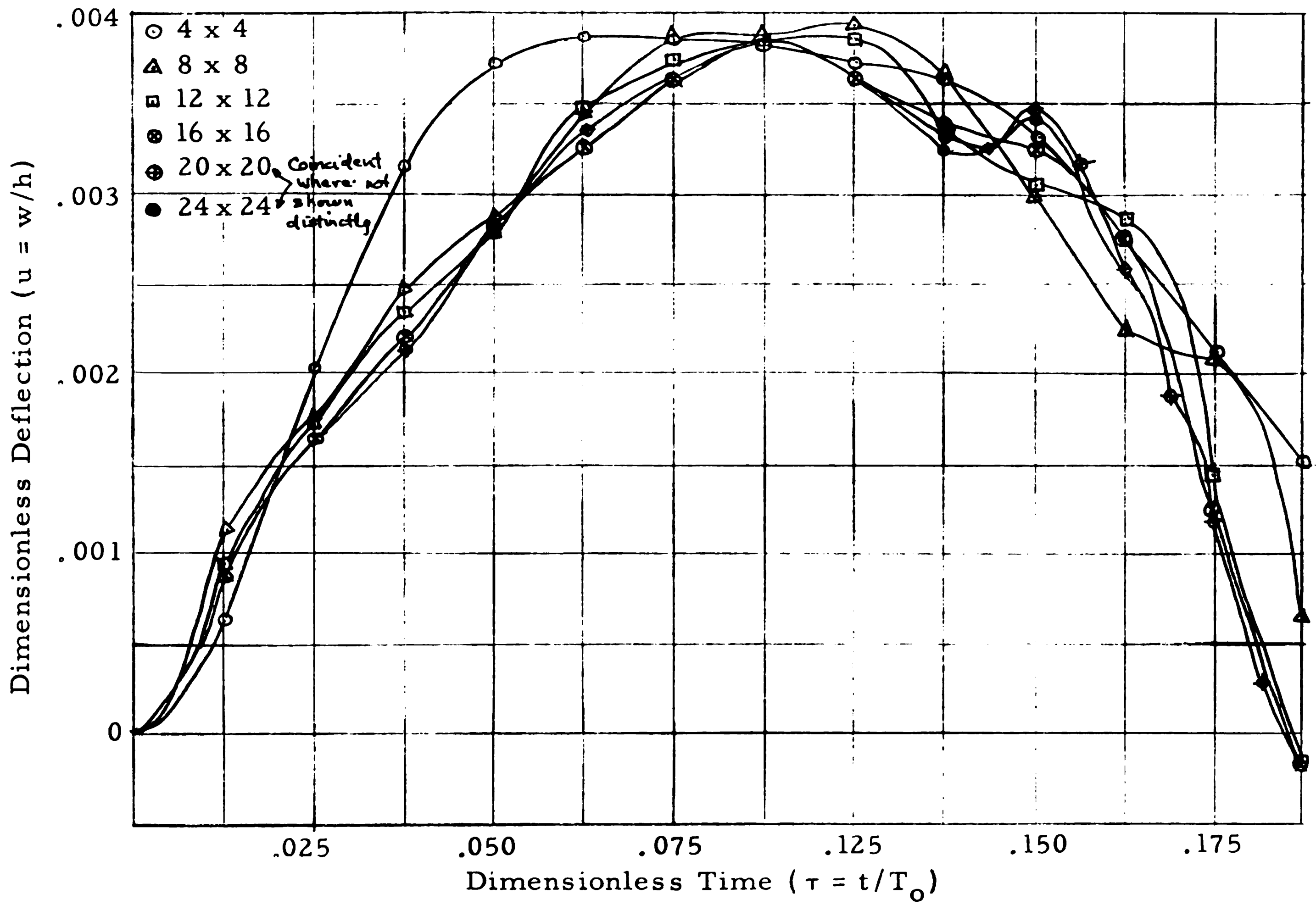

FIG. 22. CENTER POINT DEFLECTION RESPONSE HISTORIES FOR VARIOUS GRID SIZES FOR FREE PLATE

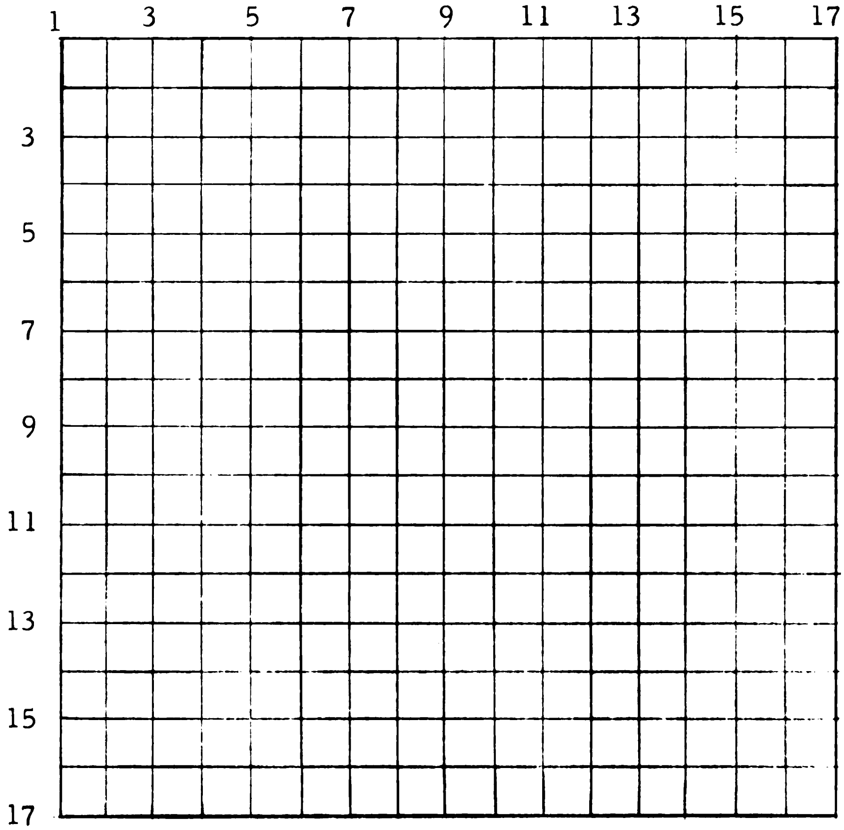

FIG. 23. COORDINATE SYSTEM FOR POINTS ON FREE PLATE FOR 16x16 GRID

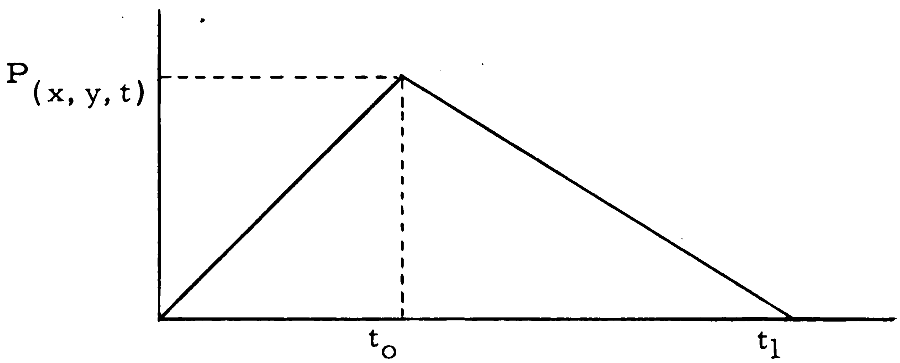

FIG. 24. LOADING PULSE WITH VARYING RISE RATE (BY VARYING t_o)

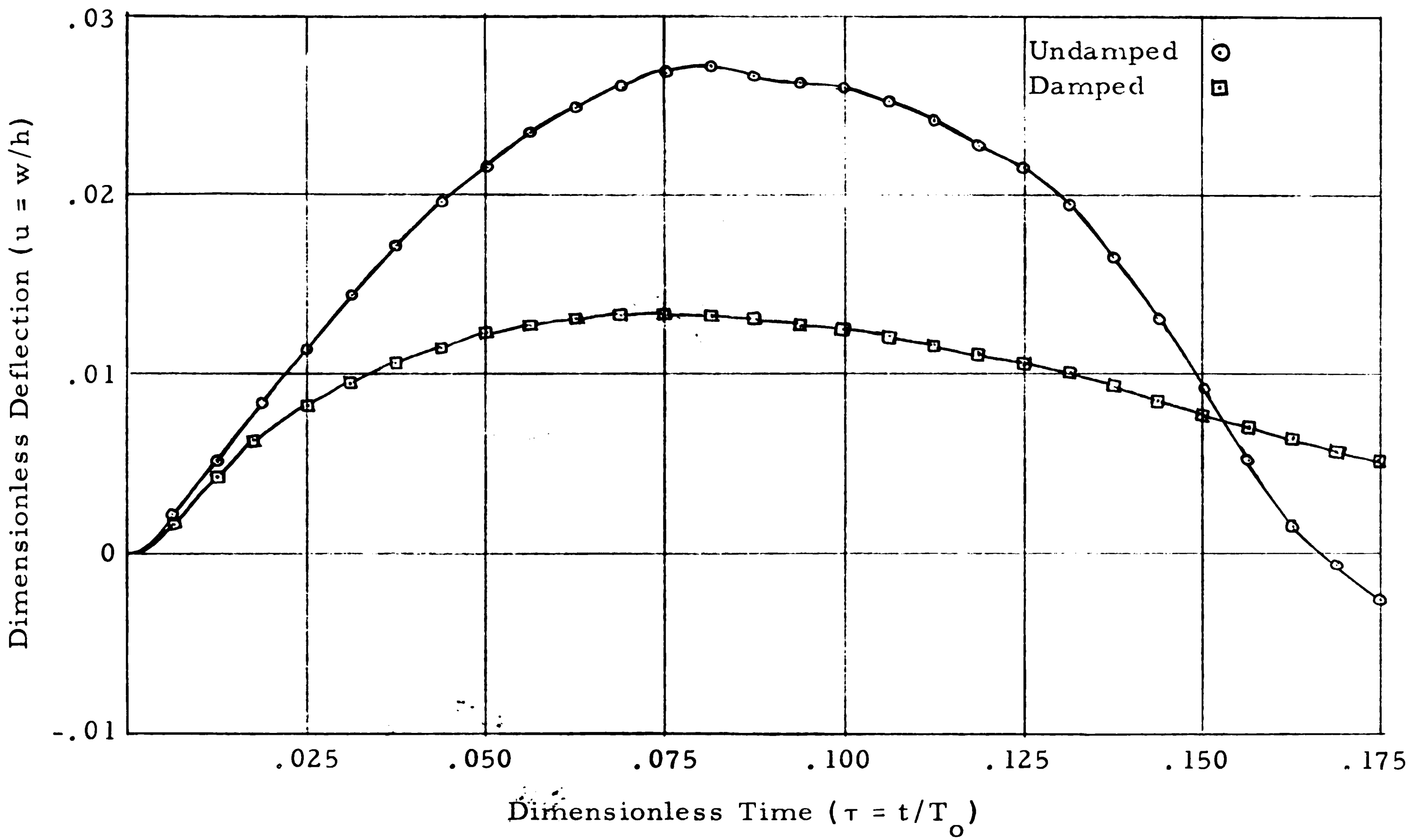

FIG. 25. RESPONSE HISTORY FOR DEFLECTION AT POINT (1, 1) DUE TO LOAD APPLIED AT POINT (1,1)

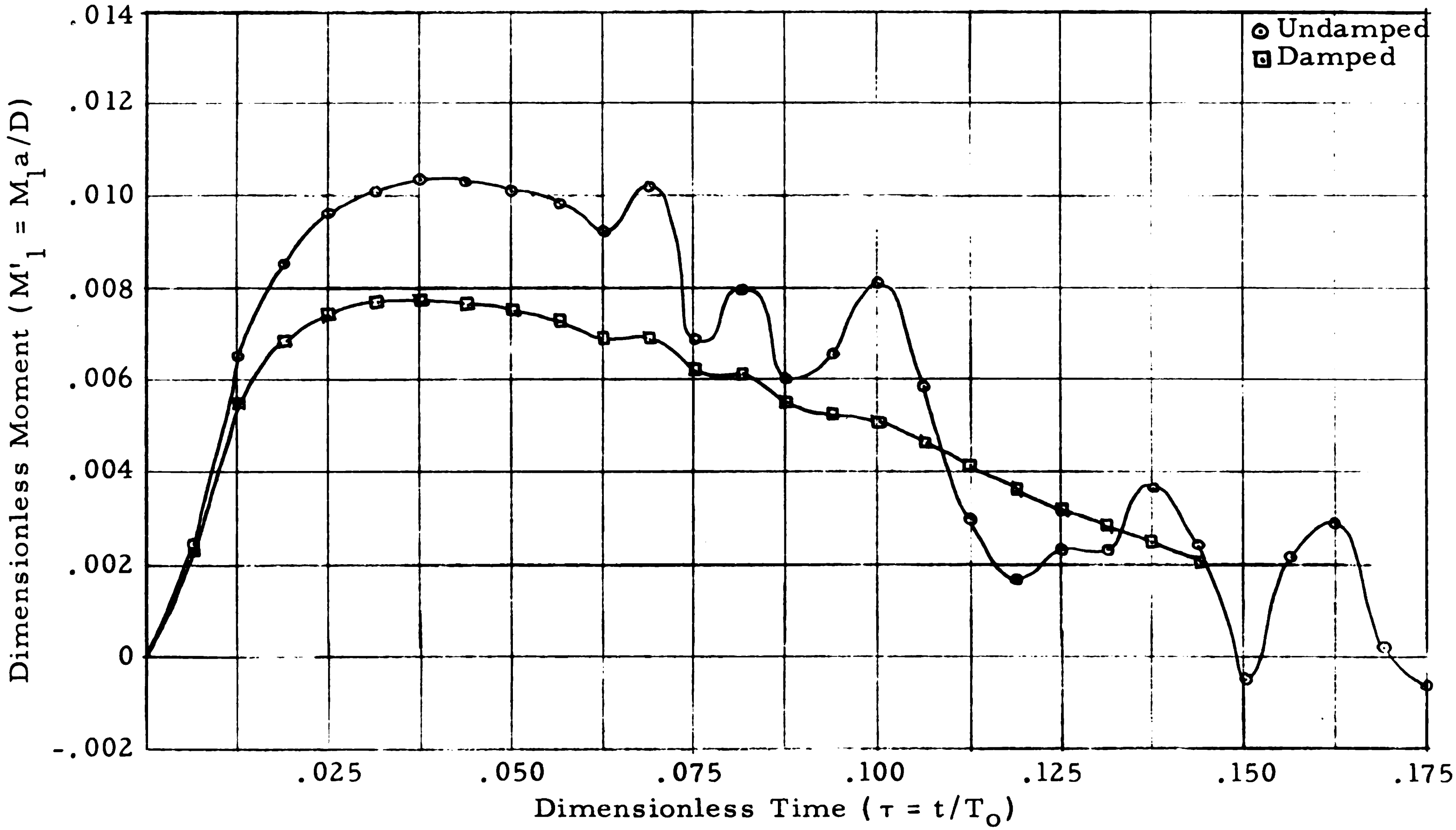

FIG. 26. **RESPONSE HISTORY FOR PRINCIPAL MOMENT M'_1 AT POINT (2,2) DUE TO LOAD APPLIED AT POINT (1, 1)**

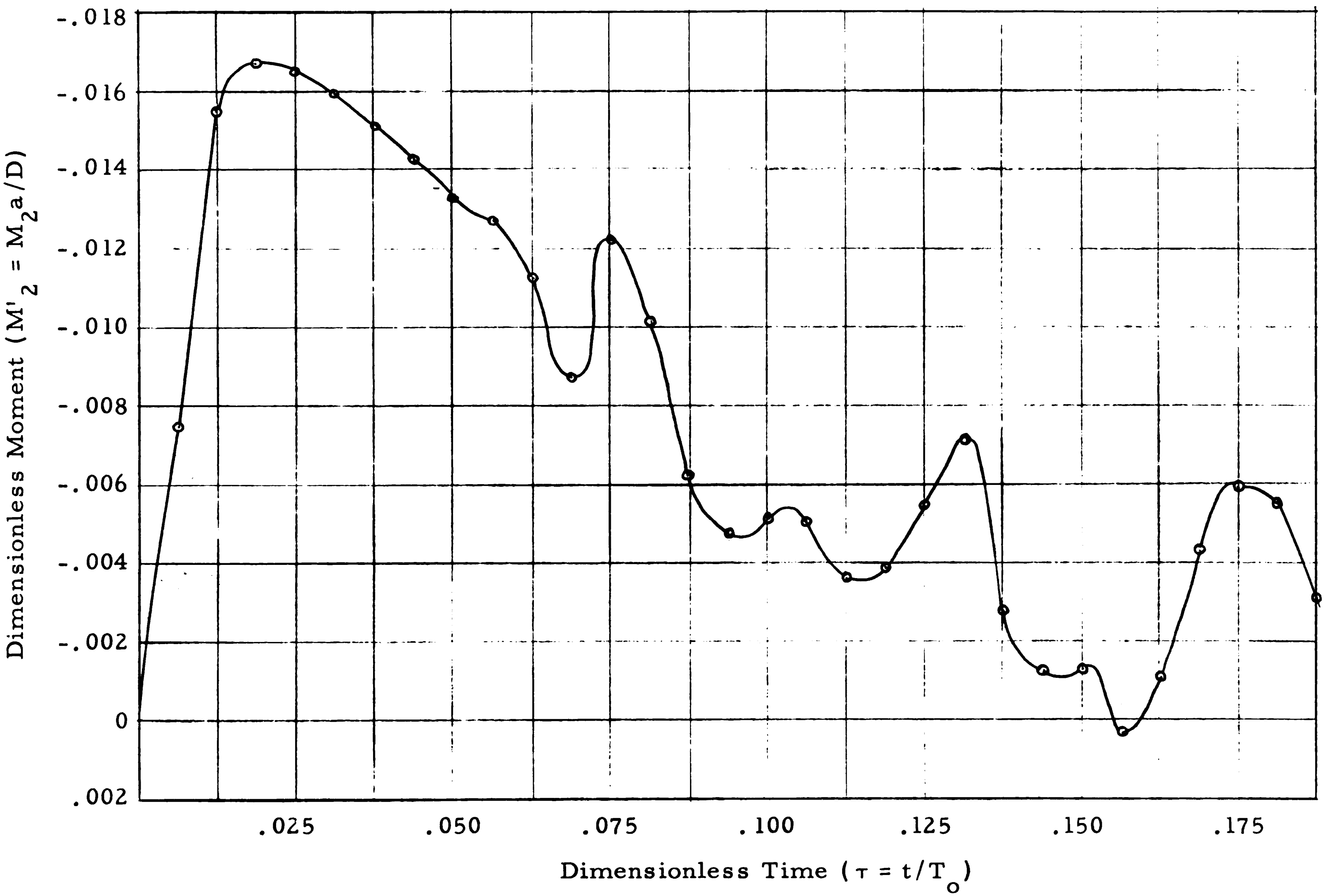

FIG. 27. RESPONSE HISTORY FOR PRINCIPAL MOMENT M'_2 AT POINT (3, 3) DUE TO LOAD APPLIED AT POINT (1, 1)

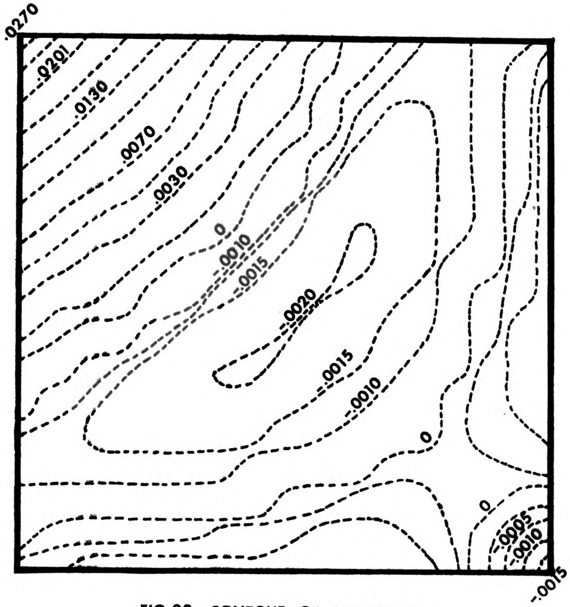

FIG. 28. CONTOUR OF DEFLECTION

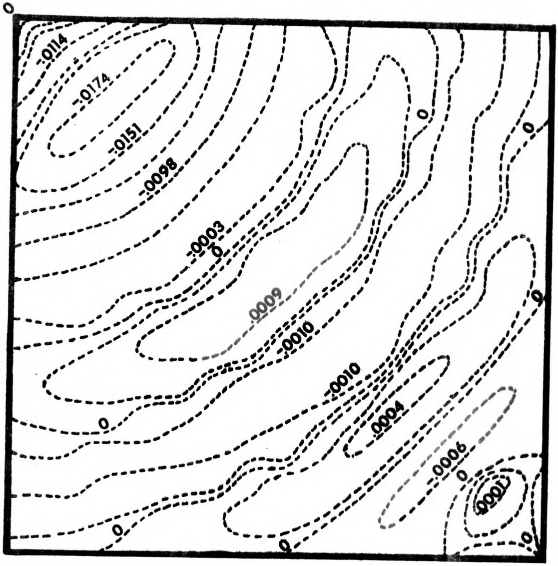

FIG. 29. CONTOUR OF PRINCIPAL BENDING MOMENT M_2'

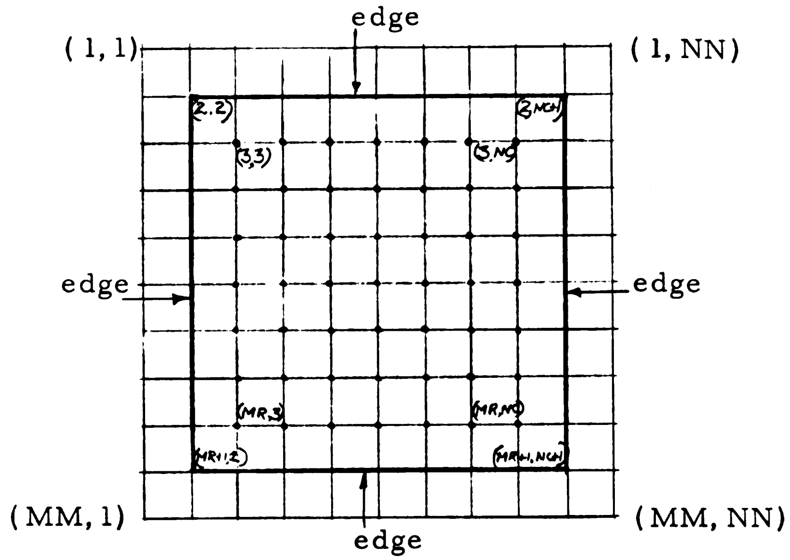

FIG. A1. GRID LINES FOR SIMPLY SUPPORTED PLATE

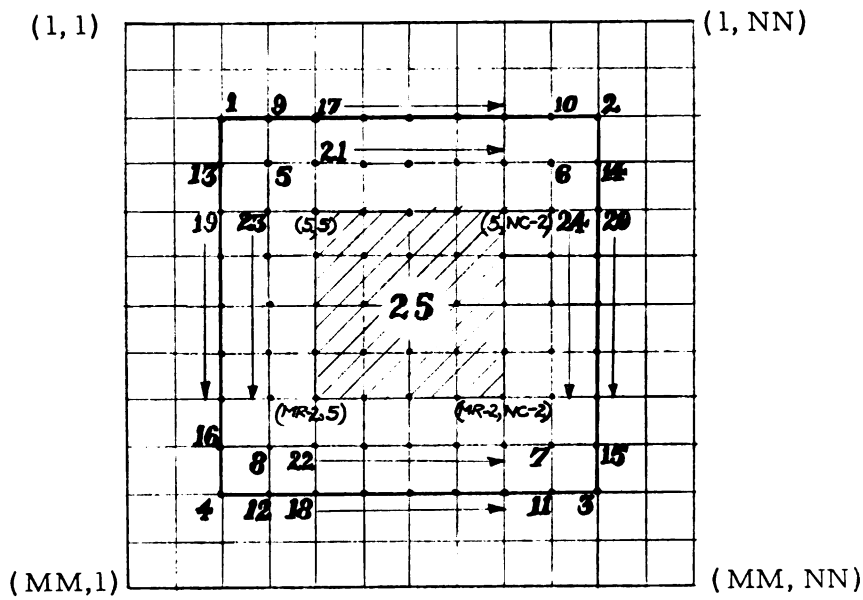

FIG. A2. LOCATION OF POINTS ON FREE PLATE AS USED IN PROGRAMMING

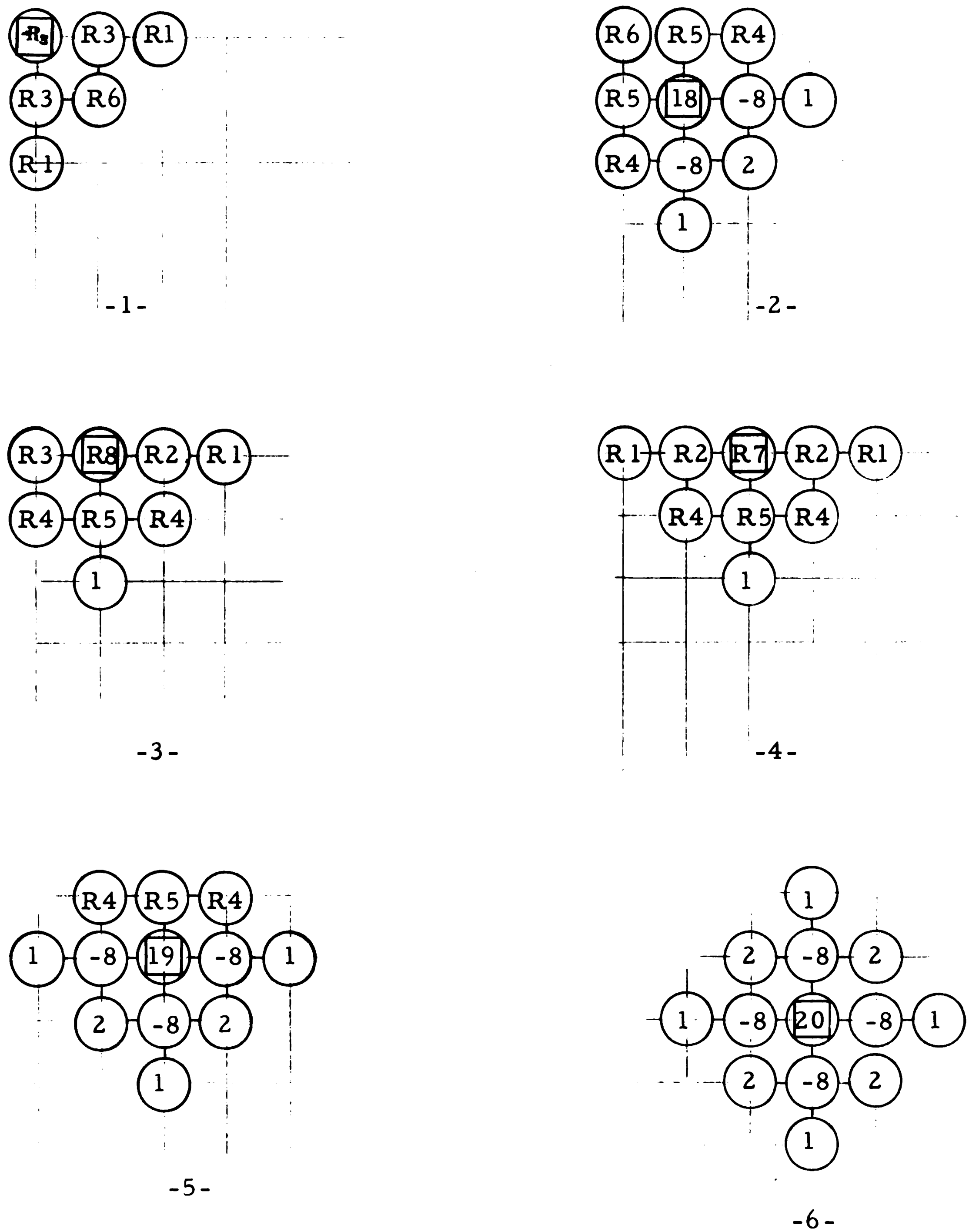

FIG. A3. SIX DIFFERENT TYPES OF "BHO" PATTERNS